Thermal Characterization of Structure-Integrated Thermal Subsystems based on the MASCOT Landing Module

AE5810 : Thesis Space

Ajay Prasad Ragupathy

Master of Science Thesis

Delft University of Technology

Space Engineering

Thermal Characterization of Structure-Integrated Thermal Subsystems based on the MASCOT Landing Module

AE5810 : Thesis Space

Master of Science Thesis

Ajay Prasad Ragupathy

27 January 2016
Student Number: 4324439
Thesis Supervisors:
Dipl-Ing. Michael Lange (DLR)
Ir. Barry Zandbergen (TU Delft)

Faculty of Aerospace Engineering · Delft University of Technology

Statement of Confidentiality

The present master's thesis comprises and affects developments which are only known to Deutsches Zentrum fuer Luft- und Raumfahrt e. V. , the German Aerospace Center, herein after referred to as "DLR". These findings and developments are therefore unknown to third parties. The contents and findings contained in the present publication - even excerpts and abstracts there from - are strictly confidential and may not be disclosed to third parties outside DLR without DLR's prior written consent. This confidentiality provision must be strictly observed. The present master's thesis must be kept under wraps following the three years after its completion. The effective date of its completion is the date on which the master's thesis is returned for assessment to the Delft University of Technology (The Netherlands). Exempted from this obligation of confidentiality is knowledge and insights in the context of assessment of the master's thesis as long as and to the extent they are not published themselves.

TU Delft Delft University of Technology

Deutsches Zentrum für Luft- und Raumfahrt e.V. in der Helmholtz-Gemeinschaft

Abstract

Accurate thermal characterisation of composite structures can help structural designers in predicting thermal paths in a spacecraft structure and assessing the effect of modifying materials on the structure's overall thermal performance. Existing spacecraft thermal analysis software lack the ability to model anisotropic thermal properties of composite materials. This in turn leads to inaccurate prediction of their thermal behaviour. The thesis describes the applied modelling methods and assumptions that are used to simulate the thermal characteristics of the MASCOT Landing Module's (LM) composite structure. MASCOT is a 10 kg shoebox-sized lander platform developed by DLR in cooperation with CNES and JAXA for the Hayabusa 2 sample return mission from the asteroid 1999JU3. The MASCOT LM structure's framework walls are made from a Carbon Fibre Reinforced Polymer/Foam sandwich. The M55J fibres used for the unidirectional sandwich face sheets are of Polyacrylonitrile (PAN) type and have high stiffness and strength properties, but poor thermal conductivity. Also, the glued connections between the framework walls are realised with PAN fibre patches. This is one reason, which necessitated a thermal sub-system consisting of heat pipes and a radiator. Both contribute with a total mass of 450 g, almost the same as the structural mass (550 g). Also, the structural design is itself influenced by the needs of the thermal subsystem. The modelling is carried out using Patran whereby methods to develop a thermal finite element model from the existing structural model are assessed and steady state analyses are carried out. To decrease the computational effort for radiation simulation, a novel method of developing radiation shell elements which are overlaid on the solid elements in the structure is described. Subsequently, the results from the finite element simulations are compared to actual temperature measurements, which were performed in a thermal vacuum chamber. The model is correlated with the test results and the method adopted is validated. The next phase of the thesis work involves the use of the developed thermal model to assess solutions for integrating the thermal functions within the LM structure. As a first step, the heat pipes are removed. The impact of the removal of the heat pipes on the LM is assessed and various design solutions are proposed for the MASCOT LM. From the simulations, it is concluded that it is indeed possible to remove the heat pipes from the LM and that a structure-integrated thermal subsystem can be achieved by introducing conductive interfaces in the structure.

Acknowledgements

First and foremost I would like to thank Dr.Christian Huehne, the head of Dept. of Composite Design at the DLR Institute of Composite Structures and Adaptive Systems, Braunschweig for giving me this opportunity to work there on my master thesis. I would like to thank my supervisors, Dipl-Ing.Michael Lange and Ir.Barry Zandbergen who guided me throughout the work. I am grateful to Mr.Lange for encouraging me to think outside the box and come up with alternate solutions when the task seemed insurmountable. By following up on an almost daily basis regarding progress, he ensured that I stayed on top of my work at all times.

I would like to thank my mother Mrs.Manimehalai and my father Mr.Ragupathy for their constant motivation and helping me pursue my dreams of becoming a space engineer. Finally, I would like to thank all my friends in Delft who supported me throughout the Masters program and have been like my second family here.

"You will begin to touch heaven, Jonathan, in the moment that you touch perfect speed. And that isn't flying a thousand miles an hour, or a million, or flying at the speed of light. Because any number is a limit, and perfection doesn't have limits. Perfect speed, my son, is being there."

~ Richard Bach, Jonathan Livingston Seagull

"Learning gives creativity. Creativity leads to thinking. Thinking provides knowledge. Knowledge makes you great."

~ Dr.A.P.J.Abdul Kalam

Delft University of Technology
27-1-2016

Ajay Prasad Ragupathy

Table of Contents

List of Figures

List of Tables

Glossary

List of Acronyms

S/C Spacecraft

LM Lander Module

PAN PolyAcryloNitrile

CFRP Carbon Fibre Reinforced Polymer

MASCOT Mobile Asteroid Surface Scout

CFRP Carbon Fibre Reinforced Polymer

MFCBS Multi Functional Composite Bus Structure

TU Delft Delft University of Technology

TCS Thermal Control System

FEM Finite Element Methods

OOP Out-of-Plane

IP In-Plane

MLI Multi Layer Insulation

MESS Mechanical and Electrical Support Structure

UD Uni-Directional

I/F Interface

List of Symbols

α	Co-efficient of thermal expansion
δ	Lamina thickness
ϵ	Emissivity
ψ	Volume percentage of fibre
ρ	Density
ρ_c	Density of core material
ρ_f	Density of facesheet material
σ	Stefan Boltzmann constant
B	Gebhart factor
c_p	Specific heat capacity
E	Young's modulus
F	View factor
k	Thermal conductivity
k_f	Fibre thermal conductivity
k_m	Matrix thermal conductivity
l	Length
Q	Heat energy
q	Radiative heat flux
t	Thickness
t_f	Face sheet thickness
T_w	Surface temperature
V_f	Fibre volume fraction
V_m	Matrix volume fraction

Chapter 1

Introduction

Composite materials are nowadays being used to develop entire spacecraft structures and their increased use has led to significant mass savings when compared to traditional aluminium structures. Although all-composite structures use state-of-the art materials, there is very little understanding of the participation of each component in a structure's thermal path and methods to predict their thermal behaviour. Thermal conductivity in such spacecraft composite structures is the central theme of this thesis. Although a few spacecrafts have flown with all-composite structures as seen in the literature study performed prior, [8] the thermal behaviour of these structures was never assessed in early design phases. This often led to uncertainties in the thermal subsystem design process. The structural design engineers create models with 2D elements that are used for simulating the structural performance using finite element software. In order to predict the temperature distribution in the structure without depending on the thermal designers, a method must be developed to convert a structural model into a thermal model which can provide an initial understanding of the thermal paths in the structure.

This chapter serves to present an introduction to the thesis work carried out. The first section describes the motivation behind the work, followed by the research objective, research question and the goals for the thesis. The thermal model development and analysis is carried out using the finite element pre-processor Patran and the solver Nastran.

1-1 Motivation

During the early design phases of a spacecraft, the only way to gain necessary thermal data is by analytical or numerical simulations of the different loads on the spacecraft. Numerical simulation techniques are the most important components for a reduction of development costs. Since each composite part is unique and tailored to a particular function, sometimes coupon level to large scale tests are always required to determine their thermal behaviour. But nowadays due to the advancements in computing, it is possible to simulate a great variety

Figure 1-1: Hayabusa 2 and MASCOT on the Asteroid Ryugu (Artist's impression) [1]

of scenarios with such an accuracy and speed that cost and time consuming tests could be avoided.

Determining the temperature distribution within a spacecraft structure helps designers determine thermal paths within the structure and optimize the design accordingly. The goal is to minimize the additional mass of a dedicated thermal subsystem by integrating it with the structure. The German Aerospace Centre (DLR) is investigating the use of composites in their planetary landers to replace the traditional aluminium based structures in order to increase the payload to structure mass ratio.

The focus of this thesis is on the MASCOT Asteroid Lander's all-composite structure. The Mobile Asteroid Surface Scout (MASCOT) is an approximately 10 kg shoebox-sized lander platform developed in cooperation with CNES and JAXA for the Hayabusa 2 sample return mission heading to the Cg-class asteroid 1999 JU3. DLR plans to use all-composite structures for future spacecraft missions and has shown an interest to investigate the thermal aspects during early design phases. (Fig 1-2)

1-2 Research Objective

A predictive thermal modelling of the heat transfer processes within the MASCOT Landing Module is aimed to be carried out. A strategy for accurate and efficient thermal investigation of composite structures by means of the Finite Element Method (FEM) is presented. During the structural design process it is advantageous to use one model for both structural and thermal analysis. Hence, the objective of the work is to ensure that the model that is used for the structural analysis of the Landing Module (LM) is adapted for thermal analysis. The primary objective will be to develop a finite element method to supply a full three dimensional

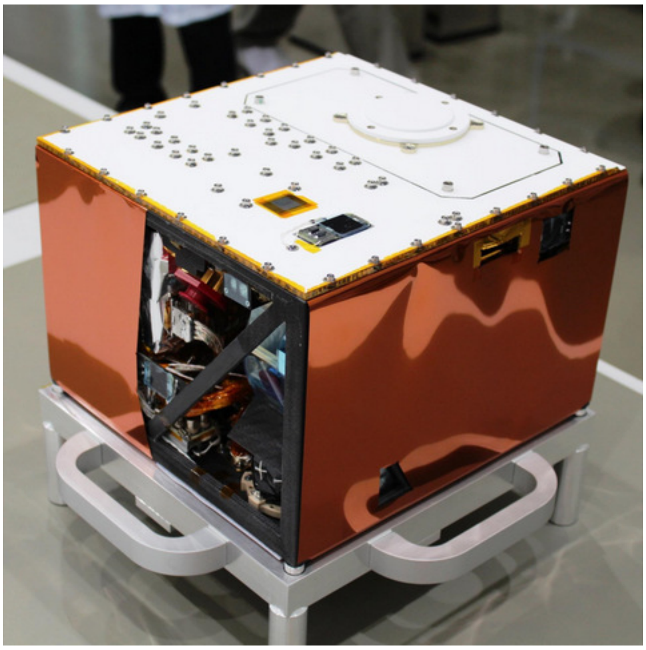

Figure 1-2: MASCOT Flight Model

temperature distribution which can be used to assess the thermal paths in the LM. The other objective for the thermal analysis will be to investigate whether a structure with integrated thermal functions can fulfill the thermal requirements of the spacecraft.

1-3 Research Questions

The thesis work seeks to answer the primary research question that is formulated:

> *What is the best modelling approach to characterize the thermal behaviour of the MASCOT Lander Module structure and what solutions can be proposed to improve the thermal behaviour of the all-composite structure?*

The research questions that were formulated based on the primary research question are:

1. What is the current thermal subsystem design?
2. What are the thermal loads introduced by payloads?
3. What are the thermal radiation sources that need to be modelled?
4. What are the methods available in Patran for converting a structural model into a thermal model for a composite structure?
5. What are the problems and anomalies that were encountered while developing the thermal model?

6. What is the temperature distribution in the MASCOT Landing Module's structure?
7. What is the accuracy needed for a thermal model to capture the physics of conduction and radiation and produce realistic results?
8. What are possible recommendations for a structure integrated thermal subsystem for MASCOT?

1-4 Goals

The structural model of the MASCOT Landing Module (LM) is modelled using the Patran pre-processor. The goal is to use the structural model developed in Patran as the baseline to develop the thermal model. The objective is not to replace the existing methods for thermal analysis performed using dedicated spacecraft thermal analysis software. The lack of the ability of these software to simulate thermal anisotropy when considering composite structures is a detriment for structural designers who might wish to gauge the thermal paths in a composite structure and select suitable materials such that the structure can perform the functions of a dedicated thermal subsystem (such as heat pipes and thermal links). The research questions generated are answered during the thesis by achieving the goals mentioned below:

1. Development of the thermal finite element model of the MASCOT Lander Module Structure.
2. Modelling the test setup and the interface values accurately.
3. Determination of the thermal paths in an all-composite structure using steady state analysis.
4. The model shall give a $\pm$ 5K error in the temperatures obtained when correlated with the test results.
5. Selection of the best combination of design solutions for improving the thermal conductivity of the structure.
6. Narrowing down the most feasible concept for thermal management based on the MASCOT Lander Module.

The thesis report is organized as follows. Chapter 2 will delve into the need for composite structures and the MASCOT heritage. Chapter 3 discusses the Hayabusa 2 Mission and the MASCOT Lander Module. Chapter 4 will describe the finite element modelling process that is carried out for the thermal characterization. Chapter 5 elaborates on the steady state analyses and the correlation of the results based on the thermal-vacuum test campaigns that were conducted previously. Chapter 6 describes the concepts for thermal management using composites that were considered applicable for the MASCOT Lander Module. In Chapter 7, the conclusions and future recommendations are put forward.

Chapter 2

Literature Review

This chapter provides a theoretical background on the focus of this thesis : composite spacecraft structures and their thermal characterisation. The payloads in a spacecraft are normally rigidly connected to the bus's structure and can dissipate heat via conduction. However also, a high thermal insulation can be required in certain cases. In contrast to an aluminium alloy structure, an all-composite structure has an overall thermal conductivity which is in the order of almost a magnitude lower [9] and thus presents a thermal challenge for designing a high thermal conductive structure.

There is a need to understand the nature of heat conduction process in CFRP sandwich structures and being able to predict how well a particular composite implemented will perform thermally. Both are of critical interest for future spacecraft structures. This chapter presents an analysis of fully composite spacecraft structures and will seek to identify the various aspects of such structures such as :

- Mass savings with respect to aluminium structures
- Effect on the thermal design
- Multifunctional capabilities

2-1 Why Composite Structures?

Composites are the most versatile materials in the spacecraft industry. Their use has grown a lot since the 1950s (Fig 2-1). By reducing the structure to total spacecraft mass ratio, the available payload mass increases. Initially, when no composite components were used in the spacecraft the structure to spacecraft mass ratio is around 20%. As the TRL levels of composite components for various aspects of the spacecraft such as antenna reflectors started increasing and with the implementation of all-composite spacecraft structures the ratio starts falling to around 5%. This reduces over the years to less than 5% when composites are used for electronics boxes. The reason why composites have been so successfully implemented in many missions with success is because of the ability to tailor the mechanical and physical properties according to mission requirements. This in turn leads to significant mass savings while giving similar or improved performance over metal structures. [8]

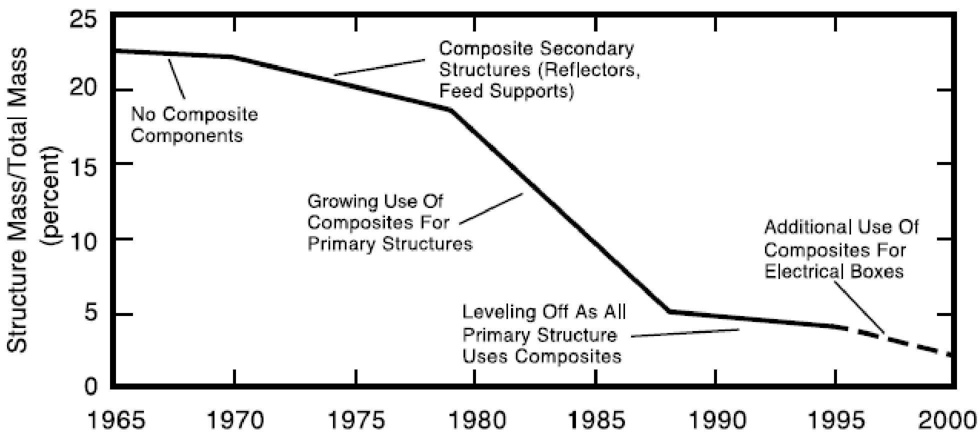

Figure 2-1: Evolution of composite usage in spacecraft[2]

Traditional structures have always contributed to approximately 20% of the total spacecraft mass [11]. Small spacecraft structures have largely stuck to using metal structure buses [12]. The use of all-composite structures in small spacecraft has not yet become mainstream as small satellite manufacturers are focussing only on developing a low cost spacecraft to fulfil the objectives of the mission. Future missions demand higher payload to structure performance ratios and hence composites can be used to achieve the desired performance ratios.

Composite materials are currently used for designing a variety of components on spacecrafts [13] :

- Primary Structures: Structure buses, payload boxes, launcher adapters and fairing, aeroshell for re-entry vehicles, tank interstage, rocket casing, pressurized modules, rover and lander chassis.
- Secondary Structures : Antenna dishes, support trusses, mounting platforms for equipment, pressure vessels, racks and protection systems;
- Tertiary Structures: Inserts, standoffs, fittings and joints

2-2 Composite Heritage

By analysing the missions previously flown with all composite structures, it can be noticed that the mass savings are in the range of 30-50% when compared to traditional aluminium structures. Due to the anisotropic nature of composite materials and the lower conductivity in both the In-Plane (IP) and Out-of-Plane (OOP) direction of PolyAcryloNitrile (PAN) fibre based composites primarily used in spacecraft structures, the thermal conduction paths normally provided by aluminium structural components are unavailable. This leads to challenges in the placement of electronics within the spacecraft in order to create a stable thermal environment and thus in turn can influence the design of the spacecraft structure to a great extent.

A comparison of the structures studied have been composed into a tabular form in Table 2-1.

Spacecraft	Total Mass (kg)	Composite Structural Mass (kg)	Mass Savings wrt a traditional Al Structure	Savings on Spacecraft Mass	Thermal Design
FORTE	236	42.6	34 %	8.45 %	Conventional
Mightysat I	63	8.6	46 %	10.51 %	Conventional
Mightysat II	130	13.6	47 %	8.70 %	Multifunctional
WIRE	250	25	50 %	9.1 %	Multifunctional
STSAT 3	150	31.9	32 %	8.98 %	Multifunctional
MASCOT	10	0.96	75 %	9.2 %	Conventional

Table 2-1: Heritage Analysis [8]

Based on the analysis of the thermal designs implemented on the missions discussed the following observations are made:

- FORTE's thermal design was conventional and the placement of the payloads was affected during the design process due to the introduction of the composite structure.
- Mightysat I followed a conventional thermal design too and the effects of a composite structure on the thermal performance were not assessed.
- Mightysat II and WIRE flew with an experimental Multi Functional Composite Bus Structure (MFCBS) where high conductivity fibres (K1100) were used at specific locations to ensure efficient heat dissipation.
- STSAT-3 exploited the concept of thermal contact conductance along with the use of combination of fibres to ensure increased heat dissipation.
- During MASCOT's design the conductive capabilities of the composite framework were not characterised and a conventional thermal subsystem was used to meet the thermal requirements.

Thermal subsystems normally contribute 2-5% to the total mass of the spacecraft [12]. It is observed that when the subsystems are downscaled for a small spacecraft, the contribution of a thermal subsystem on the overall structure bus design becomes more significant.[14] From these observations it can be noticed that there are primarily two major types of thermal design approaches that were adopted by the spacecraft designers for all composite structures.

- Conventional : The thermal subsystem is independent of the structure. The placement of components within a spacecraft is optimized and thermal systems compensate for the lower conductivity of the composite structure.

- Multifunctional : The multifunctional structure concept involves embedding passive thermal control components within the actual volume of composite materials. The goal is to ensure reduction in parasitic mass caused by dedicated thermal control components and also increase in the available volume for payloads onboard the spacecraft.

2-3 Thermal Properties

For a spacecraft, conduction and radiation are the only heat transfer processes possible. Since conduction is an important method of heat removal, thermal conductivity is a key material property. Mass is also an important factor, and consequently, material density is also significant. A useful figure of merit is specific thermal conductivity, defined as thermal conductivity divided by density.

Conductivity perpendicular to the fibres is much less as it is dominated by the polymer matrix. The ability to dissipate heat is thought to contribute to the very good fatigue properties of CFRP. The conductivity of fibres increases with graphite content and highly graphitized fibres, such as high-modulus Be/Si have thermal conductivity values of 700 W/mK in the longitudinal direction which surpass the value for aluminium (180 W/mK). [15]

Material	Specific Gravity [g/cm^3]	In-Plane Thermal Conductivity [W/m.K]	Out-of-Plane Thermal Conductivity [W/mK]	In-Plane Specific Thermal Conductivity [W/mK]	Out-of-Plane Specific Thermal Conductivity [W/mK]
2-D Carbon-Carbon	1.88	250	20	132	10.6
EWC-300/Cyanate Ester	1.72	109	1	63	0,6
Copper	8.9	400	400	45	45
Aluminium 6061	2.8	180	180	64	64
Aluminium Honeycomb	0.19	–	10	–	52
Aluminium Foam	0.5	12	12	24	24

Table 2-2: Thermal properties [9]

The thermal properties of any composite are dependent upon its constituent materials. Let us consider the simplest case of an individual lamina comprising of an unidirectional ply in a matrix material. The following notations are universal for each model.
Notations:
k = Composite thermal conductivity [W/mK];
k_f = Fiber thermal conductivity [W/mK];
k_m = Matrix thermal conductivity [W/mK];
V_f = Fiber volume fraction;
V_m = Matrix volume fraction.

According to rule of mixtures [16] , the thermal conductivities in the fibre direction (k_1) and transverse direction (k_2) can be calculated using the following formulae:

$$k_1 = k_f V_f + k_m(1 - V_f) \tag{2-1}$$

$$k_2 = k_m[\frac{k_f(1+V_f)+k_m(1-V_f)}{k_f(1-V_f+k_m(1+V_f))}] \tag{2-2}$$

V_f is the fibre volume fraction; k_m is the matrix material conductivity and k_f is the fibre conductivity. Together k_1 and k_2 are considered as the principal conductivities. All laminae are assumed to be identical in thickness and also in fibre content. The fibre orientation in each individual lamina is varied. These can be used to obtain global conductivities in the x, y and z planes of the individual lamina by:

$$k_x = |k_1 \cos\theta| + |k_2 \sin\theta|[in - plane] \tag{2-3}$$

$$k_y = |k_1 \sin\theta| + |k_2 \cos\theta|[in - plane] \tag{2-4}$$

$$k_z = k_2[out - of - plane] \tag{2-5}$$

2-4 Finite Element Modelling for Composite Structures

Anisotropic materials have properties that vary with the orientation of fibres in a structure. This makes heat transfer analysis much more complex than standard, isotropic materials. The Fourier's Law expands in order to properly govern the conduction [17]. Although it is possible to derive the governing equations and boundary conditions from first principles, it is difficult to obtain any form of analytical solution to such problems. The complexity is due to the fact that the geometry is irregular. Most problems do not allow for a closed form solution of these equations.

As a result, most analysis on anisotropic conduction is carried out numerically. Finite element modelling is a very common method being used for these problems [18]. The focus of this section will be on the Finite Element Methods (FEM) applied to characterize the thermal behaviour of the composites. The fundamental concept of FEM is to subdivide the domain for a problem into small regions; each of these small regions is called a finite element. The process of subdividing a domain into elements is called discretization, or meshing. Elements are attached to one-another at points called nodes. Each node has one or more degrees of freedom. Most finite element software packages subdivide the finite element simulation in three steps:

- Preprocessing : The mesh generation
- Solving the actual FEM
- Post processing: showing the results

2-4-1 PATRAN

NASTRAN is primarily a solver for finite element analysis. It cannot be used for developing a model or meshing. All input and output to the program is in the form of text files. PATRAN is a pre and post processing package for NASTRAN. As seen in Fig 2-3 the analysis part

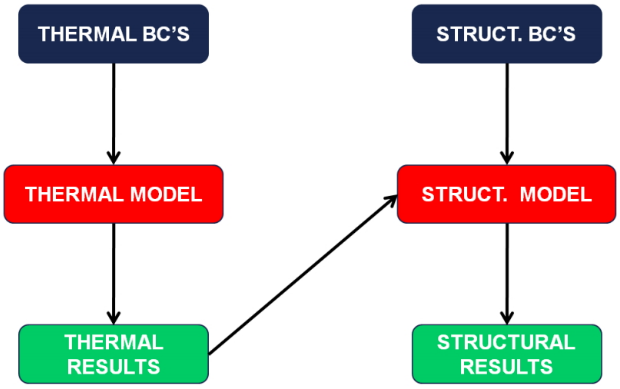

Figure 2-2: Thermo-Mechanical Coupling

is carried out by NASTRAN after receiving input model data from PATRAN and sends the solution to Patran which then is used for post processing and visualizing results.

Building a model for heat transfer analysis in PATRAN can be divided into several steps [19]:

1) Creation or importing of the geometry:

The geometry for a model can be created in Patran or imported from a CAD model.

2) Define the finite element mesh:

The goal of this step is to subdivide the geometry into elements and nodes. Temperatures are calculated at the nodal points in the analysis. Heat transfer processes take place within the elements.

3) Define material properties:

In a steady-state conduction analysis, the thermal conductivity of the materials in the model must be defined.

4) Define element properties:

The elements that define the heat conduction paths in the body can be characterized geometrically as 1D, 2D, 3D, or axisymmetric. All elements have associated material properties. One-dimensional elements must have their cross-sectional properties defined, and shell elements must have their thickness defined. Also, the co-ordinate frames of the elements must be defined properly since the orientation of fibre direction is crucial for composites.

5) Define loads and boundary conditions:

Defining loads and boundary conditions is often the most difficult step in building a model for thermal analysis. In a steady-state analysis, fixed temperatures can be specified at any nodal points in the model. This applies to structural nodal points as well as ambient nodal points. Boundary conditions such as radiation fluxes, applied surface or volumetric heat flux or heat flow are described as thermal loads.

To gain some insight into the behaviour of a complex structure, a simple model should be the starting point. Applying coordinate systems to the elements and symmetric considerations for simplification need to be considered. Discretization (mesh size) should be based on the

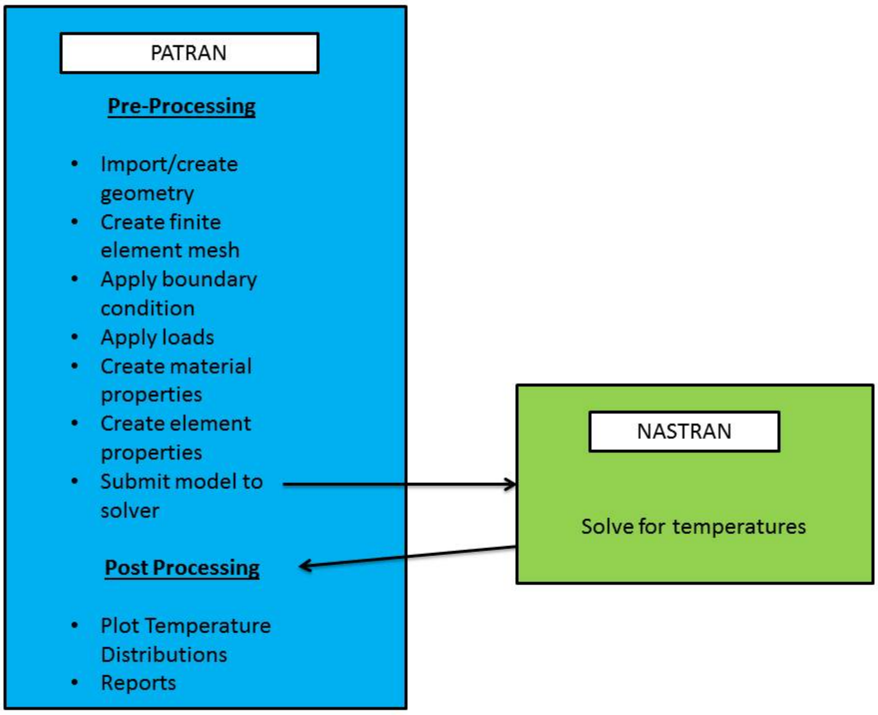

Figure 2-3: FEA Flow Chart.

anticipated temperature gradient. In areas where the heat load is introduced the mesh size has to be reduced. Element types and the mesh size are chosen based on the solution requirements for the particular thermal model. Elements that are highly distorted or stretched i.e., high aspect ratios (ratio of the longest side to the shortest side in the element) need to be avoided.

2-4-2 NASTRAN

This section describes the solution methods implemented for thermal analysis in MSC Nastran. MSC.Nastran utilizes a Newton-Raphson iteration scheme for its solutions [19]. In finite element analysis, the general equilibrium equation is given as :

$$[\mathrm{K}]\{\mathrm{u}\} = \{\mathrm{F}\}$$

where:
[K] = the conduction matrix
{u} = the unknown grid point temperature vector to be solved
{F} = the vector of known heat flows

Applying Newton's method involves the specification of a correction vector

$$\{\psi\} = [K]\{u\} - \{F\}$$

and the approximation of the vanished correction vector at the (i + 1)-th iteration, i.e.,

$$\{\psi\}^{i+1} = \{\psi\}^i + \left[\frac{\partial\psi}{\partial u}\right]^i \{\Delta u\}^i = 0$$

where

$$\{\Delta u\}^i = \{\Delta u^{i+1} - u^i\}$$

is the i-th incremental displacement vector. Rewriting the above equation as

$$[\mathrm{K}_T]^i \{\Delta u\}^i = \{R\}^i$$

where:

$[\mathrm{K_T}] = [\frac{\partial\psi}{\partial u}]$ = the tangential matrix which includes components related to the heat transfer processes

$[\mathrm{R}] = -\{\psi\}$ = the residual vector

At each iteration, the left-hand side matrix $[K_T]^i$ and the right-hand side vector $\{R\}^i$ are computed based on the temperature vector $\{u\}^i$. By solving the unknown vector $\{\Delta u\}^i$, the displacement vector at the (i + 1)-th iteration can be calculated from

$$\{u\}^{i+1} = \{u\}^i + \{\Delta u\}^i$$

The left-hand side matrix is not updated at each iteration since matrix decomposition is time consuming. In case the solution fails to converge or the iteration efficiency can be improved, the tangential matrix is updated. The residual vector is updated at each iteration.

For a steady state analysis the heat balance equation is given by:

$$[\mathrm{K}]\{\mathrm{u}\} + [\mathrm{R}]\{\mathrm{u}+\mathrm{T}_{abs}\}^4 = \{\mathrm{P}\} + \{\mathrm{N}\}$$

where:

$[K]$ = a heat conduction matrix
$[R]$ = a radiation exchange matrix
P= a vector of applied heat loads (temperature independent)
N= a vector of nonlinear heat loads (temperature dependent)
u= a vector of grid point temperatures
T_{abs} = the absolute temperature scale adjustment required for radiation heat transfer exchange or radiation boundary conditions when all other temperatures and units are specified in deg-F or deg-C.

The components of the applied heat flow vector P are associated either with heat generated inside the volume heat conduction or with surface heat transfer elements. The vector of non-linear heat flows results from boundary radiation, surface convection, and temperature-dependent thermal loads. The equilibrium equation is solved by a Newton iteration scheme. The tangential stiffness matrix is approximated by

$$[K_T]^i = [K_T]^i + 4[R]^i\{u^i + T_{abs}\}^3 - \left\{\frac{\partial N}{\partial u}\right\}$$

and the residual vector is

$$[R]^i = \{P\} + \{N\}^i - [K]^i\{u\}^i - [R]^i\{u^i + T_{abs}\}^4$$

2-4-3 Previous Work: Composite FEM Thermal Modelling

This section deals with previous finite element analysis models for thermal design that were developed for composite structures. A few cases where PATRAN/NASTRAN simulations (and one case using ANSYS) have successfully been used to predict the thermal behaviour in composite structures are presented.

Tessler et al.[20] modelled the thermal behaviour of GLARE, a fibre metal laminate developed by Delft University of Technology (TU Delft) for Airbus. The skin consists of 9 symmetrically alternating layers of aluminium and glass fibre epoxy. Since NASTRAN does not support heat conduction in the normal direction of 2D elements, the skin was modelled using solid elements. For the steady state analysis, a quarter of the panel is modelled due to symmetry. A similar analysis was carried out for a fibre metal laminate material plate made from aluminium and CFRP layers using HEX8 elements and the results correlated with the experimental values. The deviation with the experimental results were 6 deg C at maximum. [20]

Boudjemai et al. [21] created the finite element model of a honeycomb sandwich plate with inserts using Patran and carried out the analysis using Nastran. A fully coupled thermal analysis was conducted in order to predict thermal coupling phenomena caused by the adjacent inserts under extreme thermal loading conditions. The inserts were modelled with HEX8 hexahedron structural 3D solid element. In bonded constructions, a very thin adhesive layer is present and it has to be modelled correctly to find the influence of the insert on the panel. To do this, the preliminary analysis is carried on the reference joint geometry using hexagonal shape for the insert and by conserving the real thickness of the adhesive layer and which has the same shape of the honeycomb cell. It was noticed that the clearance and thermal interference between the adjacent inserts has an important influence on the satellite equipments. The representation of the adhesive model for the inserts during the analysis improved the quality of results.

Zhang et al.[22] demonstrated the power of the MSC Nastran as a thermal analysis tool for transient analysis for an antenna reflector. In the thermal modelling of the sandwich antenna structure , the top face sheet, honeycomb core and bottom face sheet is simulated by a 3 layer model. The conductivity effect of the adhesives was considered. The thermal control coating on the top face sheet was also modelled. The aluminium honeycomb core was regarded as an equivalent continuum layer. Approximations were performed to calculate the effective thermal property parameters of each layer. The view factors were calculated by means of the VIEW3D module of MSC Nastran. In this model, the face sheets were simulated by the triangular and the quadrilateral heat conduction plate elements and the honeycomb core was simulated by hexagonal and pentagonal heat conduction solid elements. In order to calculate the radiation exchange, the surface elements were added on the surface of the reflector.

Brader et al.[23] performed the thermal analysis of their CFRP electronics housing with ANSYS using soild elements. Solid thermal elements are normally used to model OOP direction temperature gradients. Typically, thermal shell elements have only one degree of freedom per node. Their test model was a composite plate consisting of uni-directional plies. All plies are oriented in the longitudinal direction. There are two K1100 plies (thickness 0.2 mm) on the surfaces and six M40J plies in the middle of the laminate. The thickness of the laminate is 2 mm. Only conduction was considered. They demonstrated that the temperature distribution is very constant already at the end where heat is generated. They also demonstrated that single-layer elements are adequate for thin laminates in steady state thermal analysis. [23]

2-5 Thermal Management Solutions

There have been attempts to integrate the functions of a thermal subsystem within the structure and make it multifunctional. As stated earlier, one of the goals of developing structures with advanced composite materials is to utilise their material properties to perform more than just the load bearing function. Multifunctional structures are broadly defined as structures that support additional tasks that may be unrelated to basic mechanical load carrying [24]. A multifunctional composite structure bus (MFCBS) that incorporates thermal management is a worthy area of research in the current generation of composite satellites structures that are being developed. Very little information is available regarding the thermal design of most of the missions that flew with a MFCBS [25]. This is attributed to the proprietary development processes of most of the composite developments carried out in contractor companies. Nevertheless, a few concepts that have flown and under development are discussed in this section.

2-5-1 High Conductivity Fibres

Using an effective conduction path to conduct heat to a radiator is a simple thermal management solution that can be implemented in small spacecraft. Mightysat II had panels with fibres that were designed to distribute the thermal loads throughout the spacecraft via thermal spools which then dissipated the heat to radiator panels. Conductivity in the OOP direction of a laminate comprising of high conductive fibres is low. A novel solution has been proposed as a particular patented design by Roberts et al. which mentions, locally increasing the OOP thermal conductivity and then allowing the high thermal conductivity fibres to spread and orient the heat flow to a heat sink. [26]

Brander et al. [23] designed a CFRP housing based on high conductivity fibres. Pitch-based K1100 carbon fibers were selected for thermal energy management. They were able to gain 29% in mass savings compared to an aluminium enclosure with two times the improvement in thermal conductivity. Table 2-3 shows us the comparison of high conductivity fibres with aluminium.

2-5-2 Thermal Inserts

The team that developed the STSAT-3 all composite structure has also investigated the use of pitch-based high-thermal conductivity fibres and additional core filling for thermal

Material	Fibre Lay-up Orientation	Fibre Volume (%)	Density (g/cm^3)	k_x (W/mK)	k_y (W/mK)	k_z (W/mK)
Aluminium 6061	Isotropic	N/A	2.70	170	170	170
K1100 carbon polymer	Unidirectional	60	1.84	595	1	1
K1100 carbon polymer	0 deg/90 deg	60	1.84	277	277	1
K1100 carbon-carbon	6:1 fibre ratio	55	1.80	700	55	50
K1100 carbon-carbon	1:1 fibre ratio	55	1.80	450	450	59
K321 carbon-carbon	4:1 fibre ratio	50	1.75	368	97	45
K321 carbon-carbon	1:1 fibre ratio	50	1.75	201	200	32

Table 2-3: High Conductivity Fibre comparison to Aluminium [8]

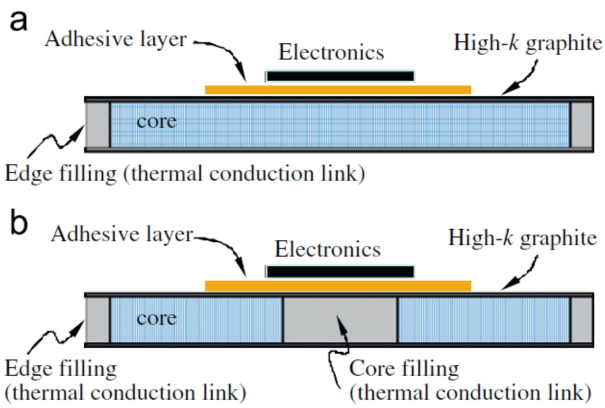

Figure 2-4: Passive thermal control with high thermal conductive fibre and thermal link:(a) edge filling and (b) core filling. [3]

management of the Spacecraft (S/C) as shown in Fig 2-4. This approach is effective to dissipate the heat generated by the high-density electronics circuitry which is bonded on the honeycomb core panel. In order to provide thermal conduction paths and isothermal areas within a single panel, John et al.[25] designed a multifunctional panel with embedded inserts . A thermal pyrolytic graphite insert is embedded into a low conductivity composite moulding compound. The graphite has an in plane conductivity of 1500 W/mK and a density of 2.26 gm/cc. When compared to aluminium, the pyrolytic graphite has 20% lower mass and provides 8.5 times the thermal conductivity. The L shaped conduction path is used to tie a component mounting spot to the spacecraft primary structure or a radiator. Since there is only low conductivity material elsewhere, the area around the graphite insert is thermally isolated.

2-5-3 High Conductivity Core Foam

Increasing the conductivity of the core material is a challenging task. Since the overall through thickness conductivity of a composite construction is low, primarily because of the thermal properties of the core, enhancing this aspect has proven to be useful. A solution proposed by Roy et al.[27] involves the use of carbon foams which can be tailored to have low or high thermal conductivity with a low coefficient of thermal expansion (CTE) and density. The graphitic foam offers the highest thermal conductivity among all carbon foams (125 W/mK). Once it was adhesively bonded the overall thermal conductivity fell to 19 W/mK for the co-cured and 6 W/mK for adhesive bonded panels.[27]

A team led by Klett et al. [9] also proposed the use of graphitic foams for heat sinks. They used ARA Mesophase pitch-derived carbonized foam at 1000^{o}C and ARA Mesophase pitch-derived graphitized foam at 2800^{o}C. For a linear increase in density from 0.27 to 0.57 g/cm^3, the thermal conductivity of the graphitized foams varies linearly from 50 to 150 W/mK. The specific thermal conductivity is around 300 W/mK and is more than six times greater than copper and five times greater than aluminium, the preferred materials for heat sinks.

Chapter 3

MASCOT Landing Module

This chapter describes the MASCOT Lander Module, the structural design and thermal subsystem.

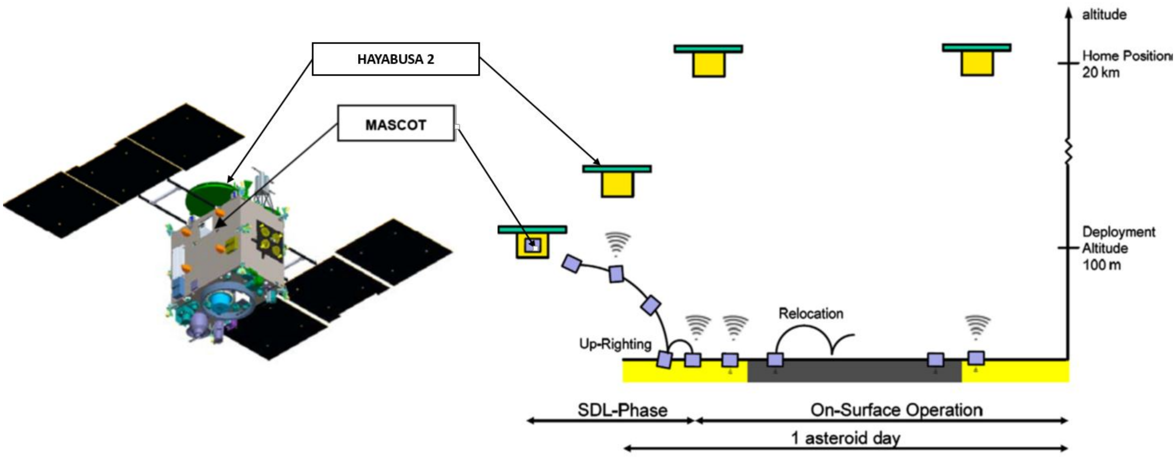

Figure 3-1: Hayabusa 2 and MASCOT mission profile [4]

The DLR Mobile Asteroid Surface Scout (MASCOT) is an approximately 10 kg shoebox-sized lander platform developed in cooperation with CNES and JAXA for the Hayabusa 2 (HY-2) sample return mission heading to the Cg-class asteroid 1999 JU3 (Named 'Ryugu'). MASCOT is dedicated to support HY-2 with landing site selection and to enhance it with in-situ surface science capabilities.

The main scientific objectives of the MASCOT Landing Module are [1]:

- "Characterization of the geological context of the surface.
- Detection of any global magnetization.

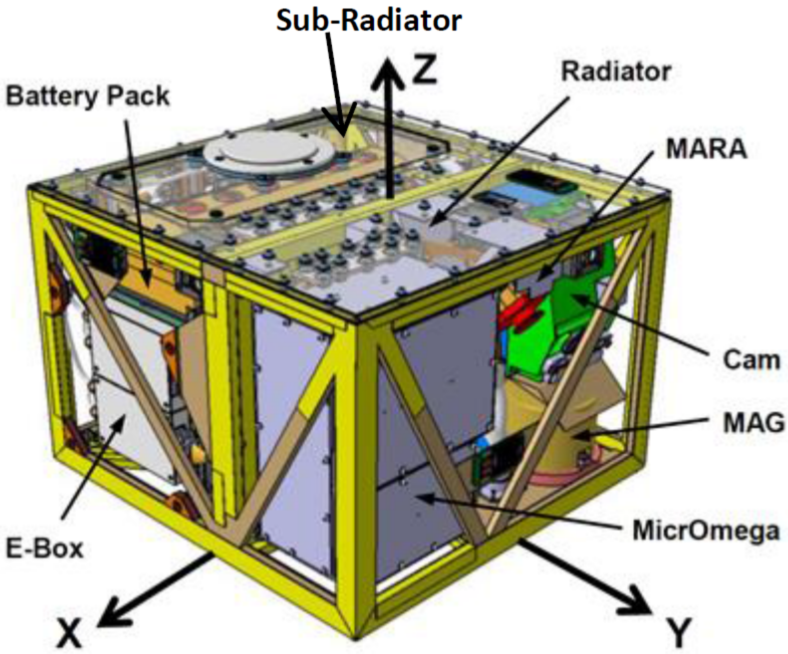

Figure 3-2: MASCOT and its Payloads [1]

- Characterization of the composition of the surface and near-surface to subsurface material, including minerals, organics and,possibly, near-surface ices.

- Characterization of the surface thermal environment and the regolith thermophysical properties."

The last phase of the Hayabusa-2 mission involves the on-surface operations of the MASCOT Landing Module on the asteroid. After reaching the target asteroid, MASCOT is released by HY-2 at a low height, lands and starts scientific investigations on the surface (see Fig 3-1). Therefore MASCOT carries four instruments: MicrOmega (near-infrared hyperspectral microscope), Cam (camera in visible range), MARA (radiometer) and MAG (magnetometer). It also houses the lander's common electronic box (EBox); the battery pack is attached to it at one end and is connected to the sub-radiator, a separate section of the radiator on the other. (Fig 3-2)

The MASCOT system itself is subdivided in two main structural parts (see Fig 3-3), the box-shaped Lander Module (LM), housing all experiments and sub-systems, and the surrounding Mechanical and Electrical Support Structure (MESS). Both are constructed as highly stiff and lightweight composite framework structures having together a total mass of around 1.4 kg. The LM alone has a mass of 550 g. [4]

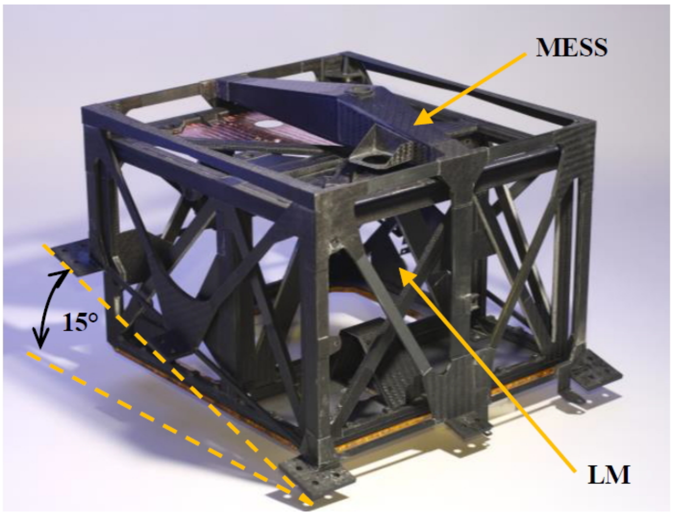

Figure 3-3: MASCOT and MESS [5]

3-1 Structural design

The structural design of the MASCOT landing module is developed as a highly integrated and ultra-lightweight load bearing framework made of CFRP-foam sandwich. The landing module's physical dimensions are 275 mm x 290 mm in area and 195 mm in height. MASCOT's entire structure consists of four external side walls, one internal vertical/middle wall, the base plate and finally a top plate, as can be seen in Fig 3-4

The LM Walls are made of one UD-CFRP facesheet ply M55J/LTM123 of thickness 0.125 mm sandwiching a foam core (Rohacell IG-31F) of thickness 5 mm. The LM Wall Connectors (Shear Straps) of 0.2 mm thickness are made of of M40J/Scheufler L160-H163. All walls and the baseplate are connected via $\pm 45^o$ M40J CFRP fabric mainly for shear load transfer. The cross section of a truss member is shown in Fig 3-5. The bottom corners are reinforced by a kind of edge/corner cap that keeps the framework walls aligned to each other and the delicate UD-trusses loaded in the strut's along-direction axis. The load bearing interface points for the instruments/EBox are connected with CFRP fabric as well.[4]

The main and sub-radiator are fixed to the side walls/inner wall respectively and to the the battery pack via screws. The same applies for the MARA support platform. Therefore the radiators and the support platform have through holes and the nuts are glued on. All payloads or rather scientific instruments and the EBox are directly bolted to the structure. MicrOMEGA and CAM are directly connected to the inner wall. Only MARA is as already mentioned, mechanically supported by an additional platform, which is bonded/bolted to the structure. MAG is connected to the base plate via a supporting plate, due to its required position inside the lander. The removable radiator plate is designed as an aluminium sandwich, mounted with screws to the other walls. [5]

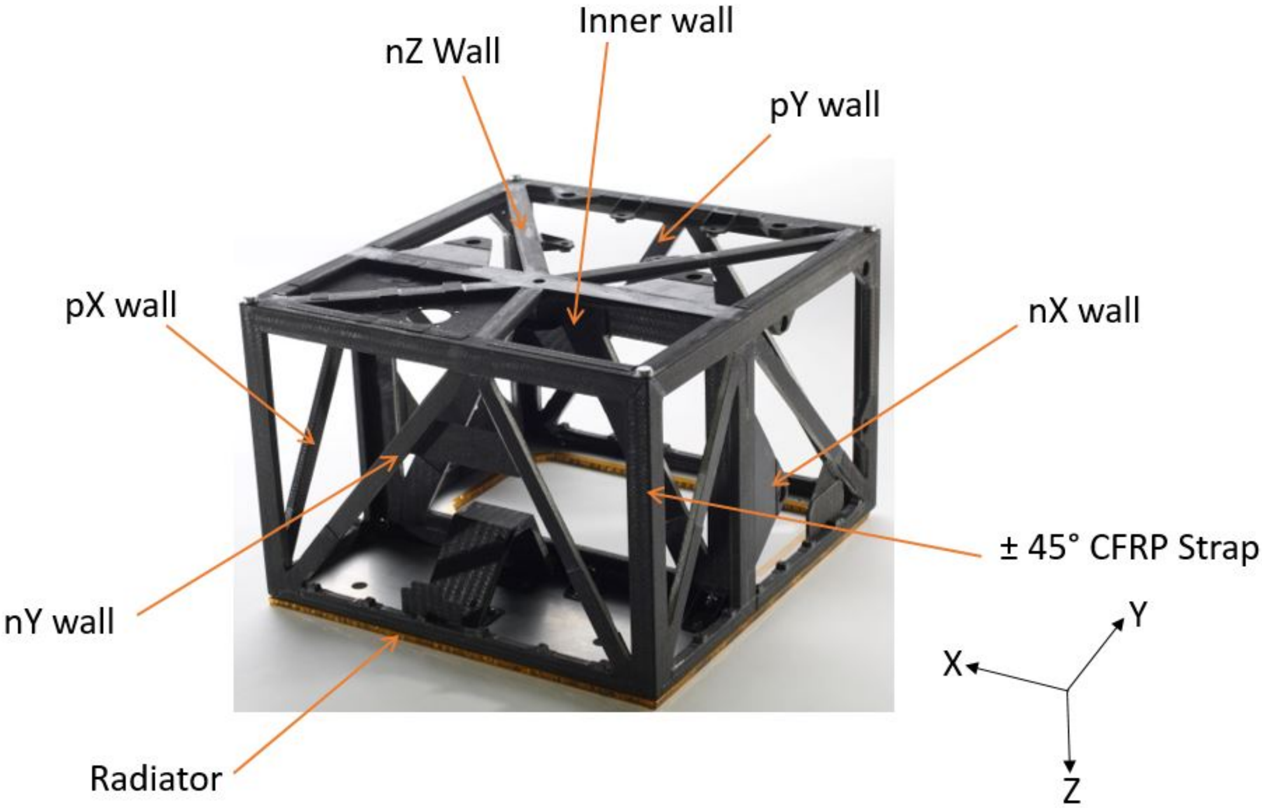

Figure 3-4: MASCOT Structure

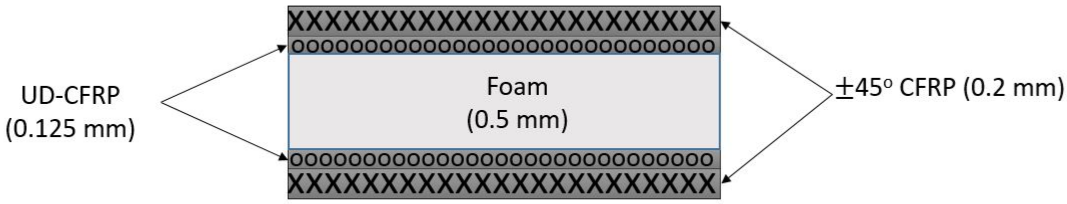

Figure 3-5: Structural member cross section

3-2 Thermal Design

The thermal design can be considered semi-active. For the cruise phase, since the LM is attached to Hayabusa 2 spacecraft, heaters powered by HY-2 are used in the cruise condition. The passive components come into play during the on surface operations. The passive system comprises of optical face sheets, multi-layer insulation and two constant conductance heat pipes carrying the thermal loads to the radiator. The design of the all composite structure was influenced by the thermal management subsystems and its placement.[28]

Due to the very short lifetime of the mission and the restricted energy available, the MASCOT thermal control system is mainly passive, i.e., using coatings and paintings as well as MLI. The only active part of the thermal design is the heater, which will be used both to grant the survival temperature of the battery during cruise and to preheat MASCOT up to the switch-ON temperature before the commissioning phases as well as shortly before landing. MASCOT survival during cold cruise phases and maximum heat rejection during on-surface phase is obtained in two ways: point distribution of the available heating power on the most critical parts and variable conductance heat pipes from the electronic box (the most dissipative element) to the radiator. The lander thermal design has a mainly passive approach, focusing on coatings selection, interfaces tuning and insulation. MLI blankets are used where space is available: to partially insulate the electronic box from the rest of the lander creating a hot compartment. [29]

3-2-1 Thermal Subsystem Mass

The approximate mass of the components of the thermal subsystem on the LM relevant to the on-asteroid phase are mentioned in Table 3-1.

Item	Mass (g)
Heat Pipe A	129
Heat Pipe B	110
Heat Pipe Thermal Foils	1.5
Heat Pipe Bolts	17
MLI EBox	72
Radiator	200
Total Mass	529.5

Table 3-1: Thermal Subsystem Mass Budgets [10]

3-2-2 Payloads and Subsystem Temperature Requirements

During launch, flight, landing and non-operational periods the payloads (P/L) and subsystems have to be kept within their non-operational temperature requirements while during surface operation all instruments must function within their operative temperatures range. The temperature requirements for mission critical components are given in Table 3-2.

Instrument/ Subsystem	Temperature Requirements (deg C)			
	Minimum non-operative	Minimum operative	Maximum operative	Maximum non-operative
Structures	-100	-100	120	120
Ebox	-55	-40	70	70
Battery Pack	-40	-40	70	70
P/L 1	-50	-40	20	50
P/L 2	-80	-55	85	125
P/L 3	-100	-100	85	85
P/L 4	-80	-80	60	60

Table 3-2: Temperature Requirements [10]

Chapter 4

Thermal Model Development

This chapter seeks to describe the modelling process that is carried out to achieve an accurate thermal characterization of the MASCOT LM structure.

As a first step, a unit cell (local model) that can be used to represent the MASCOT structure is modelled and the options available in Patran for composite thermal simulation are evaluated. The most ideal approach for modelling is then adopted for converting the baseline MASCOT structural model into the thermal model. The modelling method and the challenges faced are described.

4-1 Unit Cell Modelling

Before working on the MASCOT model, the modelling approaches that could be adopted in Patran needs to be identified. Hence, a unit cell approach is devised. A unit cell is any small section of a structure that can be used to represent the full structure. This is also called as a coupon in the field of structural engineering. Before performing any large scale tests, small sample blocks of the test specimen undergo coupon level tests. These enable the engineer to gauge the behaviour of a structural model and a preliminary understanding of the mechanics at play on a small scale. The coupon level behaviour can be scaled up to represent the performance of a large scale structure in the real world scenario in most of the cases.

The common layup in the MASCOT structure is the ± 45/UD/Foam/UD/± 45 layup. The initial goal is to determine the best method to convert a structural composite model to one that could simulate 3D temperature fields with reliable accuracy. The reason for insistence on accurate modelling is because when developing structure integrated thermal subsystems, characterizing the behaviour of the composite material and determining the thermal paths in the structure with accurate prediction of through thickness temperatures is necessary. Based on the literature study performed, three approaches to developing the thermal model from the structural model are investigated and are described below. The best method is then adopted based on the requirements that have been put forward initially.

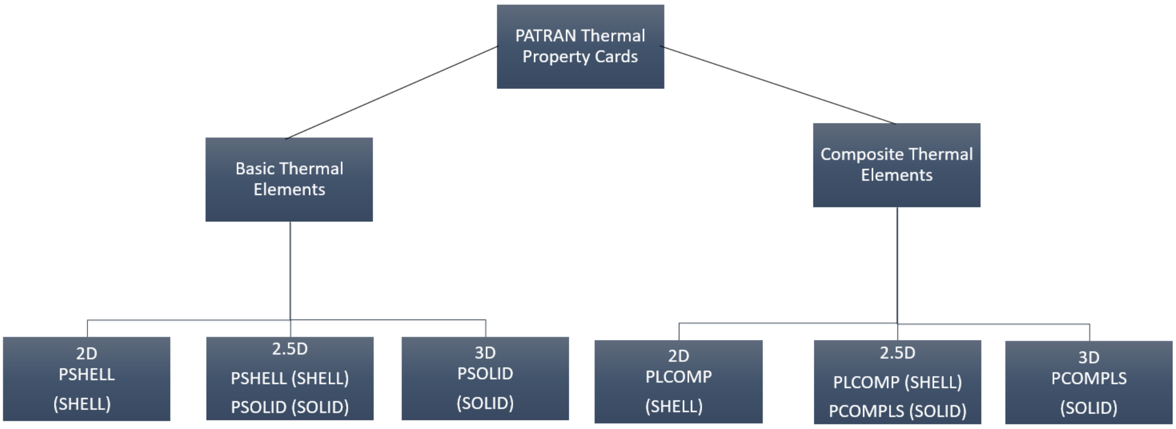

Figure 4-1: Modelling methods and associated PATRAN Property Cards

As explained in Section 2.5, Patran offers the ability to use 1D,2D or 3D elements based on the requirements of the simulation. Every element defined in the model is assigned a property card. These property cards within Patran allow us to define the formulation of the element. The formulation can be chosen based on the type of simulation to be carried out. There are the default element property cards (PSHELL and PSOLID) that are normally used for thermal analysis. But a few advanced composite property cards (PLCOMP and PCOMPLS) are provided in the software that can be exclusively used to simulate the thermal behaviour of composites and obtain results with accuracy including through thickness temperatures. These element formulations can be invoked by assigning the respective property cards to the elements in the Nastran input file. (see Fig 4-1).

All the thermal analyses for composites carried out previously as discussed in Section 2-5-1 were performed by using the default basic thermal elements. In all those cases the number of plies modelled were low. Hence, each layer is explicitly modelled and the basic thermal elements are enough for carrying out these analyses. For e.g., in case of a single ply laminate it is easier to use the PSHELL and PSOLID property cards since there is no need for invoking the advanced composite elements through the Patran Laminate Modeler. The steps involved in creating a layup using the Patran Laminate Modeler are shown (see Fig 4-2). When using the Patran Laminate Modeler, the composite thermal element property cards are assigned when creating an analysis model. When dealing with laminates with multiple plies, using composite thermal elements is desirable since Patran automatically assigns material properties to the composite thermal elements for every ply that has been created in the layup process.

In order to evaluate all the approaches for the unit cell modelling two cases of modelling composites are considered.

- Case 1 : Uni-Directional (UD) ply.
  Before assessing the thermal behaviour of a foam sandwich laminate, the extent to which the modelling methods influence the thermal behaviour are assessed on a single ply first. This gives an initial understanding of the solution approach that needs to be considered

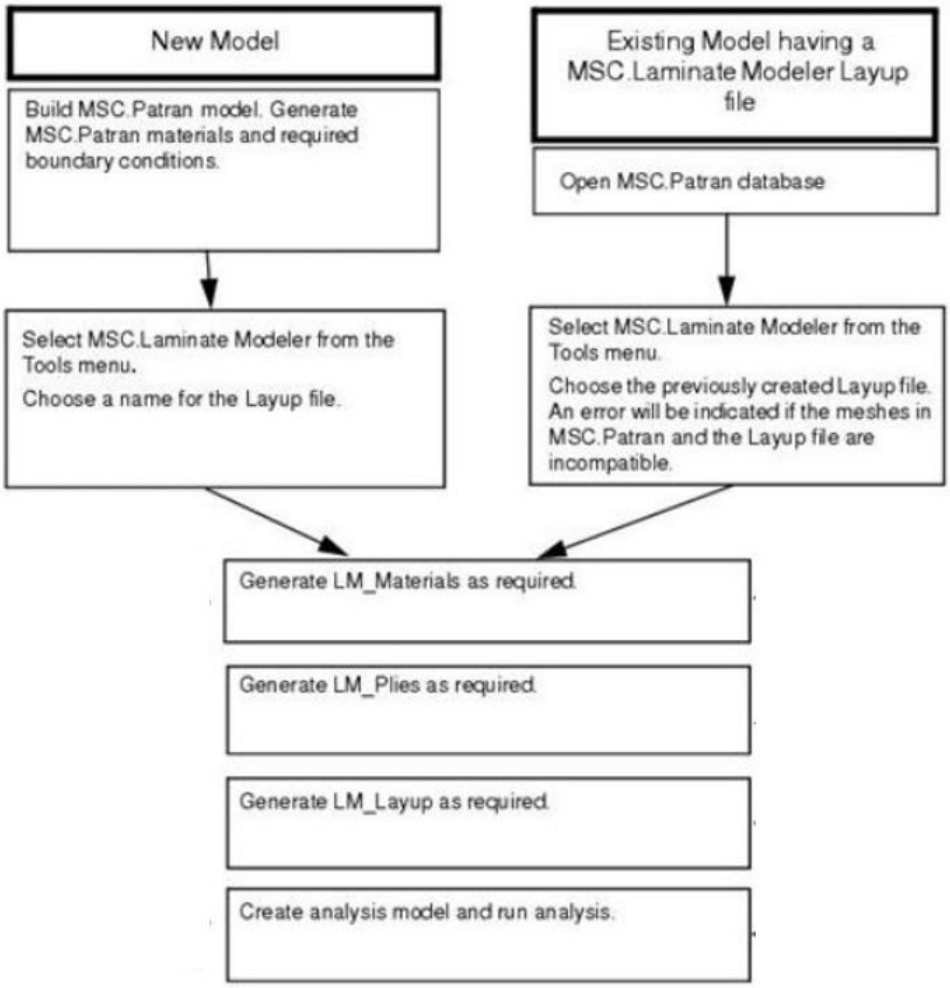

Figure 4-2: Laminate Modeler Process

while modelling. The single ply is modelled by applying the material properties directly to the elements present in the model. The Composite Laminate Modeler is not required to apply a layup since in this case there is only a single ply. If the laminate modeler is not used then the properties for the elements need to defined manually. Patran then creates property cards for the basic thermal elements. (PSHELL: for shell elements and PSOLID: for solid elements).

- Case 2 : Foam Sandwich
  The foam sandwich represents a section of the actual MASCOT structure. Hence the same methodology that was followed while developing the MASCOT structural model are followed. First, the rectangular geometry is meshed and the Composite Laminate Modeler is used to declare the materials and the plies. The layup is then defined and Patran automatically assigns properties to the elements based on the laminate properties entered into the model. The property cards assigned to the elements in this case are PLCOMP: for shell elements and PCOMPLS: for solid elements.

Using the unit cell models described in the previous section, (which is based on the 2D structural model) three different modelling techniques are investigated in order to derive a representative thermal model. The analysis setup is carried out for steady state. The mesh size that was used for the unit cell analyses are derived from the mesh size of the MASCOT structural model. For defining a simple boundary condition, a heat load of 1W is applied on one end of the unit cell and the other end is fixed at 0 deg C.

4-1-1 2D Modelling

As described earlier, the structural model comprises of 2D shell elements. A 2D shell element does not have the capability to simulate through thickness temperatures. The default composite shell elements with PCOMPG property card used for structural analysis cannot be used for thermal analysis. As an alternative, Patran offers 2D solid elements with the PLCOMP property card that have the capability to calculate the through thickness temperatures in composite laminates. Property data of upto 1024 layers in a laminate can be used in the model for the simulations. By assigning the 2D Solid to the existing 2D shell elements it is possible to adapt the mesh for carrying out thermal analysis for the laminate. The model was created by meshing a rectangle geometry of dimensions 10mm x 30mm. The mesh was created with 30 Quad4 shell elements. (see Fig 4-3)

4-1-2 2.5D Modelling

The 2.5D method refers to a hybrid modelling method whereby 3D solid elements are used at critical areas of interest in the structure. These critical areas can be defined as places where the heat load is introduced and through thickness temperatures need to be determined. And the rest of the structure is modelled using the 2D shell elements. The 3D elements could be generated by simply extruding the shell elements at the desired locations using the "Display Shell Thickness" option in Patran which then creates PSOLID Hex8 elements without any properties assigned to them. This is useful if a single ply is used. In case of a multiple ply laminate, the Patran Laminate Modeler is used to generate the 3D elements from the 2D

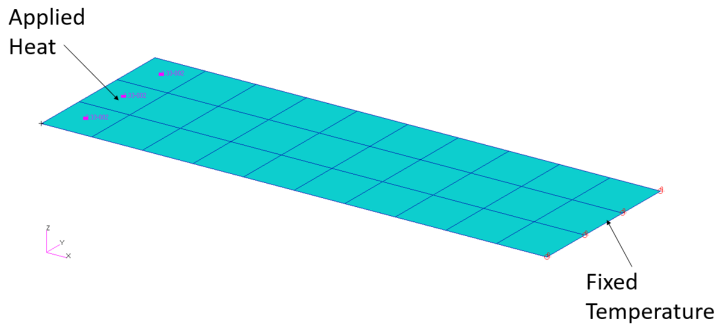

Figure 4-3: 2D model

shell elements. The material properties are then automatically assigned to all the elements through the PCOMPLS property card. 16 Quad4 elements in the middle of the model are chosen for extrusion into Hex8 elements.

Patran offers the option of defining a contact body pair between two different objects. This is used to pair a 2D shell element to the 3D solid element. This method does not work for thermal simulations at the moment although Patran extended the body pair to simulate thermal contact apart from the structural contact. The solver does not run when declaring two bodies in thermal contact. Hence, another method is devised whereby 1D conductor elements are used as interface elements to connect the 2D shell nodes to all the 3D element nodes of the face the 2D element is in contact with. The interface elements are then assigned a high conductivity value to ensure that there is no heat transfer loss at the interface nodes. (see Fig 4-4)

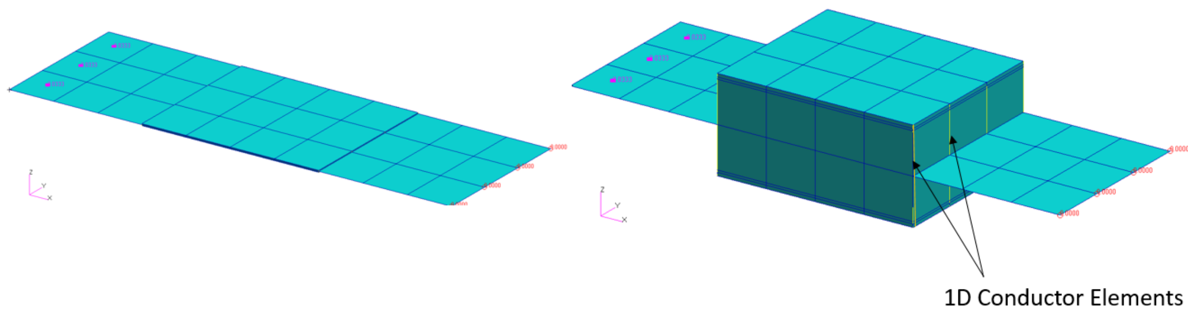

Figure 4-4: 2.5D model : Case 1 (L) & Case 2 (R)

4-1-3 3D Modelling

The most straightforward approach to create a 3D model from the 2D shell element model is to extrude all the shell elements. For case 1, this was achieved by using a function called "Display Shell Thickness" in Patran. In case of a composite layup, the material properties are assigned using the Laminate Modeler which then assigns the PCOMPLS property card to the elements. Either a single element can be used for the entire laminate or an element per ply can be generated during the extrusion process. According to Sproewitz et al. [30] and Wallin et al. [23], it is enough to use one element per layer to obtain accurate results for through thickness temperature plots. Also, if more elements per layer need to be created, the shell element size from which the solid elements are generated need to be smaller. This is because elements with bad aspect ratios will be created. An aspect ratio is the length of the element to its thickness. An aspect ratio of more than 100 will lead to inaccurate results [19]. Therefore, only one layer per element is used for the analysis and is sufficient. (see Fig 4-5)

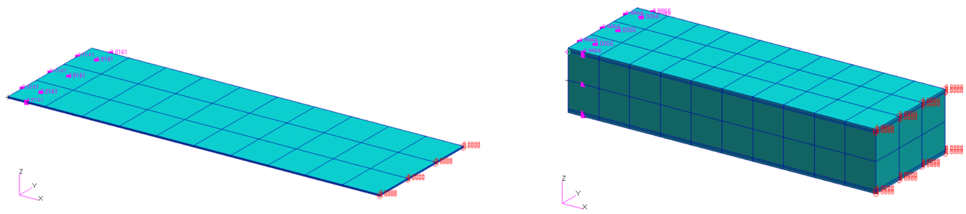

Figure 4-5: 3D model : Case 1 (L) Case 2 (R)

4-1-4 Results

Case 1 : UD ply

By comparing the results of the three approaches for Case 1, it is seen that there is almost no difference in the temperature fields in all the 3 approaches. (Table 4-1) (Fig 4-6, Fig 4-7, Fig 4-8). Although accurate, the 2D model does not allow us to determine through thickness temperatures. The hybrid model allows us to determine through thickness temperatures at specific locations as required. The solid model allows the through thickness temperature distributions throughout. Since only a single layer laminate is simulated, the material assignment is performed manually to the Hex8 elements to generate the PSOLID property card.

Case 2: Foam Sandwich

Comparing the results from the three approaches for Case 2, it is inferred that the three methods do not provide the same results. During the evaluation of the various approaches, in Case 2, a bug was discovered in the 2D Solid PLCOMP and the 3D PCOMPLS elements that are generated from the pre-existing mesh using the Patran Laminate Modeler. The bug involves the temperature gradients (T-Z) and fluxes (F-Z) in the element-normal direction that are calculated in the output (see Fig 4-12). Irrespective of the corresponding input parameters,

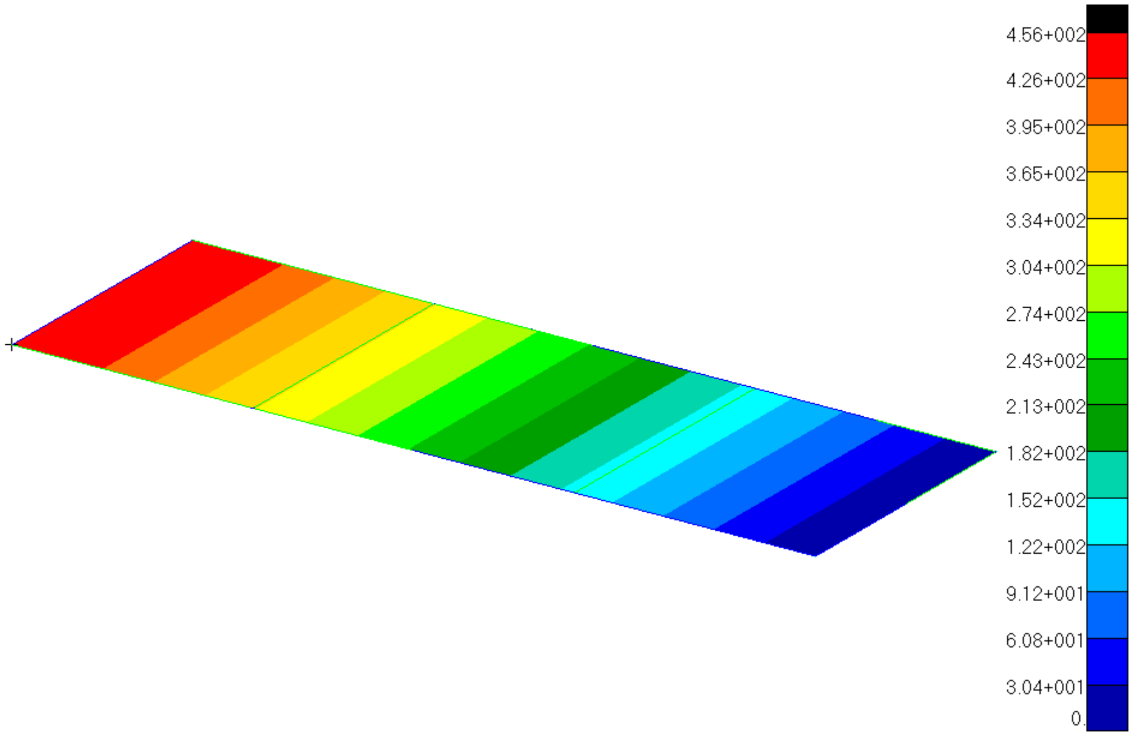

Figure 4-6: Temperature plot : Case 1-2D model

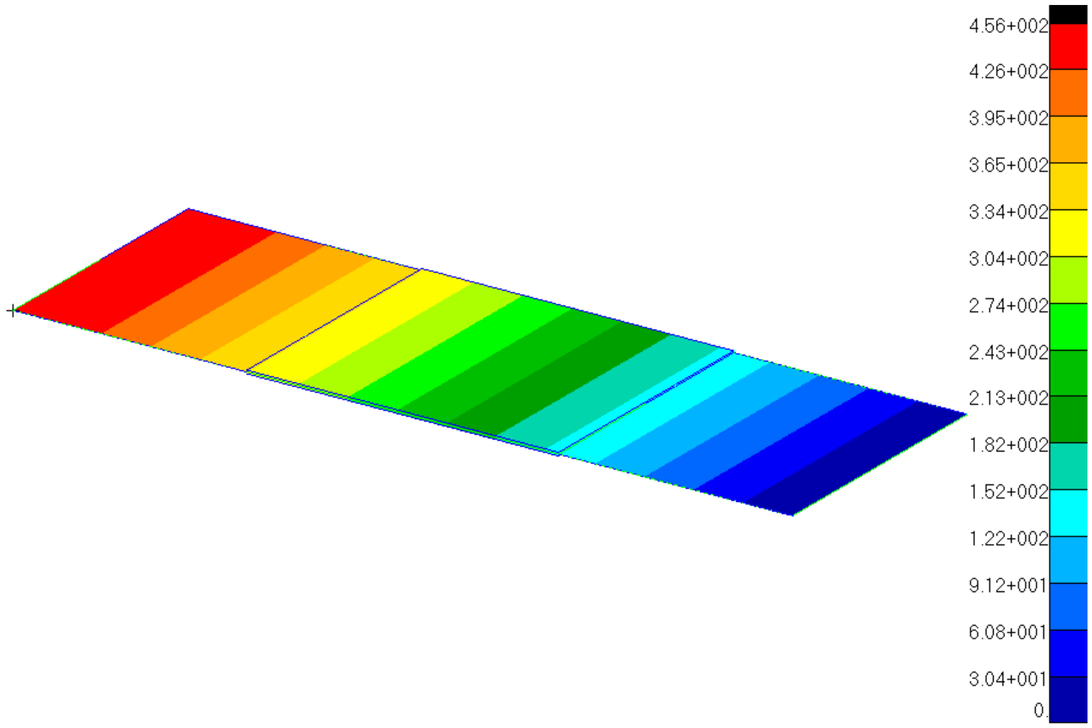

Figure 4-7: Temperature plot : Case 1-2.5D model

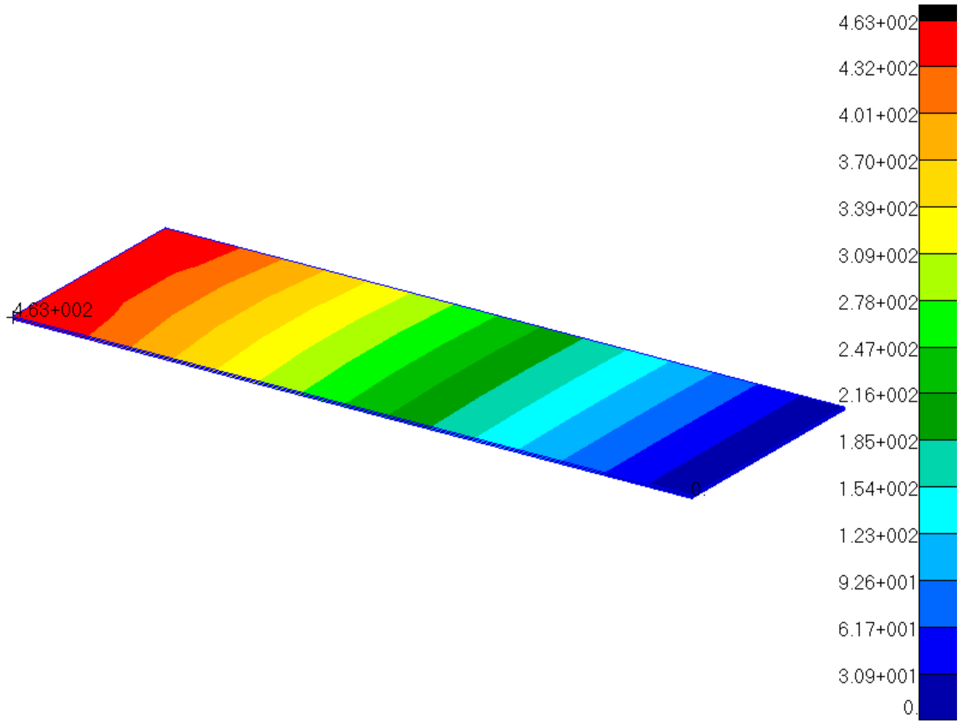

Figure 4-8: Temperature plot : Case 1-3D model

Location	Temperature (^{o}C)		
x (mm)	2D	2.5D	3D
0	45.6	45.6	46.3
3	43.2	43.2	43.8
6	38.4	38.4	38.2
9	33.6	33.6	33.9
12	28.8	28.8	29
15	24	24	24.2
18	19.2	19.2	19.3
21	14.4	14.4	14.5
24	9.6	9.6	9.64
27	4.8	4.8	4.82
30	0	0	0

Table 4-1: Temperature Field Comparison: Case 1

the output for these values was always zero. Clarification with the MSC Corporation that develops the PATRAN/NASTRAN software resulted in confirmation of the existence of the bug. The advanced 2D and 3D composite elements (PLCOMP and PCOMPLS) thus cannot be used for the analysis till the bug is fixed. The basic PSHELL elements do not have the ability to simulate the thermal behaviour of multiple ply composites as mentioned earlier. Hence, a 2D model or a hybrid 2.5D model cannot provide the desired results to meet the research objectives. Therefore, basic 3D PSOLID elements need to be assigned. The 3D

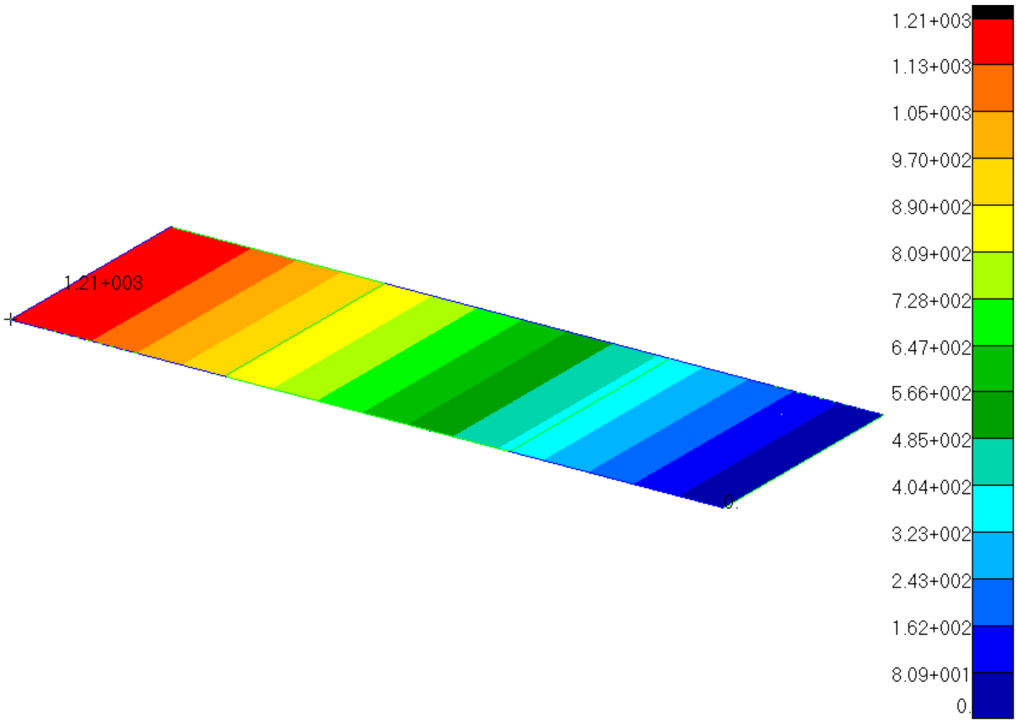

Figure 4-9: Temperature plot : Case 2-2D model

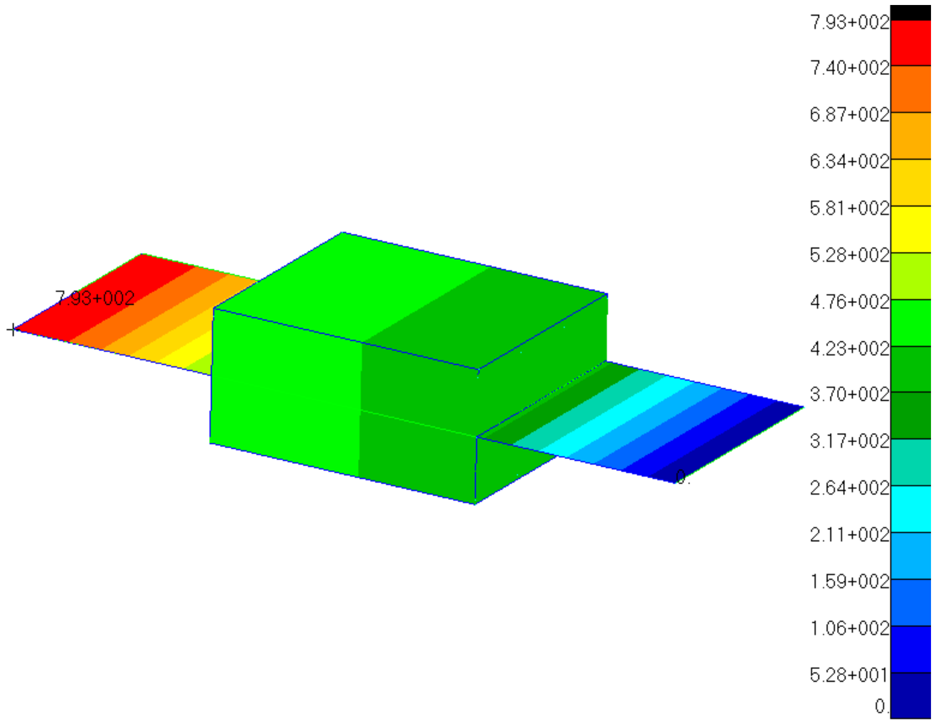

Figure 4-10: Temperature plot : Case 2-2.5D model

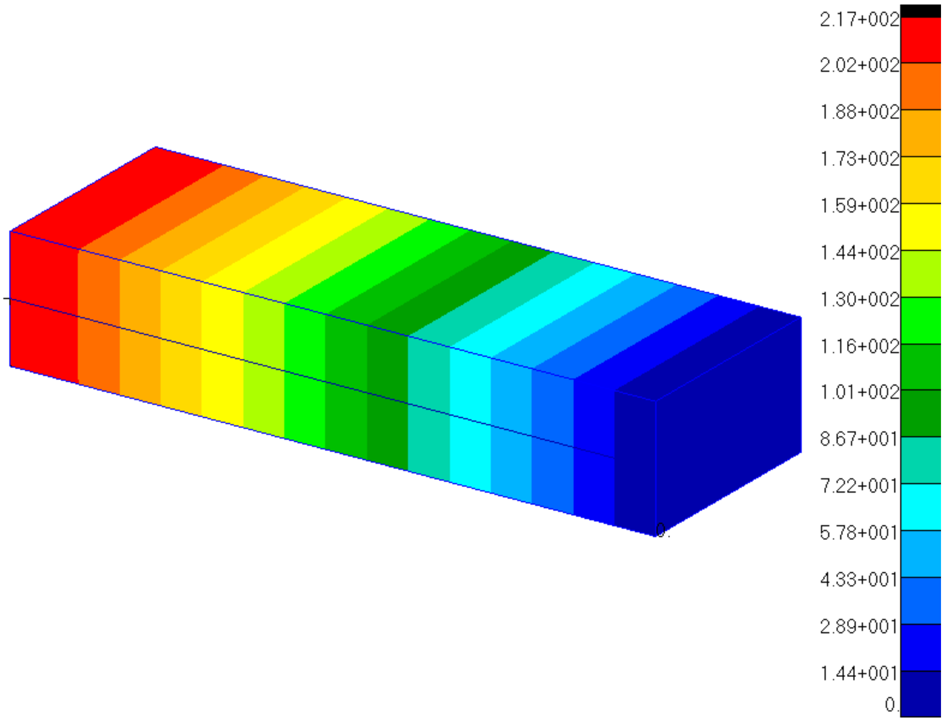

Figure 4-11: Temperature plot : Case 2 3D model

G R A D I E N T S   A N D   F L U X E S   F O R   L A Y E R E D   C O M P O S I T E   E L E M E N T S

ELEMENT ID	PLY ID	INTEG. POINT ID	T-X	T-Y	T-Z	F-X	F-Y	F-Z	T
			-------G R A D I E N T S			----------------F L U X E S			----T E M P-
1	1001	1	-2.128E+01	7.980E-06	0.000E+00	3.192E-02	-1.197E-08	0.000E+00	1.200E+03
		2	-2.128E+01	8.060E-06	0.000E+00	3.192E-02	-1.209E-08	0.000E+00	1.163E+03
	1002	1	-2.128E+01	7.980E-06	0.000E+00	1.064E+00	-7.980E-09	0.000E+00	1.200E+03
		2	-2.128E+01	8.060E-06	0.000E+00	1.064E+00	-8.060E-09	0.000E+00	1.163E+03
	1003	1	-2.128E+01	7.980E-06	0.000E+00	7.448E-04	-2.793E-10	0.000E+00	1.200E+03
		2	-2.128E+01	8.060E-06	0.000E+00	7.448E-04	-2.821E-10	0.000E+00	1.163E+03
	1004	1	-2.128E+01	7.980E-06	0.000E+00	1.064E+00	-7.980E-09	0.000E+00	1.200E+03
		2	-2.128E+01	8.060E-06	0.000E+00	1.064E+00	-8.060E-09	0.000E+00	1.163E+03
	1005	1	-2.128E+01	7.980E-06	0.000E+00	3.192E-02	-1.197E-08	0.000E+00	1.200E+03
		2	-2.128E+01	8.060E-06	0.000E+00	3.192E-02	-1.209E-08	0.000E+00	1.163E+03

Figure 4-12: Sample Output for PLCOMP/PCOMPLS elements

PSOLID elements are most commonly used to simulate composite material thermal behaviour in all the literature that deals with through thickness temperatures.[30]

To create PSOLID elements from the structural model shell elements, the Patran Laminate Modeler provides an option for extruding the shell elements into solid elements. Although this process creates PCOMPLS solid elements by default, an option is provided to not assign the PCOMPLS property card to the solid elements created while extruding. When not assigning PCOMPLS to the 3D elements, the extrusion gives PSOLID elements without any material property assigned to them. Each ply in the structure has to be matched with their respective material and coordinate frames respectively in a manual approach.

Impact on MASCOT Model Development

Initially to decide the modelling approach that needs to be adopted for the full scale modelling, a trade-off analysis was carried out with a weighted decision matrix based on the results of the unit cell modelling. Four criteria for assessing the methods are formulated. The first one is the Accuracy, which is determined by the ability of the model to predict the temperatures (including through thickness temperatures) accurately. The second being the Computation Time. It is directly proportional to the number of nodes in the model. Third comes the Adaptability which defines the ease with which the model's properties can be changed based on the requirements. Finally the Model Development Time is also considered as certain modelling methods can take a lot more time than the others. Based on their relevance to the simulation, the selected criterion are allocated weights on a scale of 1 to 4 in an increasing order. Each method is awarded a score ranging from 1 to 4, based on its performance with respect to the criteria. The total points scored by each method is the sum of the products of its individual score for a criteria and the weight of the criteria (Table 4-1). From the trade-off table it is concluded that 3D modelling is the most optimal approach for carrying out the thermal analysis on the MASCOT structure.(Table 4-2)

		Modelling Method		
Criteria	Weights	2D	2.5D	3D
Development Time	1	3	2	1
Accuracy	4	1	2	3
Computation Time	3	3	2	1
Adaptability	2	1	2	3
Score		18	20	22

Table 4-2: Trade off matrix

For 3D Modelling, the unavailability of PCOMPLS and PLCOMP property cards meant that only PSOLID elements without material properties need to be extruded and the material properties per ply need to be individually selected and assigned. There are almost 200 individual plies in the entire structure in different orientations and each ply has to be individually assigned the material properties by selecting the exact elements of the ply they belong to. This can be done only one ply at a time since the plies lie one above the other. After material property is assigned to a ply it is hidden using the plot/erase function in Patran and the next visible layer is assigned its material property. Complications might arise in junctions where plies from different structural members meet. In such cases, the ply layup sequence is used as a source of information. Hence straight sections are isolated first and the junctions are dealt with in the end for every wall of the MASCOT structure. This leads to a significant increase in the model development time but having a model that is so detailed gives an advantage with respect to the adaptability. This in turn this also means that the mesh size for the model cannot be changed without starting the manual process all over again. So, the steady state analysis that is to be performed on the thermal model developed depends on the mesh size of the structural model.

4-2 MASCOT Thermal Model

This section describes the modelling methods adopted for developing the thermal model for MASCOT. The structural model developed in Patran is used as the baseline model for developing the thermal model.

4-2-1 Baseline MASCOT Model

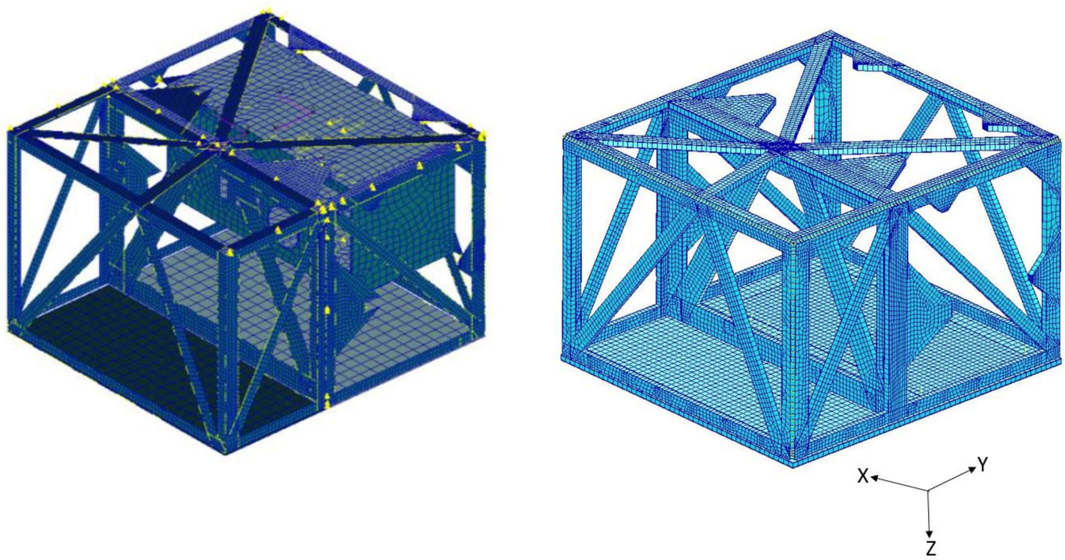

Figure 4-13: MASCOT Model: Structural Model (left) and Conduction Model (right)

The structural analysis model of the lander was modelled using MSC Patran. Quadratic 2D shell elements (Quad4) and a few triangular shell elements (Tria3) are used (Fig 4-13). The composite layup is simulated using the Patran Laminate Modeler. The instruments are modelled as point masses and connected to the structure using RBE2 elements. However, the model with shell elements does not have the capability to calculate the through thickness temperature gradient. Also, the model cannot accurately simulate the conductive heat transfer processes that occur between the structural members.

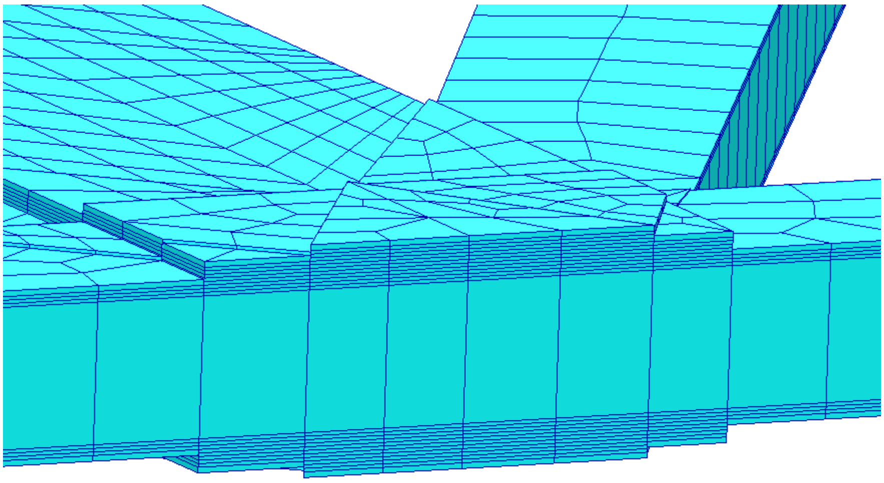

Figure 4-14: Plies at a junction: pX wall

For the structural engineer to run a thermal analysis as a subcase, a thermal model needs to be developed from the structural model. When dealing with the mostly poor out-of-plane conductivities of the sandwich structure, it is of interest to evaluate the sensitivity of the designs to changes in material properties. This is because the thermal paths in a structure depend on the fibre type and orientation of the ply. Hence a steady state analysis with solid 3D elements is used to characterize the thermal paths in the structure.

4-2-2 Model Development

The thermal model developed for the MASCOT structure is presented here. The structural model was developed using Quad4 and some Tria3 elements. Hence, extruding them using the Patran composite laminate modeler gives Hexa and Penta elements respectively. Initially the task of extruding all shell elements at once was performed. This leads to element warping at junctions within the structure where different plies meet and thus create warped elements and leads to errors. Hence, every section of every wall has to extruded individually. The development of a full 3D element model was challenging due to the fact that the automatic assignment of properties to the plies by the Patran Laminate Modeler was not available due to the bug explained earlier. During the extrusion process, only elements with PCOMPLS property card assigned to them while extruding are assigned automatically their properties. Since manual extrusion is being performed, the Hex8 elements have the PSOLID property card with no material properties assigned to them. The manual process involves isolating each part of the structure and assigning a coordinate system per structural member within the part. Next, each ply has to be selected individually and the material assigned to them. Caution was exercised when dealing with junctions in each part where plies overlap since many plies are involved and heat transfer at these intersections need to be simulated accurately.(Fig 4-14)

In the model, the walls are connected to one another using $\pm 45^o$ Carbon Fibre Reinforced Polymer (CFRP) straps. These straps are present at the wall interfaces. Hence, 1D conductor

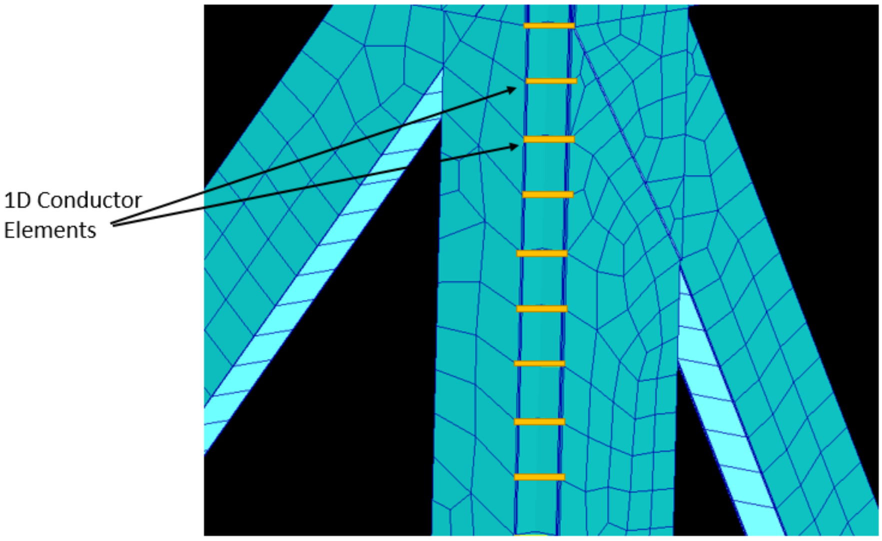

Figure 4-15: 1D Conductor Straps

elements are introduced between each edge node from one wall to the edge node of the other wall its interacting with. The conductance values assigned to these 1D CELAS1 elements are based on the conductivity of $\pm 45^o$ CFRP straps. Each node at the edge of a wall is connected to a corresponding node present on the edge of the other wall that it interacts with using the 1D conductor elements, thus simulating the straps (Fig 4-15). The conduction model including all the payloads and soil imitator comprises of the 128766 nodes and 93326 elements tabulated in Table 4-3.

Element Name	No. of Elements	Patran Property Card
CELAS1	1436	PELAS
CQUAD4	2095	PSHELL
CTRIA3	58	PSHELL
CHEXA	89261	PSOLID
CPENTA	476	PSOLID

Table 4-3: Model Summary

MASCOT Radiator

The radiator is constructed as a sandwich with aluminium honeycomb core and aluminium facesheets. In order to guarantee the possibility to have a late access to the battery pack, the panel is divided into two parts: main-radiator and sub-radiator (see Fig 4-16), the first one dedicated to spread the excessive heat from the Ebox and second for the battery pack, to which it is constrained with four fasteners. Between the two radiators, a small gap is considered, so no thermal interfaces between the two parts are taken into account. The honeycomb

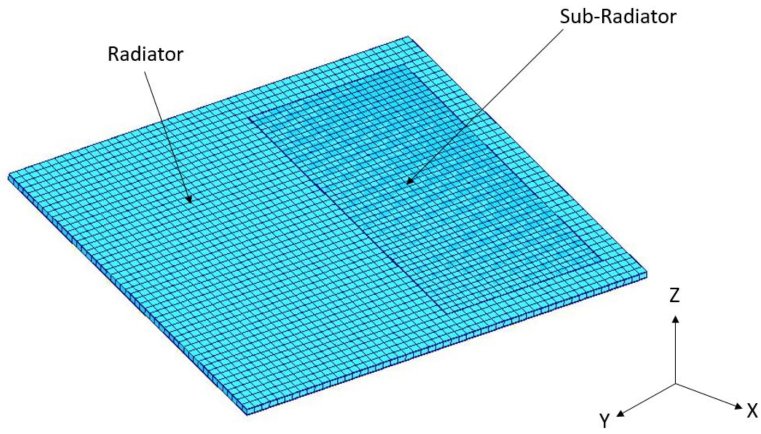

Figure 4-16: Radiator and Sub-Radiator

thickness is 4 mm, each aluminium sheet is 0.5 mm thick for both the radiator sections. The conductivities of the honeycomb core are calculated according to a paper published by Tsai et al.[31]. According to Tsai, the conductivity of a honeycomb can be roughly written as an anisotropic material with the following conductivites. The conductivites are then assigned to the solid elements that are generated to model the honeycomb.

$$k_x = \frac{3k_{Al}\delta}{2S}$$

$$k_y = \frac{k_{Al}\delta}{S}$$

$$k_z = \frac{8k_{Al}\delta}{3S}$$

The values provided are k_{Al}=155 W/mK (Conductivity of Aluminium Alloy), δ=80 μm (cell wall thickness), S=4.8 mm (cell wall length) for the honeycomb. Thus the conductivity values for the honeycomb are: k_x=0.39 W/mK, k_y=0.26 W/mK, k_z=0.69 W/mK.

Payloads

The payloads in the structural model are modelled only as point masses. The payloads in the thermal model are modelled with shell elements since they participate in the radiation processes within the spacecraft. The payloads are thermally isolated from the structure and hence the conductivity betweeen the payloads and the structure is very low. 1D Conductor elements are used to define the interface between the payloads and the structure. Since an accurate temperature field of the payloads is not required, the number of shell elements used for them is limited to one per face mostly to reduce computational time. Although the payloads are all not cuboid in shape, a simpler model was necessary due to the lack of data on the payloads. The material property assigned to the shell elements is Aluminium of thickness 0.125 mm. In case of MicrOmega, the payload is completely enveloped in Multi Layer Insulation (MLI). But to keep things simple, the radiative properties of the MLI were

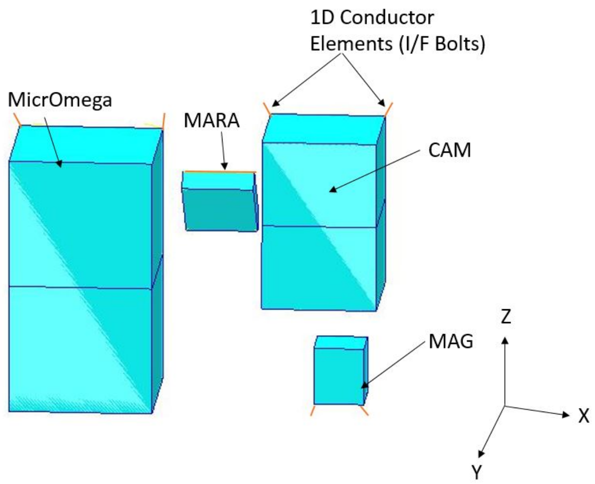

Figure 4-17: Payloads

assigned directly to the shell elements. Similarly, respective radiative properties were assigned to all other payloads. (see Fig 4-17)

EBox, Battery Pack and Heat Pipes

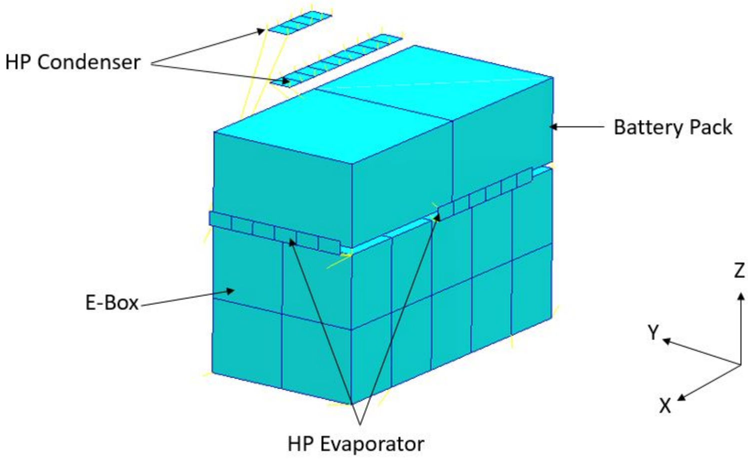

Figure 4-18: E-Box, Battery Pack and Heat Pipes

The EBox and the Battery Pack are also modelled with shell elements in the shape of cuboids. The loads in both are introduced in the form of a nodal source located at the geometric center of the cuboids and connected to the nodes on the shell elements using 1D conductor elements. The heat pipes comprise of three sections. The evaporators that are attached to the Ebox.

The heat pipes themselves and the condensers attached to the radiators. The evaporators and condensers are modelled as shell elements. The heat pipes are modelled using 1D conductor elements with the thermal conductance derived from data provided. (see Fig 4-18)

Multi Layer Insulation and External Foils

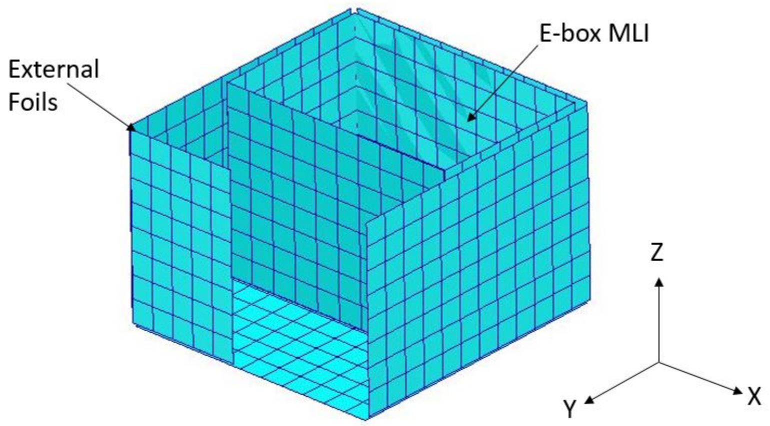

Figure 4-19: Multi Layer Insulation

The multi layer insulation for the warm compartment is modelled with shell elements with appropriate thermal properties applied. The external foils (single layer) are also modelled with shell elements. (see Fig 4-19)

Asteroid

The experimental setup used for the thermal test campaigns conducted at DLR Bremen is modelled . A setup comprising of a soil imitator with the MASCOT Lander Module is placed inside a vacuum chamber for the thermal test campaigns. The vacuum chamber walls are cooled down to 80 K. The vacuum chamber is modelled as one ambient shell element above the MASCOT model and is set at 80 K.

The soil imitator simulates the on-asteroid soil conditions. The soil imitator is an open aluminium box with heaters fitted onto the side walls to simulate the heat fluxes on the asteroid. The heaters help in maintaining the temperature of the soil imitator at the desired temperature (see Fig 4-20). The MASCOT Lander Module is placed at the center of the bottom face of the imitator with PEEK washers isolating the bottom of the lander from the soil imitator. Hence, in the model, the lander is placed 5 mm away from the soil imitator and connected to it through 1D conductors of conductance equivalent to that of PEEK washers. The asteroid soil imitator is modelled with 2D shell elements. (see Fig 4-21)

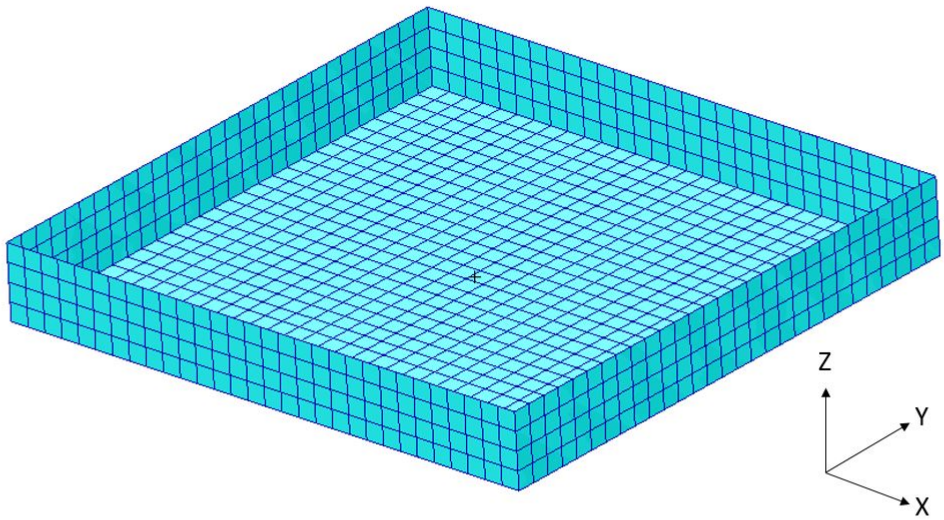

Figure 4-20: Asteroid Soil Imitator

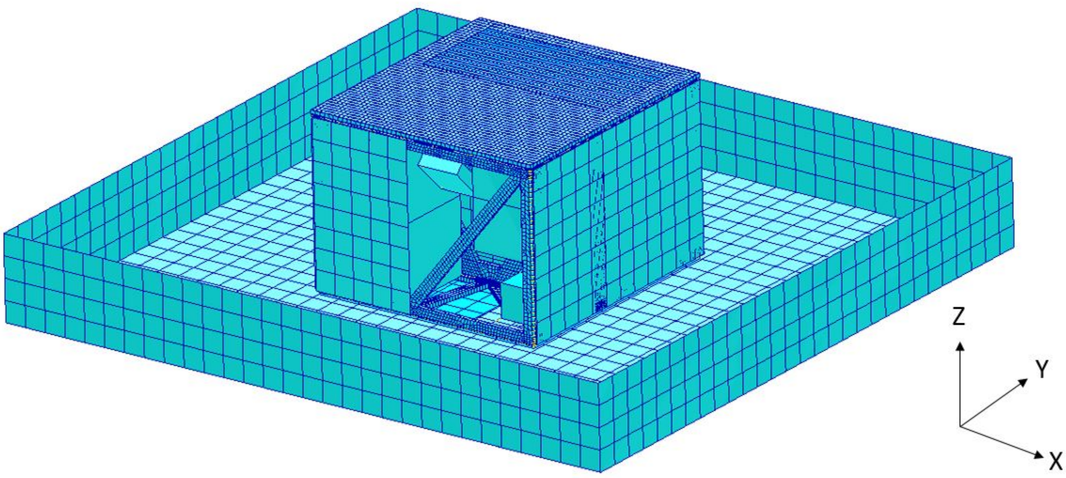

Figure 4-21: MASCOT with the asteroid soil imitator

4-2-3 Radiation Model Development

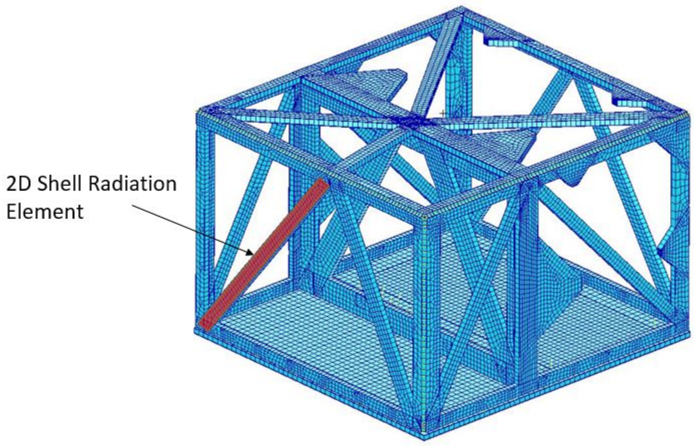

Figure 4-22: Radiation Element Modelling

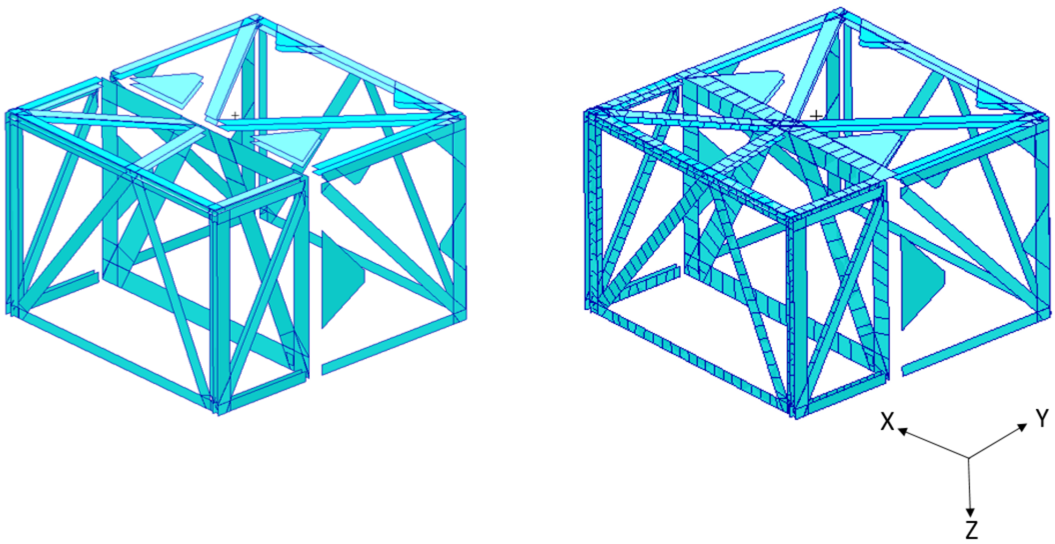

Figure 4-23: MASCOT Radiation Model: Coarse (L) and Fine(R)

In order to simulate radiation exchange in Patran, the elements that participate in radiation with the Lander Module (LM) need to be declared in the form of enclosures. All elements that belong to an enclosure or cavity participate in radiation exchange with the other components within the same enclosure only. Thus, the enclosures need to be defined carefully. A radiation model does not require as many nodes and elements as the conduction model. Also, the sheer number of faces of the solid elements that are extruded from the structural model participating in radiation exchange causes the solver to crash. As a workaround, a simplified 2D shell model was developed for the structure that represents the top layer of the framework structure. (Fig 4-22)

In order to create these elements, the four nodes that form the element need to be selected first. The next step involves assigning properties to these shell elements. The elements that are created overlap the conduction model. Each structural component of every wall is modelled with at least one element each. The energy that an element of the model receives from radiation is transferred to the surrounding elements through its corner grid points. The 2D shell elements created solely for the purpose of radiation modelling are assigned the properties of the $\pm45^o$ CFRP ply that is used throughout the structure as the reinforcement ply. The declared thickness for these elements is negligible since the through thickness conduction is simulated by the solid elements below the radiation model. Two radiation models were developed. The initial radiation model has mostly one element per structural member in a wall which is a coarse mesh with 142 PSHELL elements. To determine the effect of a refined radiation mesh on the thermal characteristics, a finer mesh of around 20 elements per structural member was developed in the payload section alone. This increases the total number of elements in the fine mesh to 557 PSHELL elements.(Fig 4-23)

4-3 Material and Interface Properties

All the material and interface properties are based on the data provided by DLR. [10]

4-3-1 Conduction Properties

The conductivities applied for the components on the MASCOT Lander Module are described in Table 4-4.

4-3-2 Radiation Properties

The radiation properties assigned to each component are put forward in Table 4-5.

4-3-3 Interface Properties

The conductance values used between various components onboard are mentioned Table 4-6. These values are applied to the 1D conductors modelled as interfaces.

Material	Thermal Conductivity [W/mm K]	Components on which the material is used
UD_CFRP	k_xx= 0.034 k_yy=0.001 k_zz=0.0005	Structure Walls
$\pm 45^o$ CFRP	k_xx= 0.015 k_yy=0.015 k_zz=0.0005	Structure Walls
Rohacell Foam	3.5E-05	Structure Walls
CFRP ISO	k_xx= 0.02 k_yy=0.02 k_zz=0.001	Inserts
Aluminium 7075	0.155	Payloads, EBox, Battery Pack, Radiators, Asteroid Soil Imitator
Al_Honeycomb	k_xx= 0.00034 k_yy=0.00026 k_zz=0.0007	Radiator Honeycomb
MLI	2.8E-04	Ebox MLI
ITO Coated Aluminized Polyimide	1.6E-04	External Foils

Table 4-4: Material Conductances

Element	Coating	ϵ	α
Structure	No surface treatment	0.9	0.95
Radiators	Outer:White	0.88	0.2
	Inner : Black	0.91	0.96
Battery Pack	Aluminium Chest	0.15	0.08
Ebox	Outer: Polished Aluminium	0.03	0.15
	Inner : Black	0.91	0.96
MicrOmega	MLI	0.035	0.15
CAM	Vapour deposited Gold	0.02	0.39
MARA	Vapour deposited Gold	0.02	0.19
MAG	MLI	0.82	0.90
Foils	Outer : ITO Coated aluminized polyimide	0.77	0.51
	Inner : Aluminium coated polyimide	0.035	0.14
EBox	Outer : ITO-Kapton	0.62	0.44
	Inner : Kapton	0.035	0.14

Table 4-5: Radiation Properties

Interface	Conductance (W/K)
Structure: CFRP Straps	0.004
Ebox-Structure	0.001
Ebox-Battery Pack	0.01
Ebox-Heat Pipes	0.007
MicrOmega-Structure	0.001
MARA-Structure	5E-05
Cam-Structure	0.001
Radiator-Structure	5E-05
Radiator-Heat Pipes	0.007
Heat Pipe A	2.5
Heat Pipe B	2

Table 4-6: Conductances

Chapter 5

Steady State Thermal Analysis

The thermal analysis is made for steady state. This means that the point of operation has remained constant long enough for the temperatures in the model to stabilise. In order to simulate the thermal paths in the structure steady state analysis is deemed enough. The analysis boundary conditions are based on the test setup that was used during the thermal qualification of MASCOT flight model. The tests were carried out with the objectives of exploring the thermal behaviour of MASCOT S/C in the critical asteroid environment and acceptance testing of MASCOT as proof of qualification within the known limits of Thermal Control System (TCS) performance. The test results are used as basis for correlation of the thermal model to the flight model in on-asteroid environmental conditions.

First, the test setup that is used as the input for the thermal model developed in this thesis is described. The results from the steady state analysis for both hot and cold cases are described. Finally, the model correlation is performed to validate the model.

5-1 Test Setup

The thermal test campaign was held in the DLR facilities in Bremen. For the asteroid phase, MASCOT was placed inside the vacuum chamber on an asteroid soil imitator (Fig 5-1). Solar flux on the Landing Module is simulated with a set of heaters that are fixed on various locations (Fig 5-2) on the top side of the radiator and the sub-radiator that provide a heat load of 20.7 W [10]. This corresponds to the average solar flux received on the asteroid by the MASCOT Radiator during the on-surface operation. This load is applied using the Total Heat option available in Patran.

Two phases of the entire thermal testing campaign are used for the model correlation. The steady state temperatures of the various components onboard are obtained and are useful for validating the thermal model developed. Phase 1 and Phase 2 environmental conditions are described in Table 5-1 and Table 5-2 respectively. The asteroid soil imitator temperature during the Phase 1 is set at 273 K and during Phase 2 at 333 K. The results from these phases are used as they provide the steady state temperatures of the various components onboard

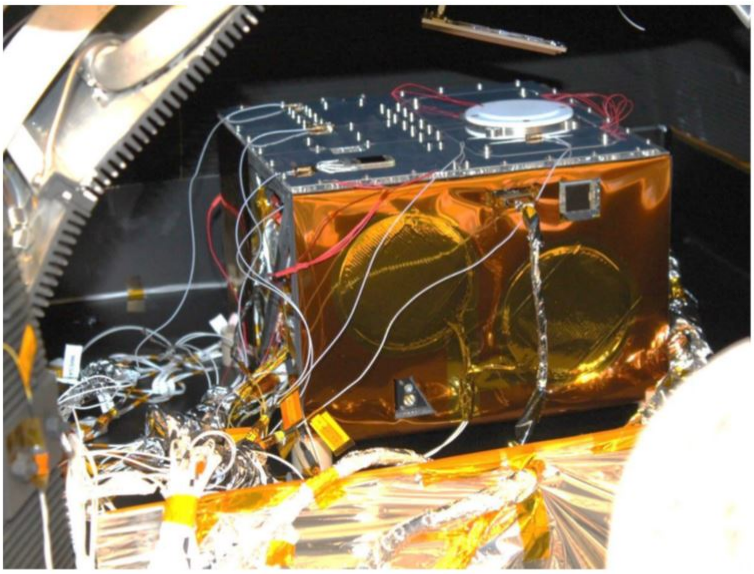

Figure 5-1: MASCOT before the chamber closure

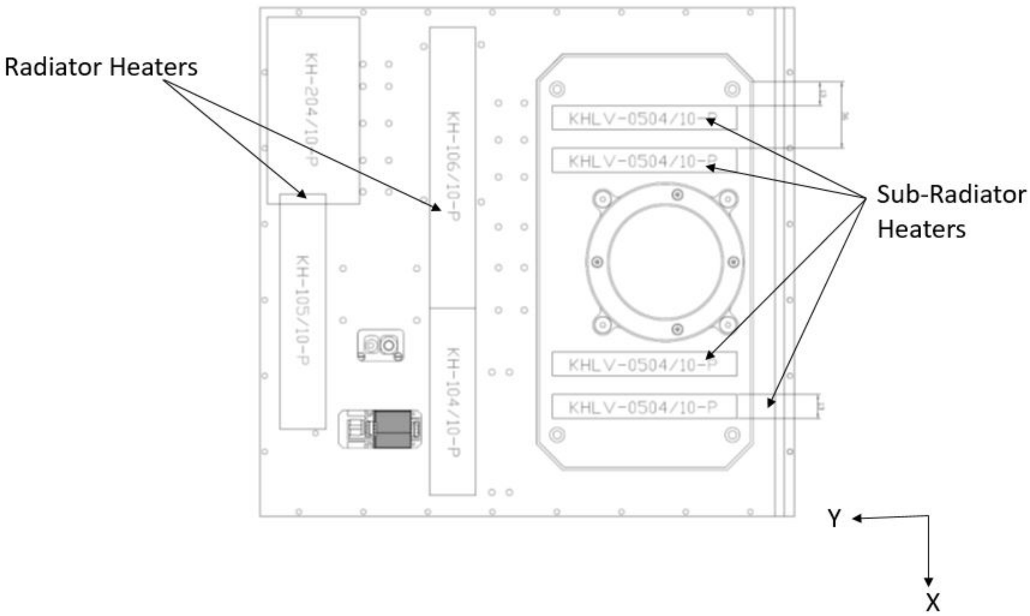

Figure 5-2: Heaters placement on MASCOT

the lander during both the hot and cold phases. In both the phases the payloads are switched off. The only heat generating components are the Battery Pack and EBox. The on-asteroid operations involve the use of only one payload at a time. Hence the effect of the environment on the lander can be gauged only when all the payloads are switched off to ensure that they

Phase 1	
Asteroid soil imitator temperature	273 K
Power set on the heaters	
-Main radiator heaters	13.3 W
-Sub radiator heaters	7.4 W
Battery power dissipation	3 W
EBox power dissipation	5 W

Table 5-1: Phase 1 Boundary Conditions

Phase 2	
Asteroid soil imitator temperature	333 K
Power set on the heaters	
-Main radiator heaters	13.3 W
-Sub radiator heaters	7.4 W
Battery power dissipation	3 W
EBox power dissipation	5 W

Table 5-2: Phase 2 Boundary Conditions

are operating within their temperature limits when they are switched on.

Out of the many thermistors used in the test campaigns, four sensors are attached directly to the structure. (Indicated by Struct 1-4 in Fig 5-3 and 5-4). These locations are chosen because of their proximity to the payloads. No sensors were placed on the structure on the other side of the inner wall. This is because the effect of structure participation in heat transfer processes with the EBox and Battery Pack is negligible due to the fact that they are isolated by MLI. The temperature readings from these four sensors will be used for the validation of the thermal model developed.

5-2 Results

The thermal test campaign results are tabulated in Table 5-3 and Table 5-4 for Phase 1 and Phase 2 respectively. From the Phase 1 tests, it is observed that there is a large difference in temperatures of Struct 1 and 2 when compared to Struct 3 and 4. The higher temperatures of Struct 3 and 4 are attributed to the fact that they are close to the region of the radiator where the heaters are attached. In Phase 2, these differences diminish owing to the fact that Struct 1 and 2 are closer to the asteroid surface and are influenced by radiation from the external foils at the bottom covering the nZ wall.

From the thermal steady state analyses performed, the thermal paths in the LM structure are characterized for both the phases. In both the phases, since the heaters that simulate the solar flux are fitted on the external face of the radiator right above the payload compartment, higher temperatures are seen in the structural members enveloping the payload compartment. The structural members in the compartment that houses the EBox and the Battery Pack are isolated from the heat transfer processes due to the components housed within because of the presence of MLI. Hence, lower temperatures are seen in that compartment. A local

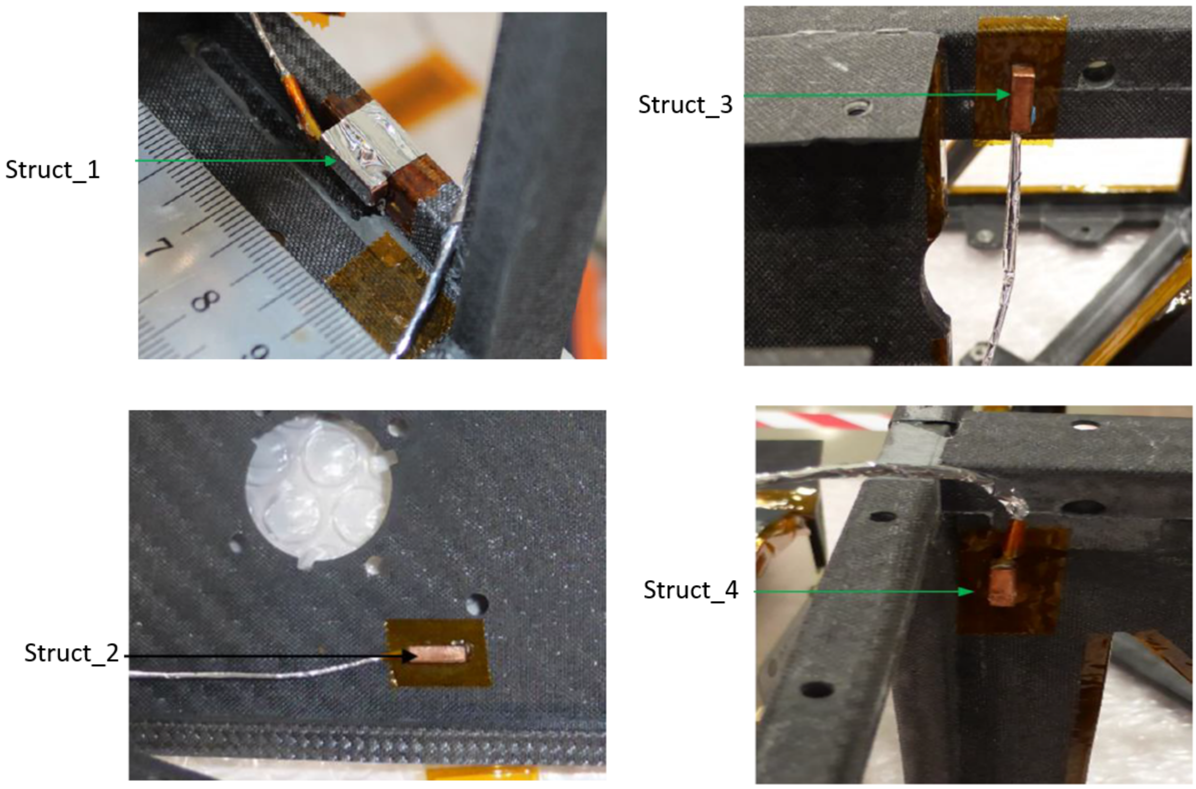

Figure 5-3: Thermistors

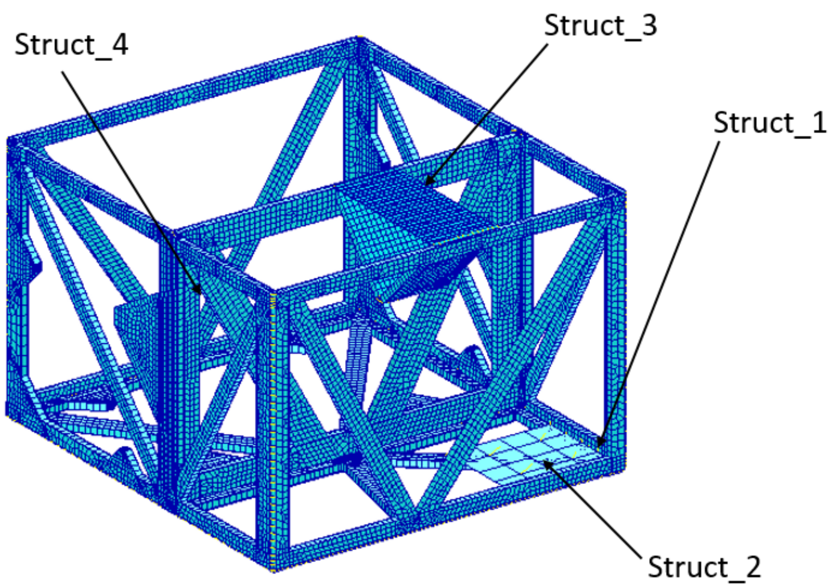

Figure 5-4: Thermistor positions on the structure

temperature build up is seen in the left section of the nY wall and the right section of the pX wall. This is due to the proximity of these sections to the MicrOmega instrument. The right section of the nY wall is open to space and not covered by an external foil in order to accommodate the field of view of the CAM and MARA payloads and hence lower temperatures are seen in that section.

The Phase 1 steady state analyses results are shown for the coarse mesh in Fig 5-5 and for the fine mesh in Fig 5-6. The temperature range for the coarse mesh is from 173 K (pY wall) at its lowest to 321 K (nX wall) at its highest. The temperature range for the fine mesh is from 166 K at its lowest (pY wall) and 314 K (nX wall). For the coarse mesh, localized heat fluxes at the corners of each truss leads to temperature rise in these areas. The Phase 2 steady analyses results are shown in Fig 5-7 and Fig 5-8. The temperature range for the coarse mesh is from 177 K (pY wall) at its lowest to 341 K (nX wall) at its highest. The temperature range for the fine mesh is from 170 K at its lowest (pY wall) and 334 K (nX wall).

In both the phases, compared to the coarse mesh, the overall range of temperatures in the fine mesh model are lower by 7 K. This might be due to the fact that when compared to 20 elements per truss member participating in radiation processes in the fine mesh, only one element per truss member is participating in the coarse mesh. This leads to localized spikes in temperatures in a truss member for the coarse mesh. This is because only the four corner nodes of the element participate in the radiation process. For the fine mesh, since more elements are present in each section the heat fluxes are distributed uniformly.

5-2-1 Model Correlation

In this section, the results of the correlation of the test results with the Patran model are shown. The standard temperature range or thermal design margin used in the space-flight industry for qualifying a thermal model is ± 5 K [12]. Hence the correlation margin of ± 5 K difference between the thermal model and the test campaign results is used. The comparison between the test result temperatures and the simulations are tabulated in Table 5-3 and Table 5-4.

The temperature differences between the test results and the simulations for Phase 1 are plotted for the coarse mesh in Fig 5-9 and for the fine mesh in Fig 5-10. In Phase 1, for the coarse mesh, when compared to the test results, the temperatures from the simulations are lower. For Struct 2 and 4, the temperature difference is -1 K. For Struct 1, the difference is higher at -2 K. And finally, for Struct 3 the difference is -4 K. For the fine mesh, all temperatures except for Struct 3 are lower compared to the test results. The reason for the spike in the temperature might be due to the radiation heat flux on the nodes in the element modelled in the region around Struct 3 which receives direct fluxes from the radiator.

The temperature differences between the test results and the simulations for Phase 2 are plotted for the coarse mesh in Fig 5-11 and for the fine mesh in Fig 5-12. In Phase 2, for the coarse mesh, similar to Phase 1, the temperatures from the simulations are lower. The temperature differences for Struct 1 is -2 K whereas for Struct 2 it goes up to -4 K. The differences for Struct 3 and 4 are the same at -1 K. In case of the fine mesh, the noticeable thing is the magnitude of the difference. For Struct 1 and Struct 4 the temperature differences

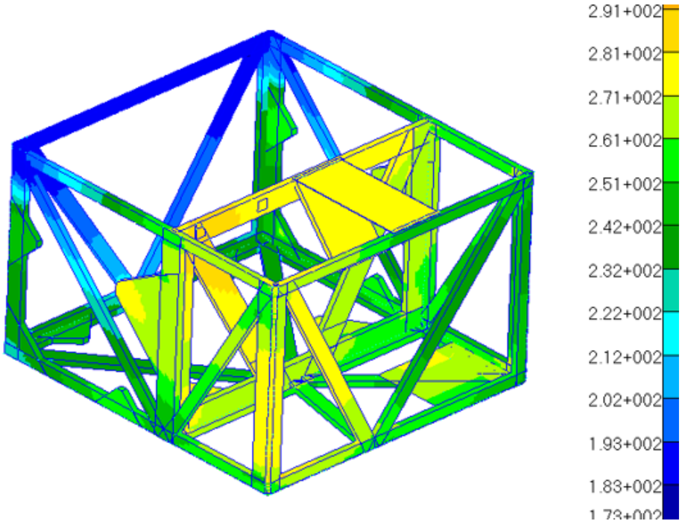

Figure 5-5: Phase 1 Coarse Radiation Mesh

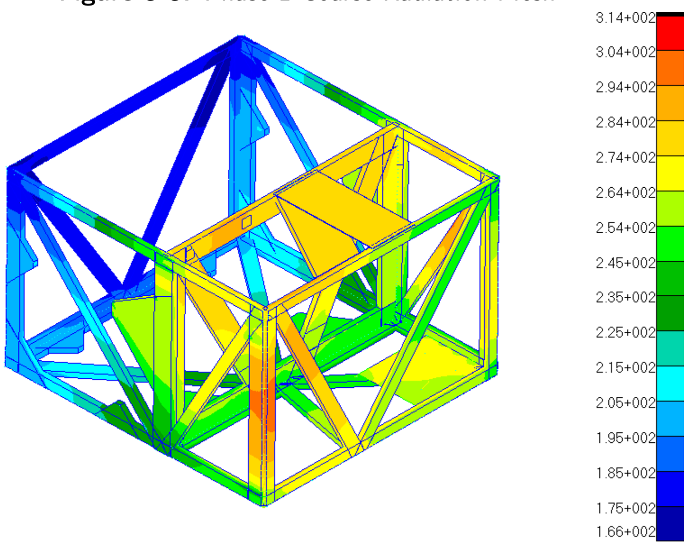

Figure 5-6: Phase 1 Fine Radiation Mesh

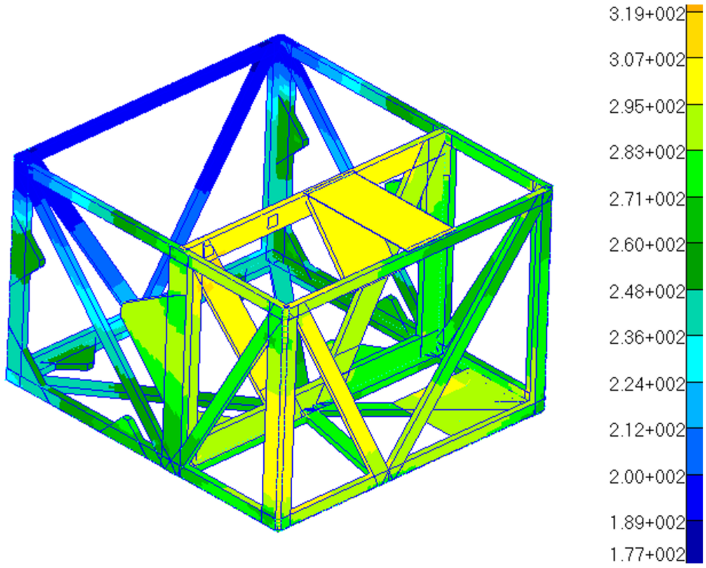

Figure 5-7: Phase 2 Coarse Radiation Mesh

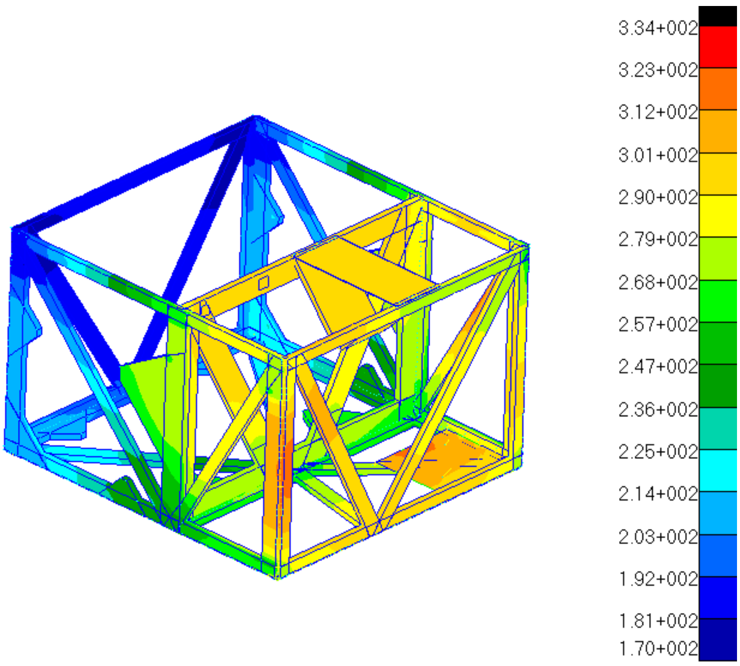

Figure 5-8: Phase 2 Fine Radiation Mesh

are above the ± 5 K limit at -9 K and -8 K respectively. The difference for Struct 2 is -1 K and that for Struct 3 is -2 K.

The uncertainties in the results can be attributed due to the radiation elements that have been modelled. Each structural member in every wall has only one radiation element in the coarse model. Hence, only the 4 corner nodes in that structural member participate in the radiation process. This is due to the fact that radiation fluxes are only introduced at these corner nodes whereas in the real world every part of the structure participates in conduction as well as radiation. The finer mesh that was developed around the payload compartment to test the influence of the mesh size on the temperatures did not yield improved results. More temperatures have been matched for the Phase 1 than for the Phase 2, i.e., in the colder phase more than in the hot one. This is observed for both the model cases. A better correlation of the colder cases is easier than in the hot ones. A reason could be the not precise, in some cases, evaluation of the coating properties, leading to more uncertainties in the hot phase correlation, because the influence of the radiative heat exchange with respect to the conductive path can be higher in the hotter phases of the mission. Thus, the coarse radiation mesh model is suitable for the analysis in the next phase for evaluating the structure integrated thermal subsystems.

	Temperature (K)		
	Test	Coarse	Fine
Struct_1	265	263	261
Struct_2	265	264	263
Struct_3	279	275	281
Struct_4	281	280	277

Table 5-3: Phase 1 Structure Correlation

	Temperature (K)		
	Test	Coarse	Fine
Struct_1	299	297	290
Struct_2	302	298	301
Struct_3	297	296	295
Struct_4	300	299	292

Table 5-4: Phase 2 Structure Correlation

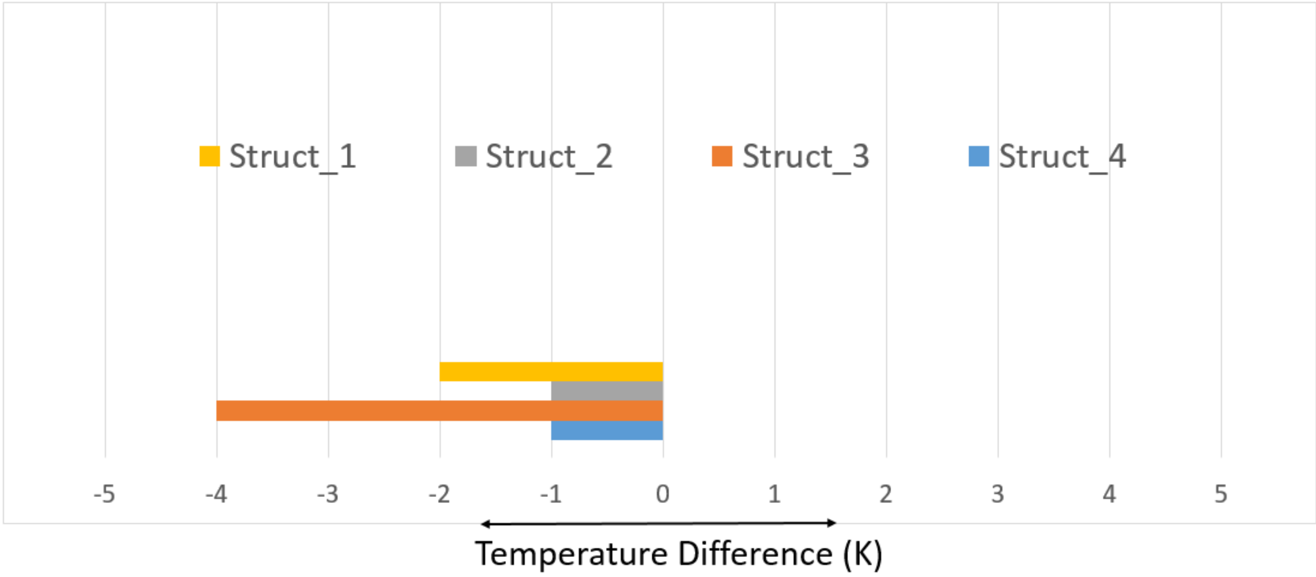

Figure 5-9: Model-Test Difference : Phase 1 Coarse

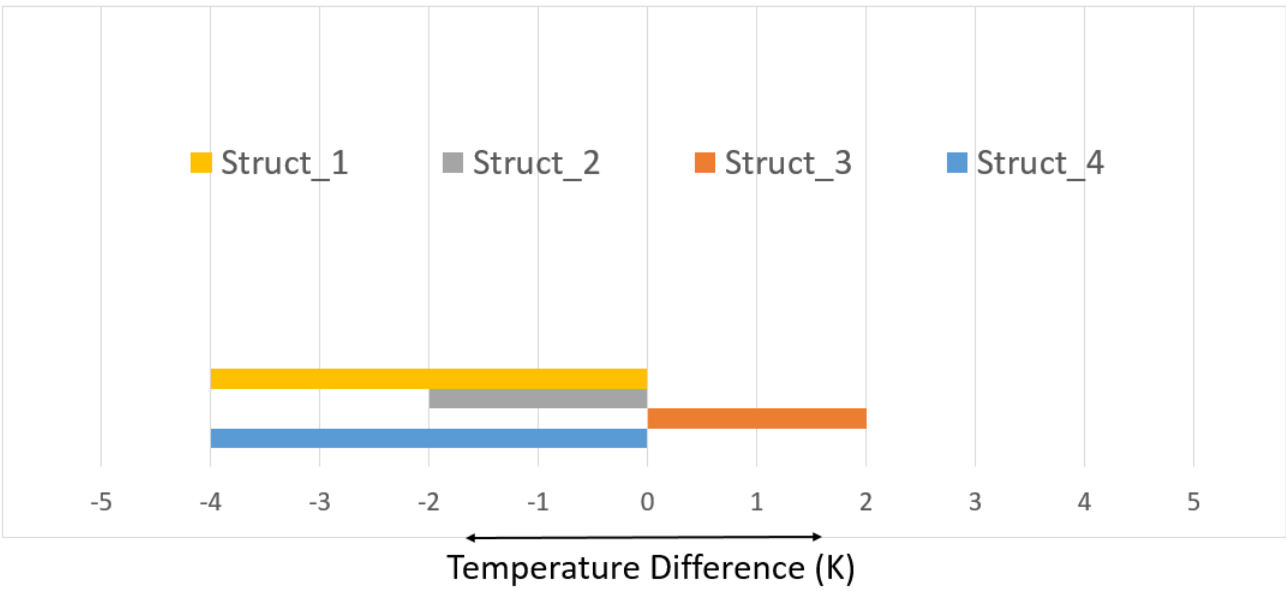

Figure 5-10: Model-Test Difference : Phase 1 Fine

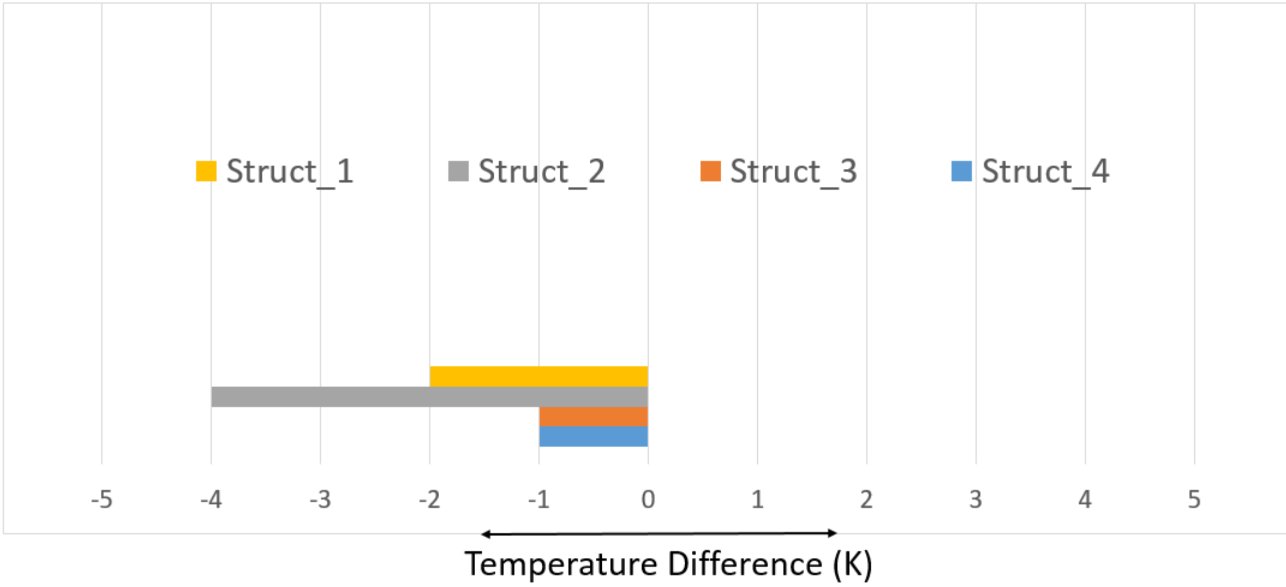

Figure 5-11: Model-Test Difference : Phase 2 Coarse

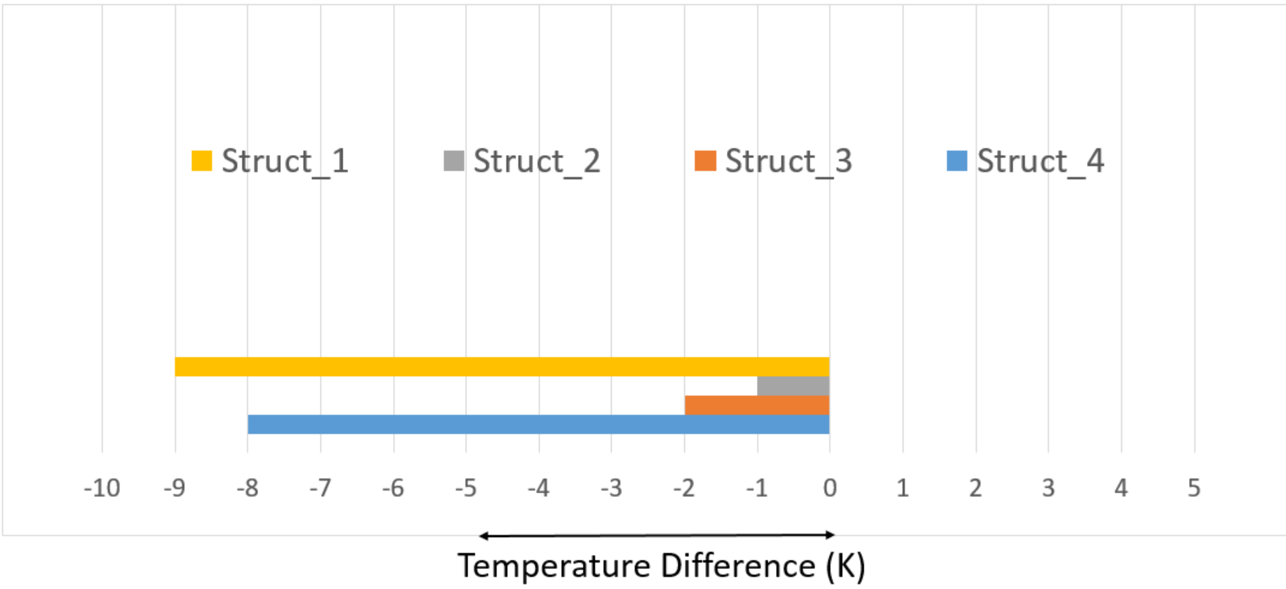

Figure 5-12: Model-Test Difference : Phase 2 Fine

Chapter 6

Spacecraft Integrated Thermal Subsystems

This chapter describes the analyses carried out with the objective of determining the temperature changes in the EBox when the heat pipes are removed. The focus will be on the heat pipes alone since the other aspects of the passive thermal subsystem such as the MLI and the external foils are vital to isolating the payloads from the external environment as well as from the heat generating components onboard and cannot be removed.

The ultimate goal for a structure integrated thermal subsystem is to minimize the ratio of the thermal subsystem mass to the overall structural mass of the system. The design and research of thermal management in multifunctional systems are primarily led by the heat absorption requirements of the system. Once the required layout is known, the influence of the components on the static behaviour of the system is simulated, and the original structure can be modified accordingly to exploit thermal characteristics of these elements. The ratio of thermal subsystem mass to the structural mass in the MASCOT LM stands at 0.96. The goal is to reduce this ratio by integrating the functions of the thermal subsystem within the structure.

By removing the heat pipes, mass of approximately 250 g can be saved on the MASCOT Lander. Due to the removal of the heat pipes, the temperature of the electronic boards on EBox might approach their maximum operational limit. This would lead to component failure. Hence, a sensitivity analysis is conducted to figure out a design solution to reduce the EBox temperature by improving the conductance values of the EBox-Structure Interface (I/F). As a first step, a steady state analysis is conducted for the lander without the heat pipe. Next, the conductive interface values are changed. To improve the thermal performance of the structure, the thermal conductivity of the $\pm 45^o$CFRP straps connecting the walls are varied. Finally, the effect of replacing the CFRP inserts in the structure at the EBox-Structure interfaces with Aluminium inserts is studied. The technical solutions that can be implemented on the MASCOT structure are identified based on the results from these simulations. One of the initial solutions was to utilise high conductivity foam for increasing through thickness conduction. However, in highly conductive graphite foams, the density of the foam is high

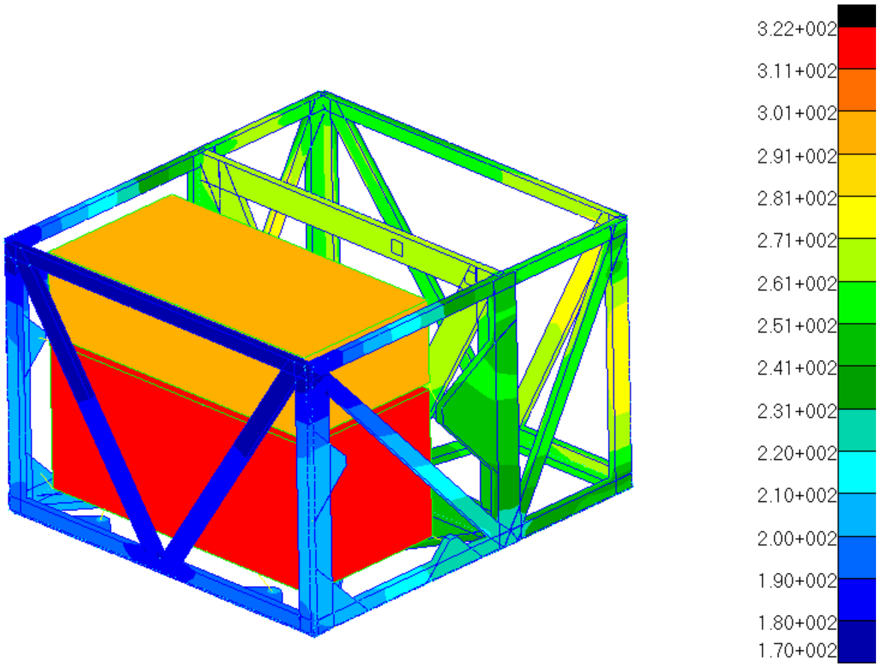

Figure 6-1: Temperature Profile: Case 1

and thus this can lead to a mass penalty. Hence, modifying foam properties are not considered for this study.

6-1 Case 1: Heat Pipe Removal

The influence of the removal of the two heat pipes on the overall system is characterised with a steady state analysis for the cold case i.e., the asteroid soil imitator is set at 273 K. The temperature of the EBox rises to 322 K due to the absence of the heat pipes. Heat exchange occurs as radiation between the MLI enveloping the EBox and the outer surfaces of the EBox and via conduction to the Battery Pack and to the structure through the 12 I/F bolts. The effect of the temperature rise in the EBox on the rest of the Lander Module is negligible since the EBox and the Battery Pack are isolated with MLI (Fig 6-1). The effect of the removal of the heat pipes on the payloads is negligible. The temperatures of the payloads on average drop by 4 K compared to the case where the heat pipes were present and thus are still within the operational requirements. The reason for this drop in temperature is due to the fact that the heat pipes are connected to the inner facesheet of the radiator and the aluminium facesheet radiates heat into the payload compartment.

6-2 Case 2: Conductive Interfaces

For the sensitivity analysis of the EBox temperature, the key parameter for evaluation is the conductive interface between EBox and the structure. Since the heat pipes are used to

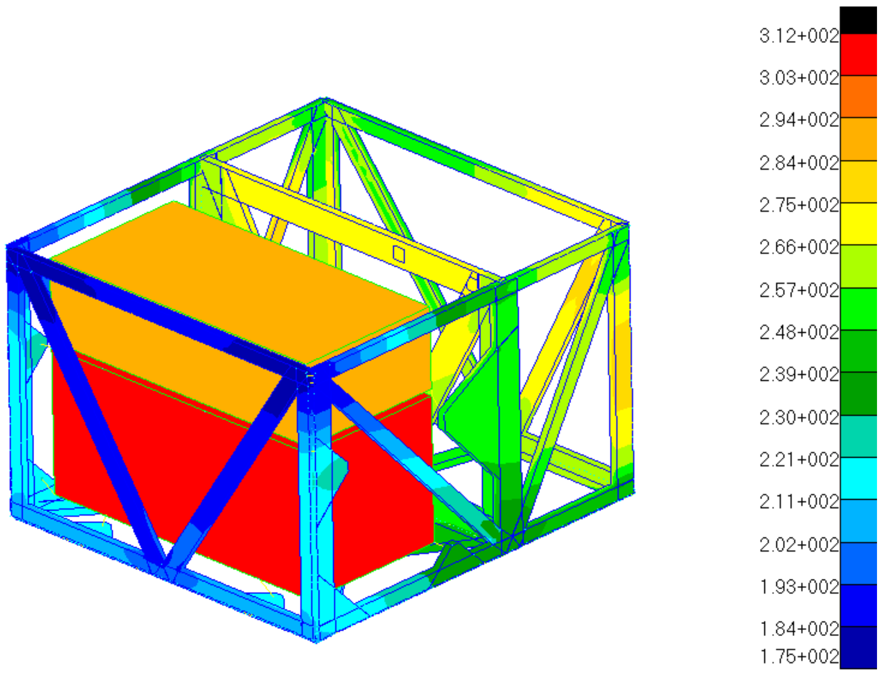

Figure 6-2: Temperature Profile: Case 2.1

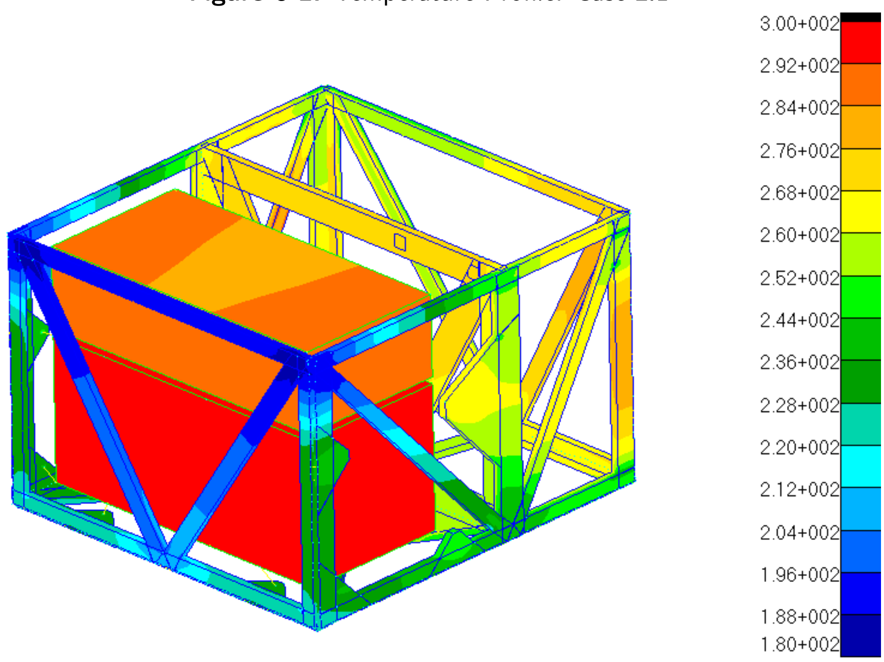

Figure 6-3: Temperature Profile: Case 2.2

carry heat away from the structure to the radiators, conductive interfaces help transfer the heat load to the structure directly. The default I/F conductance value given between the EBox and MASCOT structure is 0.001 W/K. Hence, to determine the influence of the I/F value on the EBox temperature, the conductivity is varied by a multiple of 2 (Case 2.1) and 5 (Case 2.2) for an initial estimate of the variation. It is observed that the temperature of the EBox drops to 312 K (Fig 6-2)for case 2.1 and to 300 K (Fig 6-3) for case 2.2. Thus, it is inferred that the temperature of the EBox can be controlled within its operational limits by using conductive interfaces to the structure. These conductive interfaces can be achieved by implementing lightweight graphite fibre based thermal links that are made out of pitch based UD plies. By varying the material conductivity of these thermal links, the EBox can be maintained within its operational temperature range.

6-3 Case 3 : Conductive Straps

For a structure integrated thermal subsystem, the pitch based Uni-Directional (UD) plies are traditionally added onto the PAN based plies at locations where the heat load needs to be conducted away. For the MASCOT structure too, this can be achieved by adding pitch based UD plies to the existing plies. Due to the unavailability of PCOMPLS elements, the addition or deletion of a ply to the existing layup and creating the thermal model from the layup is impossible to achieve at the moment. This is because, to add a ply, the entire process of modifying a layup, extruding elements without properties and then manually assigning properties needs to be carried out and takes a significant amount of time as explained during the MASCOT model development process.

The only component in the structure that could be used as is to improve the thermal characteristics are the $\pm 45^o$ CFRP straps. As described earlier, the walls of the MASCOT structure are connected to each other using $\pm 45^o$ CFRP straps. By changing the conductivity of the straps, it is possible to increase the thermal interaction between the walls. The CFRP straps between the walls are modelled with 1D conductor elements as explained previously. The conductance of the straps are increased by a multiple of 2 (Case 3.1) and 5 (Case 3.2) in this case too for an initial guess of the influence. From the results obtained for both cases, (Fig 6-4 and Fig 6-5) it is observed that the effect of the conductive straps on the temperature fields in the structure is negligible. The temperature difference at the junctions between the walls when compared to the default case with normal straps is only 1 K.

6-4 Case 4: Inserts

By increasing the through thickness conductivity of the structure at the EBox-Structure interface points it is possible to distribute the head load away from the top ply. This is because the heat load from the EBox is introduced only to the top ply through the use of 1D conductor elements. By replacing the CFRP inserts with an Aluminium insert the effect of using a high through thickness conductivity material at a local level is simulated. Thus the top and the bottom plies participate in the heat transfer process and help improve the thermal paths locally. Temperature differences of 5 K are observed between the top and bottom layers when CFRP inserts are used. When Al inserts are used, the difference drops

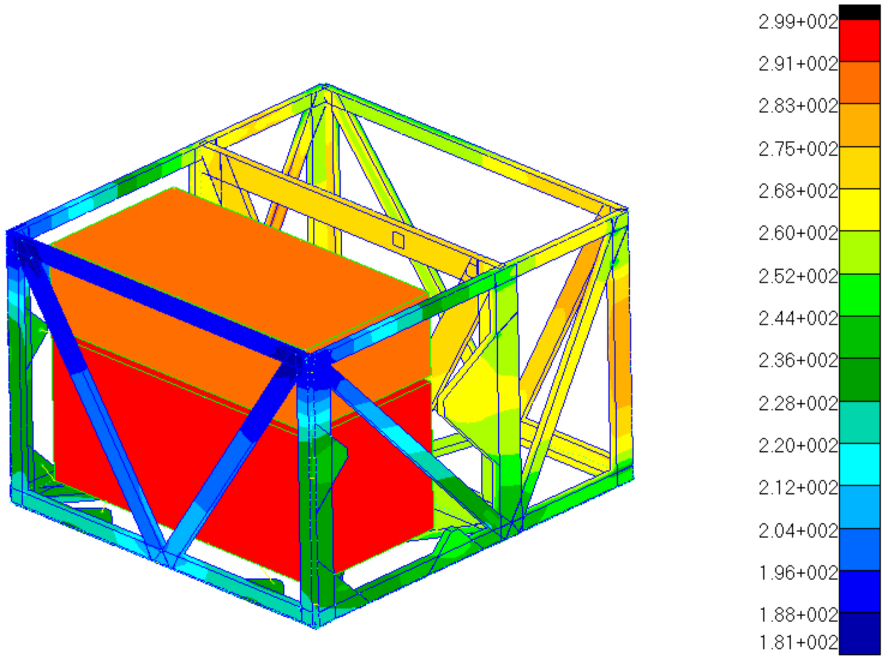

Figure 6-4: Temperature Profile: Case 3.1

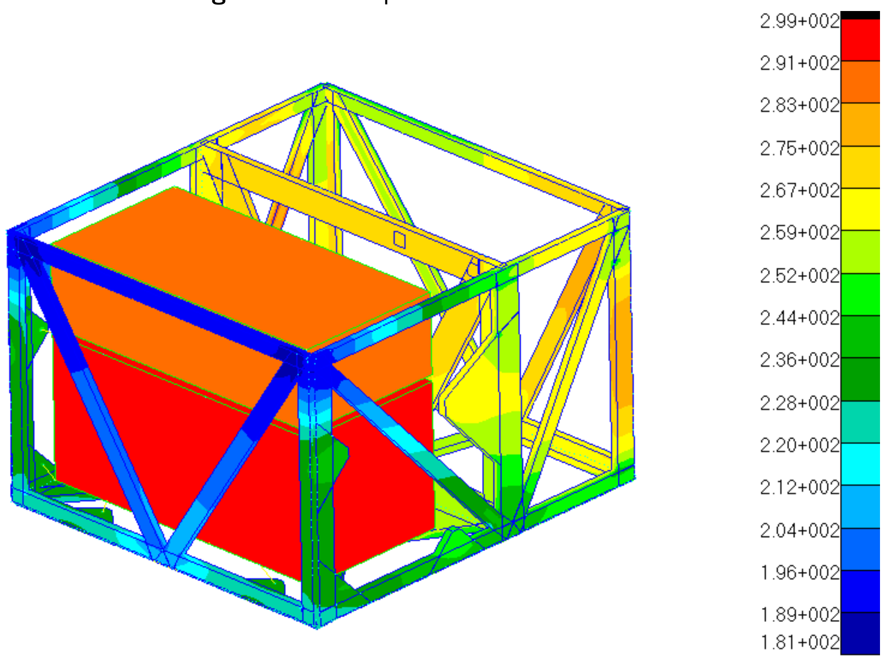

Figure 6-5: Temperature Profile: Case 3.2

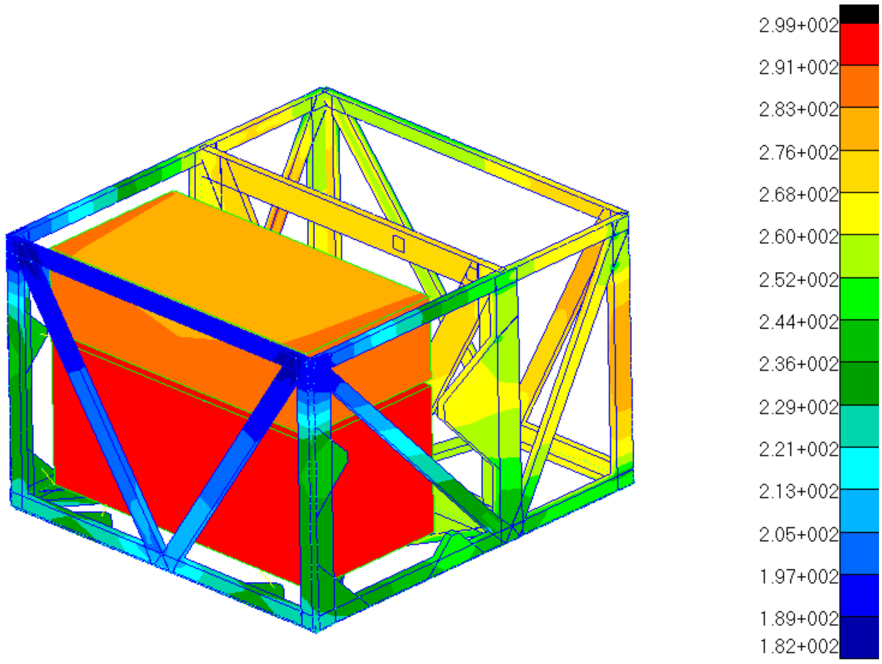

Figure 6-6: Temperature Profile: Case 4

to 1 K. The Al insert also conducts heat away from the I/F point to the walls. This can be observed by a local increase in temperatures of 8-10 K in the sections of walls that these inserts are attached to (Fig 6-6). The heat flux from these inserts could be dissipated by the walls by introducing pitch based UD conductive plies locally. The effect of this possible modification is not characterized due to the issues explained in Case 1.

6-5 Summary

By improving the conductive interface between the EBox and the structure, it is possible to control the temperature of the EBox within its operational limits. The conductive interfaces can be achieved using options such as graphite fibre thermal straps which are lightweight and are able to conduct heat from the EBox to the structure efficiently. Since the graphite thermal straps are unidirectional, they direct the heat load to the structure. The use of thermally conductive CFRP straps for the final bonding process does not improve the thermal paths between the walls. By replacing CFRP inserts at the interface points with Aluminium inserts, the heat fluxes introduced to the top layer of the structure at the I/F points are uniformly conducted to the bottom layers but unless pitch based UD plies are introduced to carry the heat load away from these interface points the temperatures will rise only locally. Thus, in this scenario it is possible to achieve a structure integrated thermal subsystem by simply removing the heat pipes and introducing thermally conductive interfaces between the EBox and the structure.

Chapter 7

Conclusions and Recommendations

This chapter describes the conclusions that are made from the work done followed by future recommendations.

7-1 Conclusions

This section seeks to answer whether the primary research question along with the other research questions have been answered in this work.

> *What is the best modelling approach to characterize the thermal behaviour of the MASCOT Lander Module structure and what solutions can be proposed to improve the thermal behaviour of the all-composite structure?*

The research questions that were formulated based on the primary research question were answered during the course of thesis work. With regards to the primary research question, there are two parts to the answer. The first part deals with the modelling method that needs to be adopted for converting the structural model into a thermal model. This was achieved by assessing all available methods in Patran and by creating a model that is able to provide results with the intended accuracy. Thus, it is possible to create a thermal model of a composite structure based on the structural model. The use of a unit cell model before going head first into the MASCOT model proved to be useful since all possible options for modelling in Patran were assessed and exhausted. The most ideal method of using advanced shell and solid composite elements (PLCOMP and PCOMPLS) would have led to a significant reduction in model development time. Due to the bug encountered during the course of the work these elements cannot be used at the moment. Hence, the work around of using one element per ply has been adopted for this purpose. This came with its own challenges since dealing with 200 plies individually is in terms of the required time impractical from the perspective of a structural designer who simply wishes to gain an initial understanding of thermal behaviour of the composite structure based on the structural model that is developed. To decrease the computational effort for radiation simulation, a novel method of developing radiation shell elements which are overlaid on the solid elements in the structure is described. The correlation of the model with the test campaign results were performed to validate the model for use in subsequent simulations. It is concluded that a coarse radiation mesh gives accurate results for both Phase 1 and Phase 2 whereas the fine mesh provides accurate results for Phase 1 but exceeds the temperature range for Phase 2. From the results it can be concluded that to estimate the thermal paths in a composite structure, it is indeed possible to convert a structural model into a thermal model which can be used to run simulations with satisfactory results although the method is inefficient.

The second part of the question deals with the characterisation of a structure integrated thermal subsystem and this was evaluated by removing the heat pipes and determining the temperature variations in the structure. The temperature rise in the EBox is simulated without the heat pipes and the only way to transfer heat away from the EBox is by means of conduction to the structure. This was demonstrated by varying the conductance values between the EBox and the structure and the impact of this variation on the temperature of the EBox were demonstrated. Other options to improve the thermal paths within the structure were also evaluated. Thus, it is concluded that the heat pipes can be removed and conductive interfaces between the EBox and the structure need to be introduced.

7-2 Recommendations

Considering the circumstances under which the thermal model had to be developed with limited flexibility (lack of advanced composite thermal elements due to bugs), the method that was adopted is not the most ideal one although satisfactory results were simulated. This is because for a structural designer the lack of an efficient method to gain an initial estimate of the thermal paths in the structure within a limited time frame is counter intuitive during the design process.

Once a thermal model is developed from the structural model, a structural designer would want to modify the material properties at specific locations and check the variation in the thermal paths of the structure. The method that was adopted for developing the thermal model involved manually assigning the properties of each ply and this was time consuming. Once the bugs in the PCOMPLS and PLCOMP property cards are fixed, manual assignment of properties for each ply will not be required since the software automatically assigns properties to the respective elements that are extruded. The most basic parameter that the accuracy of a thermal model depends on is the mesh size. In the current method, the mesh size cannot be varied. Due to the manual approach, every time the mesh size is increased or decreased to test the convergence criteria, all the elements that are generated do not have any material properties assigned to them by the software. Hence, the analyst has to start the manual material assignment process all over again. For structure integrated thermal subsystems, the availability of these advanced composite elements would be useful since the engineer has control over the conductivities of each ply. Hence, the engineer can easily perform a simple trade off on material ply combinations that would suit both the structural and the thermal requirements of the mission. This would also offer flexibility over the material assignments required for a structure integrated thermal subsystem.

Appendix A

Thermal Modelling Theory

This section deals with various analytical models that can be used to describe the thermal behaviour of composite materials. Conduction models for composite materials are discussed in detail as it is the most important form of heat transfer that occurs within a spacecraft. A general introduction to radiation modelling is also presented. Radiation is also a significant mode of heat transfer within the spacecraft and as the size of the spacecraft becomes smaller its effects are magnified.

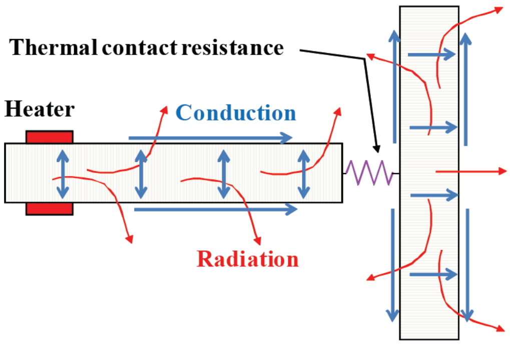

Figure A-1: Heat Transfer Mechanism of a composite sandwich T-Joint. [3]

A-0-1 Conduction

The determination of temperature distribution in a medium (solid, liquid, gas or combination of phases) is the main objective of a conduction analysis, i.e, to know the temperature in the medium as a function of space at steady state and as a function of time during the transient state. Once this temperature distribution is known, the heat flux at any point within the medium, or on its surface, may be computed from Fourier's law. [32]

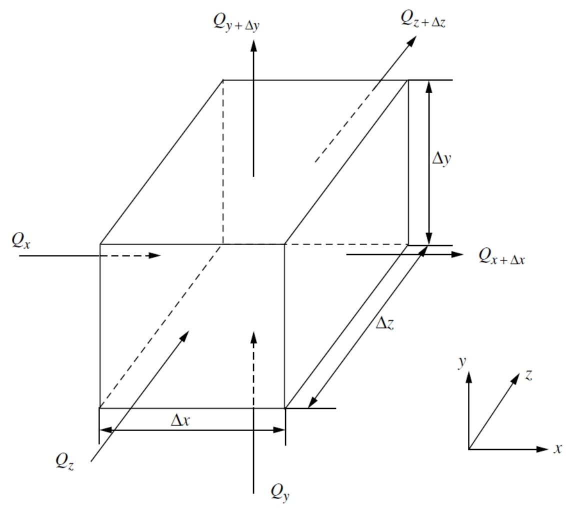

Figure A-2: Differential control volume for heat conduction analysis. [6]

A knowledge of the temperature distribution within a solid can be used to determine the structural integrity by determining the thermal stresses and distortion. We shall now derive the conduction equation in Cartesian coordinates by applying the energy conservation law to a differential control volume as shown in Figure A-2. The solution of the resulting differential equation, with prescribed boundary conditions, gives the temperature distribution in the medium.

Taylor series expansion is applied

$$Q_{x+dx} = Q_x + \frac{\partial Q_x}{\partial x}\Delta x \tag{A-1}$$

$$Q_{y+dy} = Q_y + \frac{\partial Q_y}{\partial y}\Delta y \tag{A-2}$$

$$Q_{x+dx} = Q_z + \frac{\partial Q_z}{\partial z}\Delta z \tag{A-3}$$

The heat generated in the control volume is $\Delta G \Delta x \Delta y \Delta z$. The rate of change in energy storage is given as:

$$\rho \Delta x \Delta y \Delta z c_p \frac{\partial T}{\partial t} \tag{A-4}$$

Now, with reference to Figure A-2, we can write the energy balance equation as:

Inlet energy + Energy generated = Energy stored + Exit energy

$$G\Delta x \Delta y \Delta z + Q_x + Q_y + Q_z = \rho \Delta x \Delta y \Delta z \frac{\partial T}{\partial t} + Q_{x+dx} + Q_{y+dy} + Q_{z+dz} \tag{A-5}$$

Substituting Equations A-6/7/8 into the above equation and rearranging results in:

$$-\frac{\partial Q_x}{\partial x}\Delta x - \frac{\partial Q_y}{\partial y}\Delta y - \frac{\partial Q_z}{\partial z}\Delta z + G\Delta x \Delta y \Delta z = \rho c_p \Delta x \Delta y \Delta z \frac{\partial T}{\partial t} \tag{A-6}$$

The total heat transfer Q in each direction can be expressed as

$$Q_x = \Delta y \Delta z q_x = -k_x \Delta y \Delta z \frac{\partial T}{\partial x} \tag{A-7}$$

$$Q_y = \Delta x \Delta z q_y = -k_y \Delta x \Delta z \frac{\partial T}{\partial y} \tag{A-8}$$

$$Q_z = \Delta x \Delta y q_z = -k_z \Delta x \Delta y \frac{\partial T}{\partial z} \tag{A-9}$$

Substituting Equations A-12/13/14 into Equation A-11 and dividing by the volume, $\Delta x \Delta y \Delta z$, we get,

$$\frac{\partial}{\partial x}\left[k_x \frac{\partial T}{\partial x}\right] + \frac{\partial}{\partial y}\left[k_y \frac{\partial T}{\partial y}\right] + \frac{\partial}{\partial z}\left[k_z \frac{\partial T}{\partial z}\right] + G = \rho c_p \frac{\partial T}{\partial t} \tag{A-10}$$

Equation A-15 is the transient heat conduction equation for a stationary system expressed in Cartesian coordinates. The thermal conductivity, k, in the above equation is a vector. In its most general form, the thermal conductivity can be expressed as a tensor, that is,

$$K = \begin{bmatrix} k_{xx} & k_{xy} & k_{xz} \\ k_{yx} & k_{yy} & k_{yz} \\ k_{zx} & k_{zy} & k_{zz} \end{bmatrix} \tag{A-11}$$

The preceding equation that is A-16 is valid for solving heat conduction problems in anisotropic materials with a directional variation in the thermal conductivities. The material properties are temperature dependent but for very small range of temperatures properties do not vary much and hence does not require non-linear analysis.

Noack et al [33] proposed a layerwise linear theory for prediction of heat conduction of hybrid structures. Hybrid structures are idealized as structures with homogeneous layers characterised by different thermal conductivities. Some of the assumptions taken are that the material properties are independent of temperature, perfect thermal contact between all layers, no heat flux is generated inside the layers and within each homogeneous layer and the heat conduction is described by a thermal conductivity tensor.

$$K = \begin{bmatrix} k_{xx} & k_{xy} & 0 \\ k_{yx} & k_{yy} & 0 \\ 0 & 0 & k_{zz} \end{bmatrix} \tag{A-12}$$

A-0-2 Radiation

Electronics inside a spacecraft generate heat and thus contribute towards radiation transfer within a spacecraft's body. The external sources are the sun and the albedo from earth. There is a need to quantify how much of incident radiation on it can a composite structure conduct to maintain thermal balance within the spacecraft. This section delves into the basics of radiation modelling. PATRAN uses a Gaussian integration method for calculating the radiation view factors using the VIEW3D module.

The maximum flux that can be emitted by radiation from a surface is given by the Stefan-Boltzmann Law, that is: [34]

$$q = \epsilon \sigma T_w^4 \tag{A-13}$$

where q is the radiative heat flux, (W/m^2); σ is the Stefan-Boltzmann constant (5.669×10^{-8}), in W/m^2K^4 ; T_w is the surface temperature, (K) and ϵ is the radiative property of the surface and is referred to as the emissivity.

Radiation exchange among black surfaces depends only on their temperature and how they view one another.To compute radiation exchange between any two surfaces, we must first introduce the concept of a view factor:

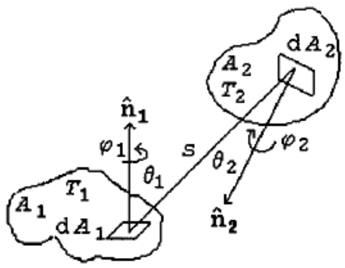

$$F_{12} A_1 = \int_{A_1} \int_{A_2} \frac{\cos\theta_1 \cos\theta_2}{\pi s^2} dA_1 dA_2$$

Figure A-3: Definition of View Factor [7]

F_{12} = radiation directly coming from A1 and impinging on A2 / radiation total emitted by A1.

The sum of view factors from a surface must be 1:

$$\sum_{i,j=1}^{N} F_{ij} = 1 \tag{A-14}$$

The radiation exchange from A1 to A2 (black surfaces) is given by:

$$Q^r_{blacksurfaces} = F_{12} A_1 (\sigma T_1^4 - \sigma T_2^4) \tag{A-15}$$

According to rule of reciprocity it can be shown that:

$$F_{ij} A_i = F_{ji} A_j \tag{A-16}$$

Exchange factor for diffuse gray surfaces includes (multiple) reflections

$$Q_{12} = \epsilon_1 A_1 B_{12} A_1 (\sigma T_1^4 - \sigma T_2^4) \tag{A-17}$$

B_{12} = radiation emitted by A1 and absorbed by A2 inclusive reflections / radiation total emitted by A1. B_{ij} known as Gebhart factor, or radiation exchange factor.For an enclosure of n surfaces:

$$B_{ij} = F_{ij}\epsilon_j + \sum_{k=1}^{n}(1-\epsilon_k)F_{ik}B_{kj} \tag{A-18}$$

Similar to the view factor, the sum of all Gebhart factors should be 1, (incl. j = i) :

$$\sum_{i,j=1}^{N} B_{ij} = 1 \tag{A-19}$$

Appendix B

IAC Paper

THERMAL CHARACTERIZATION OF A MULTIFUNCTIONAL COMPOSITE STRUCTURE IN EARLY DESIGN PHASE BASED ON THE MASCOT LANDER

Ajay Prasad Ragupathy
Delft University of Technology (TU Delft), The Netherlands, ajayprasad1223@gmail.com
Michael Lange
German Aerospace Center, Germany, m.lange@dlr.de
Barry Zandbergen
Delft University of Technology (TU Delft), The Netherlands, B.T.C.Zandbergen@tudelft.nl

MASCOT is an approximately 10 kg shoebox-sized lander platform developed by DLR in cooperation with CNES and JAXA for the Hayabusa 2 sample return mission from the asteroid 1999JU3. It consists of two parts, a Landing Module and an Interface Structure to connect the former to the mother spacecraft. This paper focuses on the MASCOT Landing Module structure, whose framework walls are made from a CFRP/foam sandwich. The M55J fibres used for the unidirectional sandwich face sheets are of Polyacrylonitrile (PAN) type and have high stiffness and strength properties, but poor thermal conductivity. Also, the glued connections between the framework walls are realised with PAN fibre patches. This is one reason, which necessitated a thermal sub-system consisting of heat pipes and an aluminium radiator. Both contribute with a total mass of approximately 450g - almost the same as the very lightweight primary composite structure (550g) of the Landing Module. Also, the structural design itself is highly influenced by the needs of the thermal sub-system. Hence, the Landing Module shall serve as a reference to investigate possible /improved thermo-mechanical design and design principles for future spacecraft missions with all-composite primary structures. In a first step, the capability of simulating the thermal behaviour of the Landing Module's structure is added. This is necessary, as the existing model was only used for mechanical finite element analysis by neglecting any thermal aspects. The paper describes the applied modelling methods and assumptions that are used to predict the Landing Module's thermal behaviour. Subsequently, the results from the finite element simulation are compared to actual thermal measurements, which were performed in a thermal vacuum chamber. The investigated design principles will help to gain a better understanding of the structure's participation in the thermal path in early design phases of future missions. By this means and corresponding measures (e.g. using materials with higher/lower thermal conductivity) the additional mass used by thermal sub-systems can be reduced by integrating the thermal functions of a spacecraft with the structure.

I. INTRODUCTION

The Mobile Asteroid Surface Scout (MASCOT) is an approximately 10kg shoebox-sized lander platform developed by DLR (German Aerospace Center) in cooperation with CNES and JAXA for the Hayabusa-2 (HY-2) sample return mission heading to the Cg-class asteroid 1999 JU3.[1]

The last phase of the Hayabusa-2 mission involves the on-surface operations of the MASCOT Landing Module on the asteroid. After reaching the target asteroid, MASCOT is released by HY-2 at a low height, lands and starts scientific investigations on the surface. Therefore MASCOT carries four instruments: MicrOmega (near-infrared hyperspectral microscope), MASCam (camera in visible range), MARA (radiometer) and MAG (magnetometer). It also houses the lander’s common electronic box (E-Box); the battery pack is attached to it at one end and is connected to the sub-radiator, a separate section of the radiator on the other. (Fig.1)

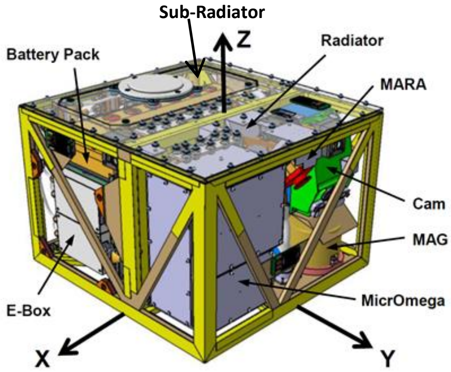

Fig. 1: MASCOT Landing Module

During its operational phase, with all the payloads switched on from time to time, the lander must be able to transfer all the heat internally produced via radiation (through the radiators) to the environment. The structure is the one of the key contributors to conductive heat transfer within a spacecraft and this influences the requirements for the construction/shape and the choice of materials during the design phase. To a great extent, the material properties determine the flow of energy that occurs due to conduction and the radiation of surfaces to each other and to space.

The payloads in a spacecraft are normally rigidly connected to the bus's structure and can dissipate heat via conduction. However also, a high thermal insulation can be required in certain cases. In contrast to an aluminium alloy structure, MASCOT's all-composite structure has an overall thermal conductivity which is in the order of almost a magnitude lower and thus presents a thermal challenge for designing a high thermal conductive structure. Although all-composite structures use state-of-the art materials, there is very little understanding of the participation of each component and connection in a structure's thermal path and methods to predict their overall thermal behaviour. During the early design phases, the only way to gain thermal data is by analytical or numerical simulations of the thermal behaviour of the spacecraft. Numerical simulation techniques are crucial for reduction of development costs of complicated systems. Hence there is a need to better understand and predict the overall heat conduction process in CFRP sandwich structures. Simulating the temperature distribution within a spacecraft structure helps the thermal and structures engineers to evaluate thermal paths within the structure and optimize the design accordingly. The temperature field is also useful for the evaluation of stresses induced by thermal expansion in a composite structure during the design phase. During the initial design phase of the structure, it is advantageous to use a single model for both structural and thermal analysis. The reference model that was used for this work is a 2D shell finite element model that was developed for structural simulations in MSC Patran/Nastran

This paper provides an insight into the modelling methods that were evaluated to adapt the structural finite element (FE) model for thermal analysis. The lander structure and the thermal subsystem are elaborated upon. The FE model development process, challenges faced and result validation process are described. The results from the FE thermal model developed are validated with test results obtained from the thermal-vacuum campaigns that were conducted on the lander during its qualification.

II. LANDER MODULE STRUCTURE

The MASCOT system is subdivided in two main structural parts, the box-shaped Lander Module (Fig. 2), housing all experiments and sub-systems, and the surrounding interface structure to the mother spacecraft. Both are constructed as lightweight composite framework structures having together a total mass of around 1.4 kg. The lander structure (excluding the radiators) alone has a mass of 450 g.

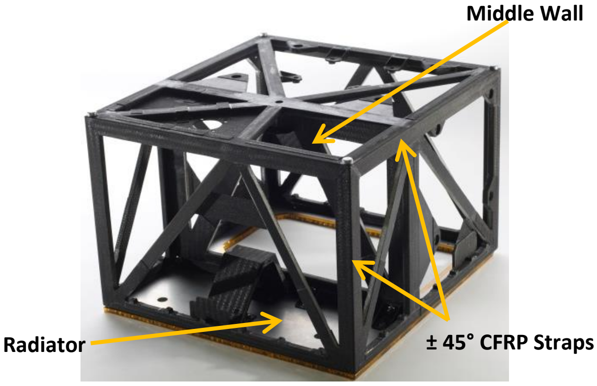

Fig. 2: MASCOT Landing Module Framework Structure

The Landing Module's structure is the focus of the investigation and the interface structure has been ignored as it remains on the mother spacecraft and is not part of the on-asteroid operations. The lander has outer dimensions of 295 x 275 x 195 mm^3 and contains two compartments separated by a middle wall. One compartment is dedicated for the payloads and the other for the E-Box including the battery pack and a mobility mechanism. The lander structure is made of sandwich components. Most of the framework sandwich walls consist of not more than one UD-CFRP facesheet ply (LTM 123/M55J) on each side and a foam core (Rohacell IG-F 31). ±45° CFRP plies (Epoxy/M40J) are used where normal and shear loads are introduced into the structure. ± 45° CFRP straps are used at the edges to connect the walls. The final design of the lander structure, especially the radiator and the subradiator, was influenced by the thermal management components and its placement.[2]

III. THERMAL DESIGN

The thermal design of the lander is primarily dependent on the on-asteroid mission phase. One side of the lander must be opened to allow the payloads to face the outside (Fig. 3). The other sides must be protected from the intrusion of dust and rocks. The lander's thermal design can be considered as semi-active [2]. For the cruise phase, since the lander is attached to HY-2 spacecraft, heaters powered by HY-2 are used to maintain the critical components above their non-operational limits. The passive system comprises of insulation foils, multi-layer insulation (MLI) sheets and two variable conductance heat pipes carrying thermal loads to the radiator. The thermal design of the Landing Module was successfully verified via multiple thermal vacuum campaigns where all the components were observed to be within the operational temperature ranges.

Fig. 3: MASCOT Landing Module Flight Model

IV. THERMAL MODEL DEVELOPMENT

IV.I Baseline Model

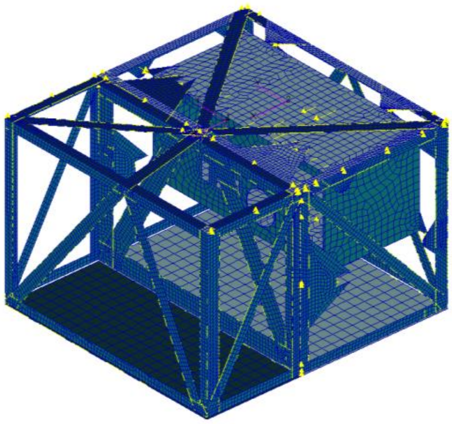

Fig. 4: 2D Shell Structural Model

The structural analysis model of the lander was modelled using MSC Patran. Quadratic 2D shell elements (Quad4) and a few triangular shell elements (Tria3) are used (Fig. 4). The composite layup is simulated using the Patran Laminate Modeler.[2] The instruments are modelled as point masses and connected to the structure using RBE2 elements. However, the model with shell elements does not have the capability to calculate the through thickness temperature gradient. Also, the model cannot accurately simulate the conductive heat transfer processes that occur between the structural members. When dealing with the mostly poor out-of-plane conductivities of the sandwich structure it is of interest to evaluate the sensitivity of the designs to changes in material properties (fibre type, orientation etc.). Hence a steady state analysis with solid 3D elements is used to characterize the thermal paths in the structure. It is expected that every single layer has to be discretized by at least one element to ensure accurate results. This is because homogenization of laminate properties using fewer elements leads to approximations that do not accurately capture the physics of the heat transfer processes that occur in the lander structure.

IV.II. Unit Cell Modelling

Before working on the MASCOT model, the modelling approaches that could be adopted in Patran needed to be identified and analysed on a unit cell model. Hence, a 2D shell model of dimensions 1mmx3mm was developed and a 5 layered sandwich layup was applied over it (Fig. 5). Three approaches to developing the thermal model from the structural model were investigated on this unit cell and are described below. The best method is then adopted based on a trade-off process between the described modelling methods.

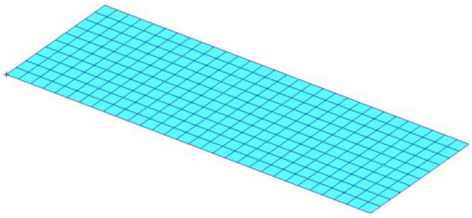

Fig. 5: Unit Cell Model

IV.II.I 2D Modelling

As described earlier, the structural model comprises of 2D shell elements. The default shell elements with PCOMPG properties cannot handle multiple composite layers for thermal analysis. As an alternative, Patran offers 2D solid elements that have the capability to calculate the through thickness temperatures in composite laminates. Property data of upto 510 layers in a laminate can be used in the model for the simulations. This is carried out using a property card for 2D Solids called PLCOMP. By assigning the 2D Solid to the existing 2D shell elements it is possible to adapt the mesh for carrying out thermal analysis for the laminate.

IV.II.II 2.5D Modelling

The 2.5D method refers to a hybrid modelling method whereby 3D solid elements are used at critical areas of interest in the structure and the rest of the structure is modelled using the 2D solids (PLCOMP). The 3D elements are then coupled with the 2D elements using 1D conductor elements. The 3D elements could be generated by simply extruding the shell elements at the desired locations using the Patran Laminate Modeler. The material properties are then automatically assigned to all the elements through the PCOMPLS property card.

IV.II.III 3D Modelling

The most straightforward approach to create a 3D model from the 2D shell element model is to extrude all the shell elements using the Laminate Modeler which then creates advanced 3D elements that can be used to represent upto 510 elements in a single element. If more accuracy is required, one element per layer can also be extruded. The PCOMPLS property card is assigned to these extruded solids which refer to the advanced composite elements. Patran also automatically then assigns the corresponding properties to the respective layers.

IV.III. Trade off analysis

After developing models using each of the three aforementioned modelling methods, the results obtained from them were compared and analysed. To decide the modelling approach that needs to be adopted for the full scale modelling, a trade-off analysis was carried out with a weighted decision matrix.

Four criteria for assessing the methods were formulated. The first one is the Accuracy, which is determined by the correlation of the results obtained to the real world values. The second being the Computation Time. It is directly proportional to the number of nodes in the model. Third comes the Adaptability which defines the ease with which the model´s properties can be changed based on the requirements. Finally the model Development Time is also considered as certain modelling methods can take a lot more time than the others. Based on their relevance to the simulation, the selected criteria were allocated weights on a scale of 1 to 4 in an increasing order. Each method is awarded a score ranging from 1 to 4, based on its performance with respect to the criteria. The total points scored by each method is the sum of the products of its individual score for a criteria and the weight of the criteria (Table.1). From the trade-off table it is concluded that 3D modelling is the most optimal approach for carrying out the thermal analysis on the MASCOT structure.

Modelling Method Criteria	Weights	2D	2.5D	3D
Development Time	1	3	2	1
Accuracy	4	1	2	3
Computation Time	3	3	2	1
Adaptability	2	1	2	3
Score		18	20	22

Table 1: Trade off Matrix

IV.IV Challenges

During the evaluation of the various FE Modelling approaches, a bug was discovered in the 2D Solid PLCOMP and the 3D PCOMPLS elements that were generated from the pre-existing mesh using the Patran Laminate Modeler. The bug involves the temperature gradients and fluxes in the element-normal direction that were calculated in the output. Irrespective of the corresponding input parameters (lambda_z), the output for these values was always zero. Clarification with the MSC Corporation that develops the PATRAN/NASTRAN resulted in confirmation of the existence of the bug. The advanced 2D and 3D composite elements (PLCOMP and PCOMPLS) thus cannot be used for the analysis till the bug is fixed. Hence, as a workaround a sophisticated 3D model comprising of the standard PSOLID Hex8 Elements was developed. Each ply in the structure had to be matched with their respective material and coordinate frames respectively in a manual approach. This led to an exponential increase in the model development time but having a model that is so detailed gives an advantage with respect to the adaptability. The model gives unprecedented control over property changes per ply.

IV.V Full Scale Modelling

The development of a full 3D element model (Fig. 6) was challenging due to the fact that the automatic assignment of properties to the plies by the Patran Laminate Modeler was not available due to the bug explained earlier. The extrusion of one element per layer without automatic property assignment meant that elements belonging to each ply had their properties to be assigned manually. This involved isolating each part of the structure and assigning a coordinate system per structural member within the part. Next, each ply had to be selected individually and the material assigned to them. Caution was exercised when dealing with junctions in each part where plies overlap since many plies are involved and heat transfer at these intersections need to be simulated accurately. The payloads, E-Box, battery pack and the MLI were modelled with Quad4 shell elements. The heat pipes were modelled as 1D conductor elements. (CELAS)

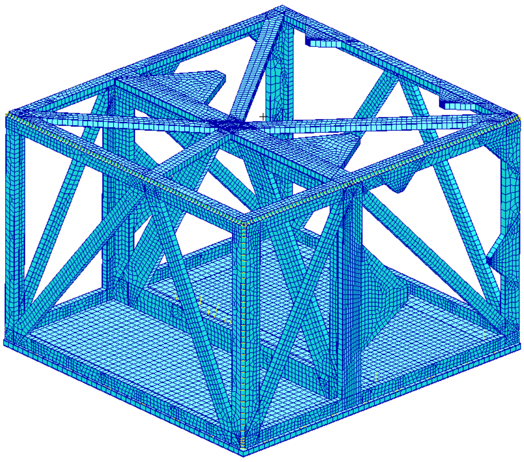

Fig. 6: 3D MASCOT FEM Model (Structure)

IV.V.I Radiation Model

A radiation model does not require as many nodes and elements as the conduction model. Hence, a simplified 2D shell model was developed that represents the top layer of the framework structure. These overlap the conduction model (Fig.7). Each structural component of every wall is modelled with at least one element each. The energy that an element of the model receives from radiation is transferred to the surrounding elements through its corner grid points. Appropriate enclosures are defined in the model based on the local radiation exchange between various components. This is required since some components onboard participate in radiation exchange with the interiors as well as the exterior asteroid environment.

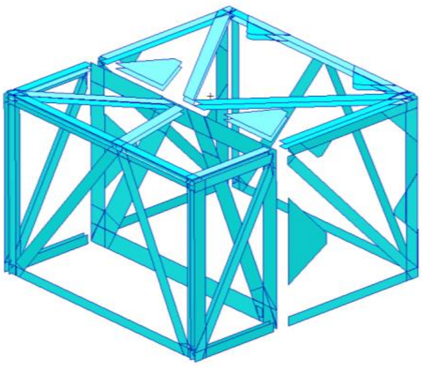

Fig. 7: Radiation Model (Structure)

IV.V.II Material Properties and Interfaces

The material properties vital for thermal modelling are conductivity, emissivity and absorptivity since only steady state analysis is carried out. These values were taken from the various tests conducted on each component during the design phase. The conductivities for the unidirectional CFRP plies and the ± 45° CFRP fabric reinforcements/patches are determined using the rule of mixtures. The interface values between the components onboard the MASCOT Landing Module have been tuned based on the thermal vacuum campaigns performed on the module over the course of the simulation model´s testing and validation process. The conductive interfaces between the components were modelled using 1D conductor (CELAS) elements with the appropriate conductance assigned to them.

IV.V.II Boundary Conditions

The boundary conditions of the model were derived from the thermal vacuum campaign setup that was designed for the MASCOT Landing Module. The Landing Module FE Model is placed on a soil imitator that simulates the on-asteroid soil conditions. The asteroid soil imitator is modelled with 2D shell elements (Fig.8). The vacuum chamber walls are cooled down to approximately around 80K. The vacuum chamber is modelled as one ambient shell element above the MASCOT model and is set at 80K. The asteroid soil imitator temperature during the Phase 0 is set at 273K and during Phase 2 at 333K. The results from these Phases are used as they provide the steady state temperatures of the various components onboard the lander during both the hot and cold phases. In both the phases the payloads are switched off. The only heat generating components are the battery pack and E-Box.

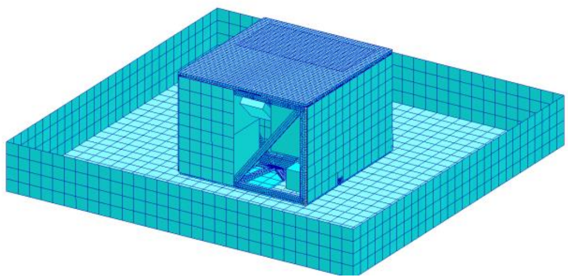

Fig 8. Lander with soil imitator

The on-asteroid operations involve the use of only one payload at a time based on the mission planning. Hence the effect of the environment on the lander can be gauged only when all the payloads are switched off to ensure that they are operating within their temperature limits when they are switched on. Solar flux on the Landing Module is simulated with a set of heaters that are fixed on various locations on the top side of the radiator and the sub-radiator that provide a heat load of 17W. This corresponds to the average solar flux received on the asteroid during the on-surface operation. Out of the many thermistors used in the test campaigns, 4 sensors are attached to the structure close to the payloads (Fig. 9). The temperature readings from these sensors will be used for the validation of the thermal model developed.

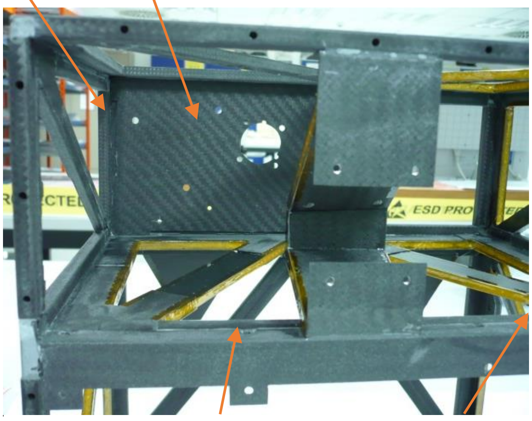

Fig. 9: Thermistor Positions in the payload compartment (Top View, Radiator removed)

V. RESULTS

V.I Correlation

The thermal model developed is correlated with the test results. During both Phase 0 and Phase 2 the temperature differences between the model results and test measurements do not exceed a ±5K range (Fig 11 & Fig.13) which can be considered as a benchmark value when evaluating the temperature limits of the components in the lander module. The uncertainties in the model can be attributed to the radiation elements that have been modelled. This is due to the fact that each structural member in every wall has only one radiation element as described earlier. Hence, only the 4 corner nodes in that structural member participate in the radiation process. Whereas in the real world every section of the structural member participates in conduction as well as radiation.

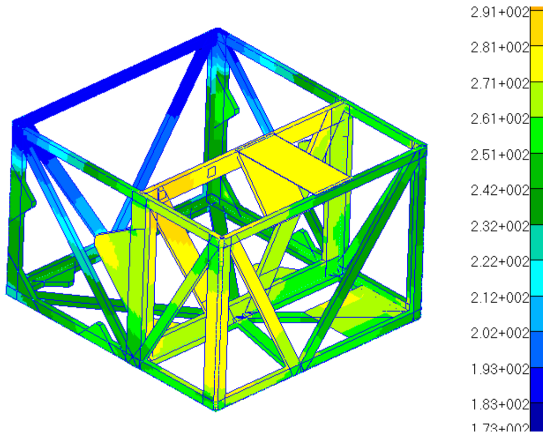

Fig 10: Phase 0 temperature plot

Sensor	Test Temp [ºC]	Model Temp [ºC]
Struct_1	-7.3	-10
Struct_2	-7.7	-9
Struct_3	6.1	2
Struct_4	8.4	7

Table 2: Temperature values for correlation (Phase 0)

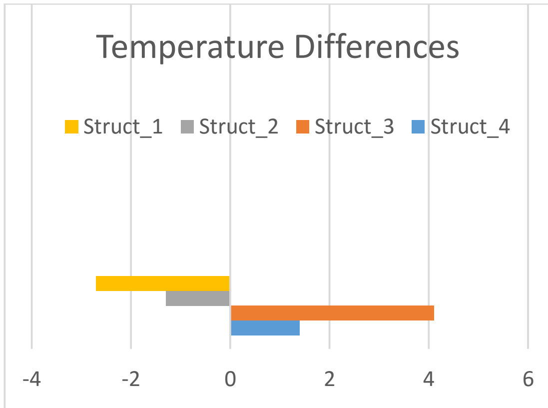

Fig. 11: Correlation temperatures, Phase 0

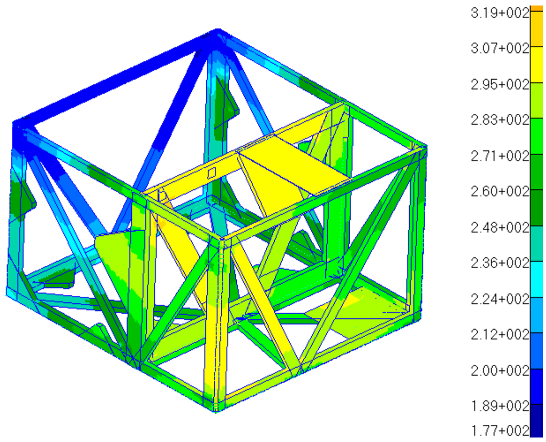

Fig 12: Phase 2 temperature plot

Sensor	Test Temp [ºC]	Model Temp [ºC]
Struct_1	26.6	24
Struct_2	29.3	25
Struct_3	23.5	23
Struct_4	27.4	26

Table 3: Temperature values for correlation (Phase 2)

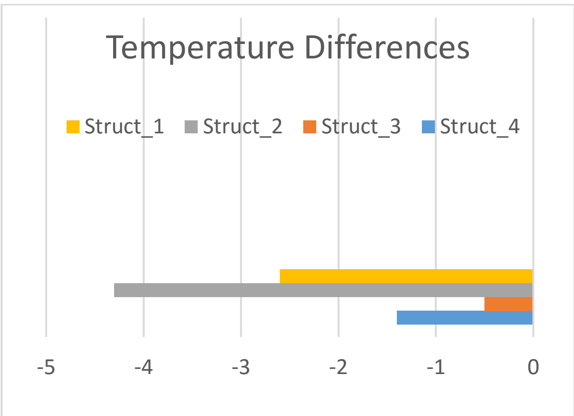

Fig 13. : Correlation temperature, Phase 2

VI. CONCLUSION

The paper provided an insight into the modelling methodology that was adopted for capturing the heat transfer processes occurring in the lander structure accurately. The finite element model developed for characterizing the thermal behaviour of the MASCOT composite structure has been correlated with test campaigns. The differences and uncertainties involved in the correlation between the simulations and tests have been explained.

VI.I Future Outlook

The model will further be used for investigating different solutions for a structure-integrated thermal sub-system that could be achieved with the MASCOT structure. This will be carried out by comparing the thermal analysis results from various solutions (such as using high conductivity fibre and foam, embedded thermal links) proposed to make the structure multifunctional.

VII. REFERENCES

[1] Lange,M. et.al, Mascot - Structures design and qualification of an organic mobile lander platform for low gravity bodies. In *Proceedings of the 13th European Conference on Spacecraft Structures,Materials and Environmental Testing,SP-727.ESA Communications.*

[2] Lange, M. et.al, MASCOT - A Lightweight Multi-Purpose Lander Platform. *European conference on spacecraft structures, materials and environmental testing 2012, 20.-23.March 2012, Noordwijk, Netherlands.*

[3] Celotti et.al, MASCOT thermal subsystem design challenges and solution for contrasting requirements. *45th International Conference on Environmental Systems ICES-2015-83 12-16 July 2015, Bellevue, Washington*

Appendix C

Original Project Planning

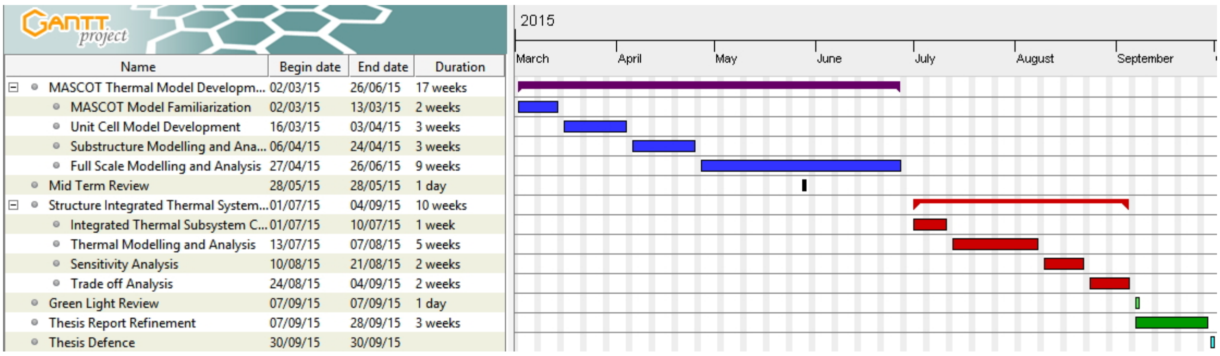

Name	Begin date	End date	Duration
MASCOT Thermal Model Developm...	02/03/15	26/06/15	17 weeks
MASCOT Model Familiarization	02/03/15	13/03/15	2 weeks
Unit Cell Model Development	16/03/15	03/04/15	3 weeks
Substructure Modelling and Ana...	06/04/15	24/04/15	3 weeks
Full Scale Modelling and Analysis	27/04/15	26/06/15	9 weeks
Mid Term Review	28/05/15	28/05/15	1 day
Structure Integrated Thermal System...	01/07/15	04/09/15	10 weeks
Integrated Thermal Subsystem C...	01/07/15	10/07/15	1 week
Thermal Modelling and Analysis	13/07/15	07/08/15	5 weeks
Sensitivity Analysis	10/08/15	21/08/15	2 weeks
Trade off Analysis	24/08/15	04/09/15	2 weeks
Green Light Review	07/09/15	07/09/15	1 day
Thesis Report Refinement	07/09/15	28/09/15	3 weeks
Thesis Defence	30/09/15	30/09/15	

Figure C-1: Project Planning

Appendix D

Appendix C- List of Analyses

Analysis	File Name
I) Unit Cell Modelling	
Case 1 - UD Ply	
2D Modelling	Lam_2D
2.5D Modelling	Lam_2.5D
3D Modelling	Lam_3D
Case 2- Composite Laminate	
2D Modelling	Comp_2D
2.5D Modelling	Comp_2.5D
3D Modelling	Comp_3D
II) MASCOT	
Steady State Analysis	
Phase 1	Phase0_rad
Phase 2	Phase2_rad
Structure Integrated	
Thermal Subsystems	
Case 1	noHP
Case 2.1	cond2
Case 2.2	cond5
Case 3.1	cond5_strap2
Case 3.2	cond5_strap5
Case 4	alinsert

Table D-1: List of Analyses

Bibliography

[1] Stephan Ulamec, Jens Biele, Pierre-W Bousquet, Philippe Gaudon, Koen Geurts, Tra-Mi Ho, Christian Krause, Caroline Lange, Rainer Willnecker, Lars Witte, et al. Landing on small bodies: From the rosetta lander to mascot and beyond. *Acta Astronautica*, 93:460–466, 2014.

[2] Scientific Advisory Board and Air Force. *New World Vistas: Air and Space Power for the 21st Century. Space Technology Volume.* Defense Technical Information Center, 1996.

[3] Kim Byoung Jim. Phd thesis : Development of stsat 3 structure with composite sandwich constructions, 2010.

[4] Michael Lange, Olaf Mierheim, and Christian Huehne. Mascot - structures design and qualification of an organic mobile lander platform for low gravity bodies. In *Proceedings of the 13th European Conference on Spacecraft Structures,Materials and Environmental Testing,SP-727.ESA Communications.*

[5] M. Lange, C. Huehne, O. Mierheim, A. Braukhane, T-M. Ho, C. Lange, S. Wagenbach, and L. Witte. Mascot - a lightweight multi-purpose lander platform. In *European Conference On Spacecraft Structures, Materials And Environmental Testing 2012.*

[6] Roland W. Lewis, Perumal Nithiarasu, and Kankanhalli N. Seetharamu. *The Finite Element Method*, pages 38–101. John Wiley and Sons, Ltd, 2005.

[7] Robert D Karam. *Satellite thermal control for systems engineers*, volume 181. Aiaa, 1998.

[8] Ajay Prasad.R. Literature study: Structure integrated thermal subystems, 2014.

[9] James Klett and Bret Conway. Thermal management solutions utilizing high thermal conductivity graphite foams. *Society for the Advancement of Material and Process . . .*, (1):1–11, 2000.

[10] M.Solyga. Mascot asteroid results interpretation and thermal correlation - thermal test campaign. 2014.

[11] Joseph H Saleh, Daniel E Hastings, and Dava J Newman. Spacecraft design lifetime. *Journal of Spacecraft and Rockets*, 39(2):244–257, 2002.

[12] Wiley J Larson and James Richard Wertz. *Space mission analysis and design*. 2011.

[13] Mauro Montabone. Spacecraft structure. *Wiley Encyclopedia of Composites*, 2012.

[14] Harald Van Weeren, Marcel Ter Brake, Rob J Hamann, Gerrit Holl, and Steve Price. Thermal aspects of satellite downscaling. *Journal of Thermophysics and Heat Transfer*, 23(3):592–600, 2009.

[15] Anthony Kelly. *Concise encyclopedia of composite materials*. Elsevier, 2012.

[16] Xingcun Colin Tong. *Advanced materials for thermal management of electronic packaging*, volume 30. Springer, 2011.

[17] Shawn Klann. Anisotropic heat conduction in composite materials. 2011.

[18] Ireneusz Kreja. A literature review on computational models for laminated composite and sandwich panels. *Open Engineering*, 1(1):59–80, 2011.

[19] MSC Patran. User's guides and reference manuals. 2014.

[20] J Tessmer, S Waitz, R Rolfes, J Ackva, and T De Vries. Thermal analysis computation and experimental validation of fiber metal laminates. In *Proceedings of the 5th International Congress of Thermal Stresses, Blacksburg, USA*, 2003.

[21] A Boudjemai, A Mankour, H Salem, R Amri, R Hocine, and B Chouchaoui. Inserts thermal coupling analysis in hexagonal honeycomb plates used for satellite structural design. *Applied Thermal Engineering*, 67(1):352–361, 2014.

[22] Lihua Zhang and Yuegen Chen. The on-orbit thermal-structural analysis of the spacecraft component using msc/nastran. *Beijing Institute of Spacecraft System Engineering*, 1998.

[23] Timo Brander, Kristof Gantois, Harri Katajisto, and Markus Wallin. Cfrp electronics housing for a satellite. In *Spacecraft Structures, Materials and Mechanical Testing 2005*, volume 581, page 144, 2005.

[24] Myer Kutz et al. *Handbook of materials selection*. Wiley Online Library, 2002.

[25] John DiPalma, Jeff Preble, Mike Schoenoff, Stephen Motoyama, James Guerrero, Capt Burks, et al. Applications of multifunctional structures to small spacecraft. 2004.

[26] Mark H Luesse and Jack C Roberts. Heat sink for increasing through-thickness thermal conductivity of organic matrix composite structures, November 2 1999. US Patent 5,975,201.

[27] Sangwook Sihn, Sabyasachi Ganguli, David P Anderson, and Ajit K Roy. Enhancement of through-thickness thermal conductivity of sandwich construction using carbon foam. *Composites Science and Technology*, 72(7):767–773, 2012.

[28] Andy Caroline Lange, Braukhane Ross, Findlay Christian, Grimm Jan Thimo, and Mi Ho Lars. How to build a 10 kg autonomous asteroid landing package with 3 kg of instruments in 6 years? 2012.

[29] L Celotti, M Solyga, R Nadalini, V Kravets, S Khairnasov, V Baturkin, C Lange, R Findlay, C Ziach, and T Ho. Mascot thermal subsystem design challenges and solution for contrasting requirements. 45th International Conference on Environmental Systems, 2015.

[30] Jan Tessmer, Tom Sproewitz, and Tobias Wille. Thermal analysis of hybrid composite structures. In *Proceedings 25th Congress of International Council of the Aeronautical Science, Hamburg, Germany*, 2006.

[31] Jih-Run Tsai. Overview of satellite thermal analytical model. *Journal of spacecraft and rockets*, 41(1):120–125, 2004.

[32] RC Progelhof, JL Throne, and RR Ruetsch. Methods for predicting the thermal conductivity of composite systems: a review. *Polymer Engineering & Science*, 16(9):615–625, 1976.

[33] J Noack, R Rolfes, and J Tessmer. New layerwise theories and finite elements for efficient thermal analysis of hybrid structures. *Computers & structures*, 81(26):2525–2538, 2003.

[34] Dutch Space. Ae4s20: Satellite thermal control course work. 2013.